工 學 博 士 學 位 論 文

Improvement in anti-cancer activity and binding affinity of the therapeutic anti-HER2 monoclonal antibody and bioprocess development

치료용 항 HER2 단일클론 항체의 항암 활성 및 결합 친화도 개량과 생산공정 개발

2016年 2月

서울大學校 大學院

協同科程 生物化學工學 專工

文 昇 基

Improvement in anti-cancer activity and binding affinity of the therapeutic anti-HER2 monoclonal antibody and bioprocess development

by Seung Kee Moon

Advisor :

Professor Young Je Yoo, Ph.D.

Submitted in Partial Fulfillment of the Requirements

for the Degree of Doctor of Philosophy

in Seoul National University

February 2016

Interdisciplinary Program

in Biochemical Engineering

Graduate School

Seoul National University

Improvement in anti-cancer activity and binding affinity of the therapeutic anti-HER2 monoclonal antibody and bioprocess development

치료용 항 HER2 단일클론 항체의 항암 활성 및
결합 친화도 개량과 생산공정 개발

指導敎授: 劉 永 濟

이 論文을 工學博士 學位論文으로 提出함

2016年 2月

서울大學校 大學院

協同科程 生物化學工學 專工

文 昇 基

文 昇 基의 博士學位 論文을 認准함

2016年 2月

委 員 長 _____

副委員長 _____

委 員 _____

委 員 _____

委 員 _____

ABSTRACT

To generate a bio-better which has improved therapeutic activity than that of hu4D5 (Herceptin), the hu4D5 antibody was used as a model system. scFv libraries were constructed by random mutagenesis of several resides of CDR-H3, L3 and L2 of hu4D5, and the scFv clones isolated from the phage display libraries using the "stringent" panning, and their anti-proliferative activity as IgG1 against breast cancer cells was evaluated as a primary selection criterion.

Among 139 variants variant, AH06 was the best candidate as a bio-better antibody that has an increase by 7.2-fold in anti-proliferative activity (IC_{50}: 0.81 nM) against gastric cancer cell NCI-N87 and by 7.4-fold in binding affinity (K_D: 60 pM) to HER2 compared to hu4D5, respectively.

AH06 specifically bound to domain IV of HER2 and did not have cross-reactivity with other receptor tyrosine kinases (RTK) except HER2, and decreased the level of phosphorylation of HER2 and AKT to a similar extent, but most of all, highly increased the overall level of p27 in gastric cancer cell NCI-N82 as compared to hu4D5.

Binding energy calculation indicated that the substitution of residues of CDR-H3 to W98, F100c, A101 and L102 could stabilize binding of the antibody to HER2. And molecular modeling stimulation indicated that the direct hydrophobic interactions

between the aromatic ring of W98 within AH06 and the aliphatic group of I613 within antigen HER2 domain IV, and the inter-chain hydrophobic interactions between the phenyl ring of F100c in CDR-H3 and the hydrophobic groups that consist of Y36, P44 and F98 located in V_L could have synergistic effects on improvement in binding affinity of AH06 to HER2.

The expression vector for producing AH16 was constructed, and the AH16 producing AH16F1-3-14-80-26 clone whose antibody growth rate and productivity had been consistently maintained during 1~15 passages was finally screened as a stable producer cell line. One basal media and 3 additives were selected, and the final productivity of AH16 using the optimized media mixture was approximately 1.3g/L in flask culture.

The three chromatography steps using Protein A resin column (1st step) and two steps of ion-exchange chromatography provided the yield of 93.8% and the purity of 99.9%, and non-Protein A-based cation-exchange chromatography provided the yield of 99% and the purity of 97.5%.

Also, analysis of physico-chemical, biological and immunological characteristics of AH16 verified that it meets the standards set based on the “Specifications and Analytical Procedures”.

Through this study, the upstream antibody engineering technology required to discover and improve biological efficacy of various therapeutic lead antibodies and the downstream bioprocess

technology required to produce antibody were able to be established and applied.

Keywords : Antibody engineering, Antibody optimization, HER2, Phage display, Random mutagenesis, Anti-proliferative activity, Binding affinity, Herceptin, Bioprocess optimization, Stable cell line development, Culture process, Purification process

Student Number: 2004-30222

CONTENTS

LIST OF TABLES

LIST OF FIGURES

LIST OF ABBREVIATIONS

Amino acid

A (Ala)	Alanine
R (Arg)	Arginine
N (Asn)	Asparagine
D (Asp)	Aspartate
C (Cys)	Cysteine
Q (Gln)	Glutamine
E (Glu)	Glutamate
G (Gly)	Glycine
H (His)	Histidine
I (Ile)	Isoleucine
L (Leu)	Leucine
K (Lys)	Lysine
M (Met)	Methionine
F (Phe)	Phenylalanine
P (Pro)	Proline
S (Ser)	Serine
T (Thr)	Threonine
W (Trp)	Tryptophan
Y (Tyr)	Tyrosine
V (Val)	Valine

CDR	complementarity determining region
V_L	variable region of light chain

V_H	variable region of heavy chain
pIII	M13 bacteriophage gene-3 minor coat protein
HER2-ECD	extracellular domain of erbB2 or p185HER2
hu4D5	humanized version of the monoclonal antibody 4D5
TBS-T	TBS containing 0.05% Tween 20
pHER2	phosphorylated HER2
pAkt	phosphorylated Akt
API	active pharmaceutical ingredient
HCP	host cell protein
HCD	host cell DNA
SDS-PAGE	sodium dodecyl sulfate-polyacrylamide gel electrophoresis

CHAPTER 1

Introduction

1.1 Research Backgrounds

Antibody seems to be ideal molecule as targeting reagent by binding with high specificity and affinity to a wide variety of molecules, and therefore, widely used in research, diagnosis and treatment for disease. In particular, the engineered antibody has been used as a disease-curing agent in clinical fields via neutralizing disease-inducing target antigen or regulating cellular function of target cells expressing the disease-related specific antigens.

It is possible to develop human antibodies designed to increase efficacy, to reduce side effects, and to increase productivity of the antibody in a variety of diseases such as cancer, immunological disease, infective disease and metabolic diseases. The reasons why the antibody has been widely used for curing various diseases are that it is a natural product of humans with low toxicity and high safety, and its stability and specificity are relatively superior to those of small molecule drugs in human body (Imai and Takaoka, 2006).

Various target antigens have been studied for the development of therapeutic antibodies used for curing cancer and immunological diseases. One of the antigens is HER2 protein over- expressed on the breast and gastric cancer cells.

HER2 is a receptor tyrosine kinase located in cell membrane and a

member of the ErbB/HER (Human epidermal growth factor receptor) family that consists of EGFR, HER2, HER3 and HER4. HER2 has been implicated important roles in growth, differentiation and survival in cancer cells as well as in normal cells (Whenham et al., 2008). In contrast to other HER family members, HER2 does not require ligands for the receptor-receptor interactions (Nicolas et al., 2008). In cancer cells, the HER2 protein can be expressed up to 100 times more than in normal cells (2 million versus 20,000 per cell, respectively) (Shepard et al., 1991). Such overexpression or amplification of HER2 promotes the formation of receptor homo- and heterodimers with other HER family members, leading to uncontrolled cell proliferation and tumor growth (Mayumi et al., 2006).

Therefore, HER2 has been investigated as a promising therapeutic target for cancer. Particularly, targeted-therapy using anti-HER2 monoclonal antibodies such as Herceptin (Trastuzumab, hu4D5: binding to domain IV), Kadcyla (Trastuzumab-maytensinoid: antibody-drug conjugate) and Perjeta (Pertuzumab: binding to domain II) has been used to treat HER2 positive cancers.

Herceptin (trastuzumab) launched by Genentech in October 1998 is a humanized version of murine monoclonal antibody, hu4D5. It binds extracellular domain (ECD) IV of HER2 receptor, subsequently inhibits its downstream PI3K-Akt signaling (Hudziak et al., 1989; Yakes et al., 2002; Sliwkowski et al., 1999) and induces

cell cycle arrest via induction of cyclin-dependent kinase inhibitor p27/kip1 and apoptosis (Carter et al., 1992) in metastatic HER2 positive breast and gastric cancer cells, which in turn inhibits HER2-meidated tumor growth.

A combination of Herceptin with chemotherapy has shown significant improvements in cancer treatment. Disease-free survivals were 75.4% and 87.1% with chemotherapy alone and in combination with Herceptin, respectively, in patients with HER2-overexpressing metastatic breast cancer (Romond et al., 2005). However, despite its proven clinical benefit, most patients who have an initial response to Herceptin develop resistance within one year of treatment initiation.

Accordingly, it is required to develop another anti-HER2 antibody having improved affinity, efficacy or the like. For this purpose, various approaches are as follows: screening a novel anti-HER2 antibody with different epitope, random mutagenesis strategies of Herceptin (hu4D5) variable region or Fc-engineering technologies enhancing antibody effector function (e.g., antibody dependent cell–mediated cytotoxicity, ADCC) by increasing its binding to FcγIII on effector cells such as macrophages.

For this purpose, a strategy to improve the binding affinity and efficacy of the antibody is mutagenesis, and particularly substitution of the residues at some positions of CDR-H and CDR-L would be considered. Based on this way, it was previously reported that substitution of residues in the CDRs of hu4D5

influences antibody affinity (Gerstner et al., 2002).

In the previous report, Gerstner et al. constructed phage-displayed Fab libraries targeting 19 positions of hu4D5 (Gerstner et al., 2002) including R50(V_H), W95(V_H), Y100a(V_H) and H91(V_L) known to be important to bind with HER2 molecule (Kelley et al., 1993). The libraries were divided into five groups by 5~7 residues, respectively. The binding affinity of a single mutant D98 (V_H)W (K_D 0.11 nM) was increased by 3-fold compared to the parent antibody hu4D5, but the anti-cancer activity of the variant was not reported. They also suggested that further improvement in binding affinity could be found using alternative methods of binding selection or targeting more plastic or variable positions (Gerstner et al., 2002). However, there were no reports of success in screening variants superior to D98(V_H)W in binding affinity and functional activity such as anti-cancer activity until now.

Therefore, screening was carried out using Herceptin as a template antibody to discover the biobetter antibody with improved activity and bioprocess study was performed for the production of the resulting antibody.

1.2 Research Objectives

The aim of our study was to investigate whether further modifications of the antibody that has been already affinity-maturated could improve its binding affinity and subsequent biological activity or efficacy, and to establish antibody optimization technology for antibody improvement strategy, using hu4D5 as a model system. Also, it was aimed to set up a series of bioprocess technologies required to produce the selected antibody, and to apply the bioprocess platform technologies to discover and develop new antibody therapeutics.

Firstly, the CDR regions of Herceptin that already has high binding affinity to specific antigen HER2 were changed by random mutagenesis, and the following screen was planned to select the variants with improved anti-cancer activity and binding affinity. In addition, since there was a possibility to increase those activities by mutating the framework part (or region) instead CDR regions (Ding et al., 2010; Kobayashi et al., 2010), it was aimed to select new improved HER2-targeting therapeutic antibodies through error-prone random mutagenesis of the entire variable region from the selected variants and the well-established phage display technology.

Secondly, *in vitro* functional anti-tumor activity, binding affinity,

target cross-reactivity (specificity), mechanism of signaling inhibition and *in vivo* anti-tumor activity of variants were evaluated, and, it was also speculated how to attribute the modification of hu4D5 to improvement in binding affinity using molecular modeling analysis.

In addition, to produce and supply the selected antibody samples required to proceed development process for clinical trials and launch, the following bioprocess has progressed.

Thirdly, to produce the stable cell line producing a large amount of the selected antibody, the study on screening of high-producing stable cell line was conducted. By screening, the stable cell line with high-producing and stable growth was selected, and was used to perform the following study for optimization of antibody production.

Fourthly, the screening of basal media and additives for improving growth, survival rate and the antibody productivity of the selected stable cell line and the optimization of purification process for the purpose of establishing antibody separation and refining methods were performed.

Fifthly, in this way, the "Specifications and Analytical Procedures" for the biobetter antibody was established by

evaluating the physical-chemical and biological characteristics of the highly purified final antibody produced through the validated bioprocess. In addition, feasibility and robustness of the validated bioprocess were determined by evaluating the quality of antibody produced through the bioprocess.

Distinctively, in this study, mutagenesis was performed on CDR residues affecting the heavy and light inter-chain interaction as well as CDR resides participating in binding to the antigen unlike Gerstner et al. carried out only the latter strategy (Gerstner et al., 2002). Another distinctive point is that the sublibrary construction and combinatorial expression by mutagenesis of each heavy and light CDR instead of mutagenesis of heavy and light CDRs in one scFv library, which can reduce the enormous size of library construction .

Therefore, the objectives of this work are summarized as follows.

- To screen and discover improved antibody variants by random mutagenesis and phage display technology using CDR and FR region of Herceptin as a template

- To evaluate biological activities of the isolated variants and to analyze the improved binding affinity using molecular modeling analysis (simulation)

- To produce the stable cell line, screen basal media & additives, set up process for antibody purification, and establish “Specifications and Analytical Procedures”

CHAPTER 2

Literature Survey

2.1 Clinical needs of therapeutic antibody

Antibody seems to be ideal molecule as targeting reagent by binding with high specificity and affinity to a wide variety of molecules, and therefore, widely used in research, diagnosis and treatment for disease. Studies in genomes and proteome have made it possible to identify a wide variety of molecules as therapeutic targets.

In vertebrate, immune system can produce antibodies that have high affinity for any kinds of antigen based on genetic diversity. Recently, therapeutic monoclonal antibodies are emerging as the therapeutic agent for the wide range of diseases including cancer, autoimmune and infectious diseases.

By using the technologies of developing therapeutic antibody such as humanization and optimization of antibody, it is possible to develop human antibodies designed to increase efficacy, to reduce side effects, and to increase productivity of the antibody in a variety of diseases such as cancer, immunological disease, infective disease and metabolic diseases. Now, monoclonal antibodies used for therapeutic and diagnostic reagents for a long time are now emerging as a major biologics following chemical drug.

Since the clinical importance and industry of therapeutic antibody have continuously increased, many pharmaceuticals and bio-ventures worldwide have invested to develop novel monoclonal therapeutic antibodies and technologies. And the therapeutic

monoclonal antibody is expected to lead the market as the next generation of antibody-based therapeutic agents. Consequently, following this trend, more than 30 therapeutic antibodies were developed (Table 2-1) (Janice, 2012) in year 2012, and currently, over 1,000 antibodies are being discovered and developed.

Table 2-1. Therapeutic monoclonal antibodies marketed or in review in the European Union or United States in March 2012 (Janice, 2012).

International non-proprietary name (Trade name)	Manufacturing cell line	Type	Target	First EU (US) approval year
Abciximab (Reopro®)	Sp2/0	Chimeric IgG1κ Fab	GPIIb/IIIa	1995* (1994)
Rituximab (MabThera®, Rituxan®)	CHO	Chimeric IgG1κ	CD20	1998 (1997)
Basiliximab (Simulect®)	Sp2/0	Chimeric IgG1κ	IL2R	1998 (1998)
Palivizumab (Synagis®)	NS0	Humanized IgG1κ	RSV	1999 (1998)
Infliximab (Remicade®)	Sp2/0	Chimeric IgG1κ	TNF	1999 (1998)
Trastuzumab (Herceptin®)	CHO	Humanized IgG1κ	HER2	2000 (1998)
Alemtuzumab (MabCampath, Campath-1H®)	CHO	Humanized IgG1κ	CD52	2001 (2001)
Adalimumab (Humira®)	CHO	Human IgG1κ	TNF	2003 (2002)
Tositumomab-I131 (Bexxar®)	Hybridoma	Murine IgG2aλ	CD20	NA (2003)
Cetuximab (Erbitux®)	Sp2/0	Chimeric IgG1κ	EGFR	2004 (2004)
Ibritumomab tiuxetan (Zevalin®)	CHO	Murine IgG1κ	CD20	2004 (2002)
Omalizumab (Xolair®)	CHO	Humanized IgG1κ	IgE	2005 (2003)
Bevacizumab (Avastin®)	CHO	Humanized IgG1κ	VEGF	2005 (2004)
Natalizumab (Tysabri®)	NS0	Humanized IgG4κ	α4-integrin	2006 (2004)
Ranibizumab (Lucentis®)	*E. coli*	Humanized IgG1κ Fab	VEGF	2007 (2006)
Panitumumab (Vectibix®)	CHO	Human IgG2κ	EGFR	2007 (2006)
Eculizumab (Soliris®)	NS0	Humanized IgG2/4κ	C5	2007 (2007)
Certolizumab pegol (Cimzia®)	*E. coli*	Humanized IgG1κ Fab, pegylated	TNF	2009 (2008)
Golimumab (Simponi®)	Sp2/0	Human IgG1κ	TNF	2009 (2009)
Canakinumab (Ilaris®)	Sp2/0	Human IgG1κ	IL1b	2009 (2009)
Catumaxomab (Removab®)	Hybrid hybridoma	Rat IgG2b/mouse IgG2a bispecific	EpCAM/CD3	2009 (NA)
Ustekinumab (Stelara®)	Sp2/0	Human IgG1κ	IL12/23	2009 (2009)
Tocilizumab (RoActemra, Actemra®)	CHO	Humanized IgG1κ	IL6R	2009 (2010)
Ofatumumab (Arzerra®)	NS0	Human IgG1κ	CD20	2010 (2009)
Denosumab (Prolia®)	CHO	Human IgG2κ	RANK-L	2010 (2010)
Belimumab (Benlysta®)	NS0	Human IgG1λ	BLyS	2011 (2011)
Raxibacumab (Pending)	NS0**	Human IgG1κ	*B. anthrasis* PA	NA (In review)
Ipilimumab (Yervoy®)	CHO	Human IgG1κ	CTLA-4	2011 (2011)
Brentuximab vedotin (Adcentris®)	CHO	Chimeric IgG1κ; conjugated to monomethyl auristatin E	CD30	In review (2011)
Pertuzumab (Pending)	CHO	Humanized IgG1κ	HER2	In review (in review)

2.2 Types of therapeutic antibody

2.2.1 Mouse antibody

In 1975, a murine monoclonal antibody, which is produced from 'hybridoma' technique invented by Kohler and Milstein in Britain (Köhler and Milstein, 1992), has high selectivity and specific binding affinity. Therefore, it has been used for various fields efficiently. Especially, because monoclonal antibody can target variety antigens and be produced for large-scale, it is widely used for clinical diagnosis and research agents (Fuchs et al., 1992; Vieira and Messing, 1987). Currently, there are six mouse antibodies approved for the treatment of diseases.

However, the application of murine monoclonal antibodies for therapy has raised several problems. One major drawback is, for instance, that mouse Abs are recognized as antigen in human and can induce the formation of a human anti-mouse antibody (HAMA) response after repeated injection. It causes the low response rate for efficacy of therapy. To solve these problems, a humanized antibody such as Herceptin was designed and developed (Carter et al., 1992).

2.2.2 Chimeric antibody

In order to reduce the HAMA response, a technique of replacing the constant region of a mouse antibody with a constant region of a human antibody has been developed. Chimeric antibody contains approximately 65% human sequences. It may significantly decrease the HAMA response but still have immunogenicity due to the mouse Fv sequences. Rituximab (Reff et al., 1994) and Remicade (infliximab) (Knight et al., 1993; Scallon et al., 1995) are examples of the typical chimeric antibodies approved for lymphomas and rheumatoid arthritis, respectively.

2.2.3 Humanized antibody

Antibody can be divided into variable and constant regions, and the variable region consists of CDR (complementarity determining region) which directly binds to the specific antigen and FR (framework region) which supports the structure of CDR loop (Marchalonis et al., 2006). The humanized antibodies such as Herceptin are made using CDR grafting technology that the CDR loops of mouse antibody is grafted into FR of human antibody (Kettleborough et al., 1991).

Since the humanized antibodies contain about 5~10% of mouse antibody sequences and have less HAMA (human anti-mouse

antibody) response than the mouse antibodies, they may have better efficacy than the mouse antibodies. And since the productivity and thermodynamic stability of Herceptin is relatively high, and the immunogenicity of Herceptin is very low as about 0.5%, the framework region of Herceptin is sometimes used as a template for generating the humanized antibody (Carter et al., 1992).

Humanized antibodies are produced by grafting hypervariable regions of a murine antibody onto the human antibody framework. As compared to murine and chimeric antibodies, it greatly reduces immunogenicity increases a half-life *in vivo*. However, the affinity of the humanized antibody is decreased in the process of the CDR grafting. In this case, it could be solved by re-introducing the murine framework residues that play an important role in the structure of the CDR or the affinity maturation.

Herceptin (trastuzumab) (Carter et al., 1992) is a representative humanized antibody approved for breast cancer therapy.

2.2.4 Fully human antibody

Although humanized antibodies comprise murine sequence to less than 10%, they might still be immunogenic. Thus, researchers have tried to develop a fully human antibody by using transgenic mice or display technologies.

Advances in techniques for the manipulation of the germline of mammalian embryos led to the creation of transgenic mice technology. These mice directly generate high affinity human sequence antibodies de novo in response to immunization. Vectibix (panitumumab) is the first antibody developed by immunization of transgenic mice that produce the human immunoglobulin light and heavy chains (Yang et al., 2001). More fully human antibodies will be developed using this technology.

2.3 Antibody engineering technology

2.3.1 Phage display technology and its application

Besides human hybridoma technique, human mAb has recently been produced using two skills, 'Phage display' and 'Transgenic Mice'. Particularly, the technology of Phage Display is a typical technique to reproduce the discovery of antibody in test-tube scale (Pasqualini and Ruoslahti, 1996; Cheng et al., 2005).

The phage display has many advantages. It can produce antibody fragments such as scFv and Fab in bacterial hosts such as *E. coli* in quantity, more efficiently, quickly and at a lower cost, compared to production of whole antibody. And these fragment antibodies induce less immune responses than murine mAb and have better penetration into tumor tissue than whole IgG (Farajnia et al., 2014).

In the mid-1980s, George P. Smith invented the cell surface-expression system in which peptides or small proteins are fused to pIII of a filamentous phage. Since then, the research on the secretion mechanism of microorganisms was actively progressed, and a new field called "Cell Surface Display" that expresses target proteins on the surface of microorganisms, was appeared (Rader et al., 1998; Baca et al., 1997).

Cell surface display is a technique that a foreign target protein is stably expressed on the surface of microorganism such as bacteria and yeast through fusion with the surface anchoring motif. Using ssDNA of filamentous phage, a foreign antigen fused to the coat protein is expressed in host bacteria cells, and then the foreign protein is expressed through the replication system of a helper phage and the phage coat protein (Rader et al., 1998; Baca et al., 1997). This process is called phage display (Fig. 2-1).

Phage display technique is used to express antibody library that has high diversity through genetic recombination on the surface of bacteriophage. Because a specific antibody for antigen is easily isolated and amplified using this skill, it is a very important tool for antibody engineering. (Clackson et al., 1991; Hoogenboom and Chames, 2000; Hoet et al., 2005). Phage display makes antibody discovery more efficient and takes less time. Especially, human antibody for development of new therapeutic antibody can be produced by this skill; phage display is widely exploited in the

field of biotechnology and the pharmaceuticals industry (Winter et al., 1994).

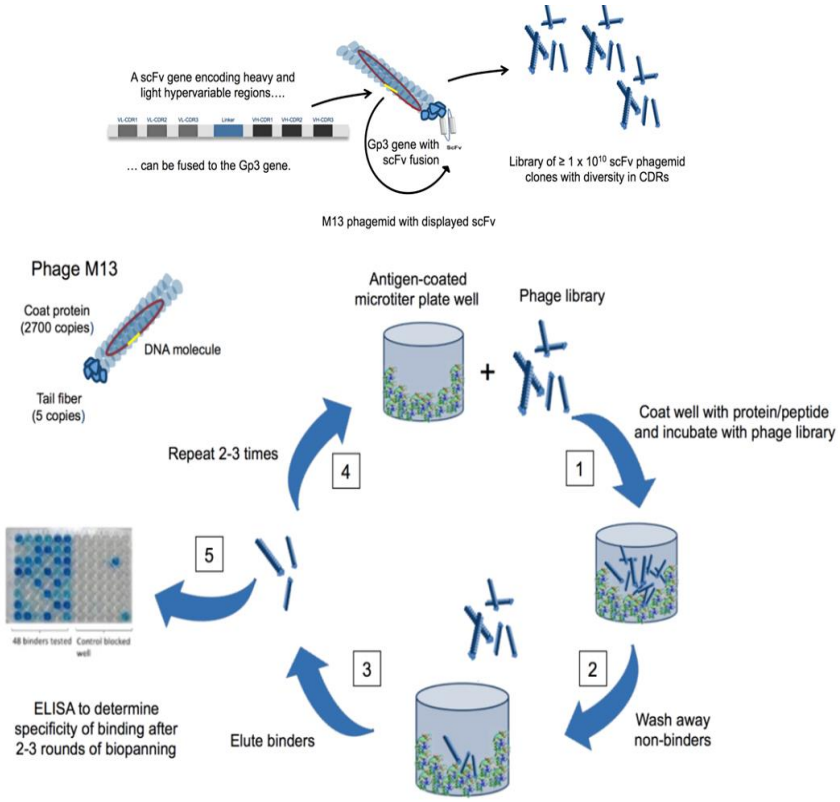

Fig. 2-1. The method of panning using recombinant phage displayed library.
(Source from http://axiomxlab.wpengine.com)

Phage display technology first developed by British Medical Research Council in 1990s is a technique that peptide, particularly the antibody fragment such as Fab and scFv, is fused with the coat

protein of bacteriophage and expressed on surface of phage. These proteins organize phage antibody library. A phage clone, which has peptide or antibody fragment specific to particular antigen, is selected by phage library. (Parsons et al., 1996; Barbas et al., 2004)

Phage display is a fundamental technology showing superior selection power among biotechnologies developed until now. (Giordano et al., 2001; Yang et al., 1999; Krebs et al., 2001; Dower et al., 1988) (Fig. 2-4). However, it is possible for the selected human antibody to have low affinity. (Knappik et al., 1995; Krebber et al., 1996; Azzazy et al., 2002; Baek et al., 2004; Corisdeo et al., 2004). In this case, it is necessary to perform affinity maturation.

In this phage display, a skill called 'panning' is needed to select the protein that specifically binds to the target antigen among recombinant phage library expressing recombinant fusion pIII with various sequence (Rader et al., 1998; Baca et al., 1997) (Fig. 2-1).

2.3.2 Phage display technology: system requirements

The phage display system is composed with 1) phage vector system using bacteriophage genome as a cloning vector, and 2) phagemid vector system using phagemid vector, a fusion type of phage genome and plasmid. The vector mentioned above is recombined with specific peptide or foreign protein through

genetic cloning, and then target protein is successfully exposed (displayed) on the surface of phage as fusion to phage-coated protein, p3 or p8.

In case of displaying foreign protein such as antibody, the phagemid vector system can be utilized. Unlike peptide display with phage genome, phagemid has only part of phage genome, and there is no gene for replication, assembly of real type bacteriophage and coat protein in phagemid. Thus, phagemid vector cannot produce new phage particles by itself.

In phagemid vector system, a helper phage needs to be added for replication, assembly of a recombinant phage and production of coat protein, this process is called phage rescue. On the surface of the recombinant phage obtained through the phage rescue, there are not only fusion-pIII, the fusion protein of antibody and phage coat protein p3, but also a lot of wild type pIIIs. This problem makes numerous technical difficulties in selection of recombinant phage targeting specific antigen from phage library. To solve these problem, various types of helper phage (Ex-phage, CT-phage, hyper-phage, VCS M13, Phaberge, etc) have been developed and utilized (Steiner et al., 2006).

From the 'phage display library' that is a complex of recombinant phage particle expressing random peptide or various foreign protein, a recombinant phage fused peptide or protein specific

binding to target protein or ligand is selected and acquired by searching method called 'bio-panning' (Fig. 2-1). The isolated recombinant phage has a phenotype-genotype linkage between gene in phagemid genome and target-specific peptide or protein expressed on the surface of phage. Thus, genetic information of target peptide or protein can be confirmed (Rowley et al., 2004).

2.3.3 Yeast display

Yeast surface display technology was reported by Boder and Wittrup in 1997 (Boder and Wittrup, 1997). This technique has become a powerful tool for protein engineering and library screening. The principle of this technique is to use a yeast mating adhesion receptor α-agglutinin (Aga) that is a glycoprotein composed of two subunits, Aga1p and Aga2p. Aga serves to anchor recombinant proteins to the cell surface. Aga1p is an anchoring subunit tethered to the yeast cell wall via a β-glucan covalent linkage at its carboxyl terminus and Aga2p is an adhesion subunit covalently linked to Aga1p by two disulfide bonds (Zou et al., 2000).

The use of an eukaryotic host provides the significant advantage in posttranslational processing and modification of proteins of animal origin. Also, it allows the quantitative analysis in

conjunction with FACS cytometry and thus enables efficient screening for proteins having a high affinity. However, it is difficult to produce a large size library due to the limited yeast transformation efficiency (Benatuil et al., 2010).

2.3.4. Ribosome display

Ribosome display reported by Hanes and Plückthun in 1997 (Hanes and Plückthun, 1997) is a powerful *in vitro* technology for screening proteins. It is a method for selecting ~~a~~ proteins specifically binding to a target using a cell-free translation system.

The mRNA library is generated by *in vitro* transcription from a cDNA library produced by PCR. After *in vitro* translation, a stable ribosomal complex is achieved as a result of coupling the phenotype and genotype. After the selection process, the mRNA–protein complexes are then reverse-transcribed to cDNA and their sequences are amplified using PCR. After repeating this process, it is possible to obtain the sequence of the protein binding to the target antigen.

Ribosome display has two advantages. First, the large size library whose diversity is not limited can be made quickly and easily. Second, additional mutations can be introduced easily.

2.3.5. Humanization of mouse antibody

Antibody humanization technology is the representative technique to reduce the immunogenicity of the mouse antibodies. When a mouse antibody administered to a human, HAMA (human anti-mouse antibody) response is induced. The HAMA response influences the safety, efficacy and half-life of the antibody (Khazaeli et al., 1994).

There are two common techniques for antibody humanization. One is chimerization, replacement of the constant region of a mouse antibody with that of a human antibody (Boulianne et al., 1994; Morrison et al., 1984; Neuberger et al., 1984). HAMA response of some mouse antibodies is reduced through chimerization.

However, other antibodies may still have immunogenicity due to sequences of the mouse Fv. Thus, Jones et al. reported the technology to implant the CDR regions of a mouse antibody onto the Fv framework of a human antibody (Jones et al., 1986; Riechmann et al., 1988; Verhoeyen et al., 1988). Immunogenicity of the humanized antibody is minimized by using only the sequence of the mouse antibody necessary for the antigen binding.

2.3.6 Fc engineering

Antibodies can act on other cells or proteins and induce various biological activity, such as ADCC (antibody dependent cell cytotoxicity) and CDC (Complement dependent cytotoxicity), which is referred to as antibody effector functions (Strohl, 2009). Effector function of the antibody is derived by the Fc region of the antibody heavy chain. A receptor capable of reacting with the Fc region of an antibody is called the Fc receptor. The Fc gamma, Fc epsilon and Fc alpha receptors bind IgG, IgE and IgA, respectively.

Antibodies reacting with the Fc receptors induce effector functions such as ADCC (antibody dependent cell cytotoxicity) and CDC (Complement dependent cytotoxicity) responses (Daëron, 1997). Thus, Fc engineering technology to control ADCC, CDC and the half-lives of antibodies has been developed.

Lazar et al. described a triple mutant (S239D/I332E/A330L) with a higher affinity for FcγRIIIa and a lower affinity for FcγRIIb resulting in with enhanced ADCC (Lazar et al., 2006; Ryan et al., 2007). Notably, alanine substitution at position 333 was reported to increase both ADCC and CDC (Presta et al., 2000; Idusogie et al., 2001). It has been shown that an increase in the binding affinity of the antibody to FcRn leads to an increase in the half-life of IgG1 *in vivo* (Hinton et al., 2004; Vaccaro et al., 2005).

2.4. Bioprocess development technology

2.4.1 Development of stable cell line

The dihydrofolate reductase (dhfr) (Urlaub et al., 1983; Kaufman et al., 1985; Werner et al., 1998) expression system or glutamine synthetase (GS) system (Wurm, 2004; Birch and Racher, 2006; Cockett et al., 1990) are widely used for development of stable cell lines with high productivity. Cells are transfected with a construct containing a selectable marker and subjected to selection. After screening the highly productive stable clones, bioprocesses are further developed and optimized for large-scale production.

DHFR is an amplifiable and selectable marker, so routinely use to establish cell lines. The parental CHO cell was mutagenized to yield DG44, a cell line with deletion of DHFR. DG44 was adapted for the large-scale suspension culture (Trill et al., 1995). DHFR converts 5, 6-dihydrofolate into 5, 6, 7, 8-dihydrofolate, which is required for the de novo synthesis of nucleic acid precursors, such as purine. This purine plays central role in cell division and maintenance of cell survival through DNA replication after synthesizing nucleic acids (Hamlin, 1992).

Purine precursors, hypoxathine and thymidine (HT) are therefore necessary for growth and survival of DHFR-deficient DG44 cells. If the construct containing DHFR and a target gene is stably integrated into the chromosome of DG44 cells by transfection, the

transfected cells can survive in the media without HT.

DHFR also functions as a genetic marker for amplification of a target gene using MTX (methotrexate) selection. If MTX is present in the media, the cells amplify DHFR gene copy number in the genome to overcome inhibition by MTX. Since the target gene is integrated into the same locus as DHFR gene, it can also be amplified, leading to an increase in expression of the target protein (Gu et al., 1992; Ng, 2012).

2.4.2 Optimization of cultivation media and additives

Basic carbon source (sugar), energy source (glucose), nitrogen source (amino acids), inorganic salts, trace elements, vitamins, growth factors and buffering agents should be included in the culture media used in the cultivation of the antibody-producing cells such as mammalian animal CHO DG44 cells (Kim et al., 1999; Parampalli et al., 2007). In addition, 5~20% of serum could be added.

Animal serum has been generally used in cell culture media, but since then the recombinant protein drugs was accidently produced in animals cell cultures, using the serum was gradually became to be removed due to the trend in biopharmaceutical approvals to remove unknown (or uncertified) constituents and risk of infection of the animal-origin ingredients (Butler, 2005).

In addition, the serum is expensive and the separation and refining process of the products from cell culture is very complicated due to proteins and peptides within the serum. Since the sterilization method of serum is not heat sterilization but only filtration, there is an increasing possibility of mycoplasmas or virus contamination. And since the composition of serum varies considerably in quality from batch to batch, it is difficult to obtain the reproducibility of experiments (Witzeneder et al., 2005).

Therefore, in order to overcome these issues, the research to find which element is suitable to replace a serum (Mariani et al., 1991; Barnes and Sato, 1991), in other words, the study on the media development regarding the required ingredients and their combination has been developed.

In addition to glucose, glutamine, amino acids and salts, insulin, transferrin and selenium could be used in serum-free media to replace serum (Iscove and Melchers, 1978; Parampalli et al., 1978). And since the components composition of the serum-free media is clearly known and defined, it is easy to standardize the media composition, to give high-reproducibility of the experiment, to easily sterilize and to purify the products.

However, there are problems in the use of serum-free media: the cost of media is expensive if specific hormones or growth factors needs to be added; the rate of cell growth is slower than the serum containing media; it should be a personalized production

depending on the intended use; different cell lines requires the different media composition (Grillberger et al., 2009).

Therefore, it needs to study on screening of serum-free media additives to complement the disadvantage of the media and to increase the cell growth and productivity of the recombinant proteins.

2.4.3 Optimization of antibody purification process: Protein A and non-Protein A process

Protein A column is an affinity chromatography column based on an interaction between protein A and immunoglobulin G (Jendeberg et al., 1996). Protein A column may need to be carefully selected because it is expensive as well as has a significant impact on the efficiency of the process. Therefore, selecting the appropriate protein A resin is a critical step in development of purification process based on Protein A affinity chromatography (Shukla et al., 2007; Liu et al., 2010; Kelley, 2009; Moser and Hage, 2011). And ligand leaching should be considered as a key factor for resin selection because it affects purity of purified product, capacity and life cycle of column (Carter-Franklin et al., 2007).

Antibody purification process can be divided into Protein A-based purification and non-Protein A-based purification processes,

depending on the use of Protein A resin. A Protein A-based purification step is only having the advantage of being able to purify the antibody in high purity, high efficiency, but its cost of the resin is expensive (Kent, 1999; Fahrner et al., 2001; Marichal-Gallardo and Alvarez, 2012), and ligand leaching could be a possible problem.

Non-Protein A process can be established at lower costs than Protein A process and does not require monitoring leached protein A. In addition, new specialized resins that and enable efficient antibody purification with high purity have been developed. Therefore, it is worth developing non-Protein A-based purification processes.

Cation exchange chromatography is based on the principle that it holds on positive electric charged molecules and flows negative electric charge. Isoelectric point of IgG is known about 6.1 ~ 8.5 (Bumbaca et al., 2012). Therefore, antibodies are positively charged at the pH of neutral or below and can be separated by cation exchange chromatography.

For example, the material with a pI value of 9 is positively charged in the neutral buffer solution and it means that it interacts with cation exchanger. Protein is in folded state, so its surface charge is more important than the net charge. However, it is general to refer to the theoretical pI in cation exchange chromatography initial try.

In general, non-protein A capturing process is known to be

slightly inferior to Protein A process in terms of the yield and purity, but Non-protein A-based process has the advantages: there is no need to keep track of the leached Protein A toxicity and it is cheaper than Protein A process in production cost.

2.5 HER2 as a therapeutic target of anticancer antibody

2.5.1 Biological functions of HER2 on cancer

One of the representative features that appear in many species of cancer is deregulation such as over-expression of tyrosine kinases (RTKs). HER2 (also known as Neu or ErbB2), a receptor tyrosine kinase that belongs to the human epidermal growth factor receptor (EGFR) family including HER1 (ErbB1/EGFR), HER3 (ErbB3) and HER4 (ErbB4) (Calogero et al., 2007), exists on the normal and cancer cell membranes and plays an important role in cell growth, differentiation and survivals (Fig. 2-2). Over-expression of HER2 on the cancer cells induces homodimerization as well as heterodimerization with other family members such as HER1 and HER3, which initiates a variety of signaling pathways and promotes cell proliferation and survival.

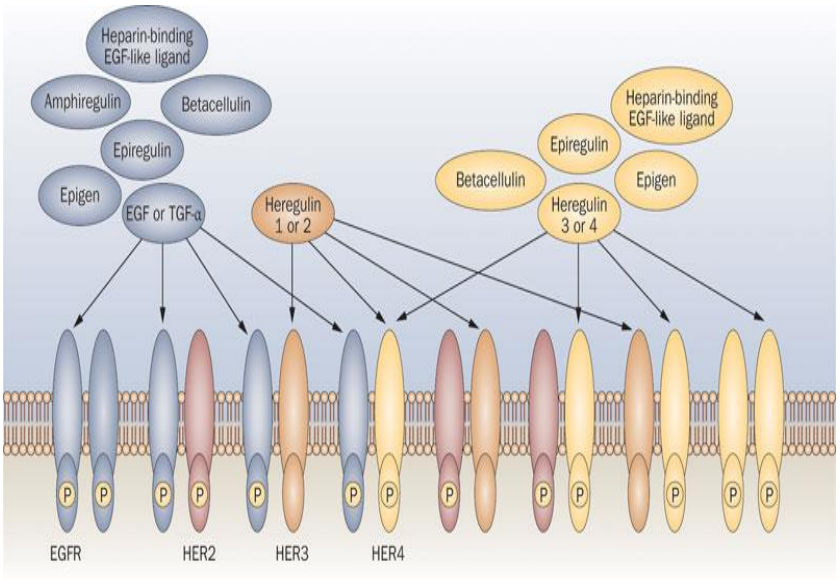

Fig. 2-2. HER family and their ligands (Okines et al., 2011).

The unique feature of HER2, which differentiates HER2 from the other members of the family, is the absence of a known ligand. Its activity is subsequent to homo- or hetero dimerization with the other family members. Breast cancers can have up to 25~50 copies of the HER2 gene and up to 40~100 fold increase in HER2 protein expression resulting in up to 2 million receptors expressed at the tumor cell surface (Shepard et al., 1991).

In particular, overexpression of HER2 has been reported in about 20~30% of invasive breast cancer patients and in other forms of cancers such as ovary (15~30%), stomach (23%), Lung (11~32%),

kidney (30~40%), colon (17-90%), pancreas (26~45%), bladder (44%), prostate (12%) and head and neck (29~39%). (Baxevanis et al., 2004; Swanton et al., 2006; Mineo et al., 2004; Lara et al., 2002; Høgdall et al., 2003; Matsui et al., 2005; Lei et al., 1995; Seliger et al., 2000; Ménard et al., 2001; Bei et al., 2004). Therefore, HER2 is a promising therapeutic target for cancer drug discovery.

HER2 has no known direct activating ligand and may be in an activated state constitutively or become active upon heterodimerization with other family members such as HER1 and HER3. The HER2 receptor has an important role in normal cell growth and differentiation. However, overexpression of the HER2 promotes the formation of HER2 heterodimerization, which leads to more aggressive tumor growth (Davoli et al., 2010). Because of the oncogenic pathway of HER2, a number of monoclonal antibodies such as Herceptin or Perjeta directed against the HER2 receptor have been actively developed.

2.6. Needs for new anti-HER2 antibody

Herceptin (Trastuzumab, hu4D5 : humanized version of 4D5, Genentech) was approved as part of a treatment regimen containing doxorubicin, cyclophosphamide and paclitaxel for the adjuvant treatment of women with node-positive, HER2

overexpressing breast cancer in 1998. Herceptin selectively blocks HER2-HER2 dimerization through binding to domain IV of the extracellular segment of the HER2 receptor and subsequently inhibits tumor growth (Molina et al., 2001) (Fig. 2-2). In addition, Herceptin binding to HER2 blocks proteolytic cleavage of the extracellular domain of HER2, resulting in diminished levels of the more active p95-HER2 form of HER2. However, Herceptin did not suppress tumor growth completely by failing to disrupt HER2-HER3 heterodimerization (Fig. 2-2).

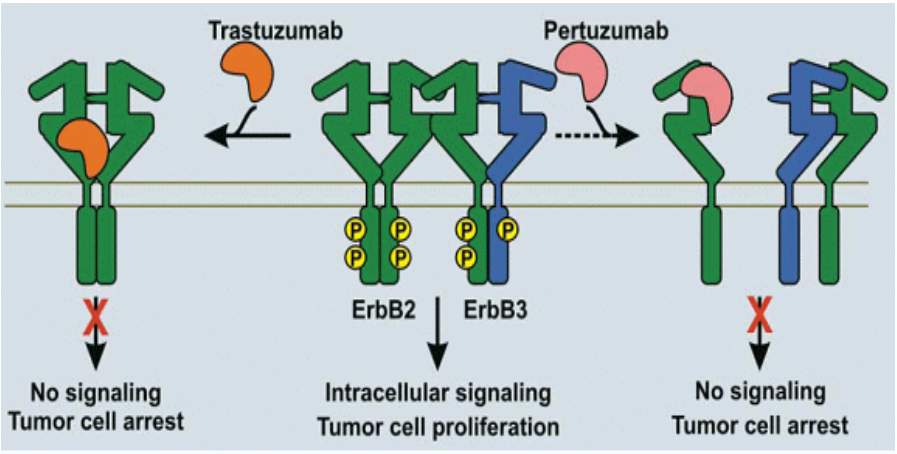

Fig. 2-3. Action mechanism of Herceptin (Trastuzumab) and Perjeta (Pertuzumab).

Herceptin is indicated for HER2-overexpressing metastatic breast cancer and adjuvant treatment of HER2 overexpressing node positive or node negative breast cancer. The objective response rates of Herceptin with cytotoxic drug range from 38 to 50%. However, the objective response rates to Herceptin monotherapy range from 12 to 34% and acquired resistance to Herceptin has been increasingly recognized as a major obstacle in the clinical management of this disease. In addition, incidence of congestive heart failure was 2~7% in women with Herceptin monotherapy and 11~28% in women with Herceptin plus chemotherapy. One in 10 women could not receive Herceptin due to the risk of heart failure (Hudis et al., 2007).

Sporadic cases of congestive heart failure were reported in major side effects of Herceptin. A total of 27% of patients treated concurrently with Herceptin and anthracyclines, 13% with Herceptin and paclitaxel, and 5% with Herceptin alone experienced cardiotoxic effects (Hudis et al., 2007).

Despite benefits of Herceptin in adjuvant and neoadjuvant uses, its efficacy was not perfect. Several issues are under investigation, including cardiac safety, the optimal treatment duration, the benefit of treatment after disease progression, combinations with additional anti-HER2 targeting agents, and health care costs. Therefore, the community needs to develop another anti-HER2 antibody with improved efficacy and reduced cardiac toxicity risk.

Therefore, HER2-overexpressing breast cancer led to development of another HER2 targeted antibodies. Perjeta (Pertuzumab, Omnitarg, Genentech), a new anti-HER2 antibody, has been approved in 2013 by the European Medicine Agency.

Pertuzumab, a monoclonal antibody directed against a portion of the extracellular domain II of HER2, sterically blocks the ability of HER2 to heterodimerize with other members of the family and induces apoptosis and cancer cell death (Fig. 2-2). Clinical efficacy of Pertuzumab was reported to be low when used alone but very striking when used in combination with Herceptin. Therefore, Perjeta is used only in combination with Herceptin for the treatment of HER2-overexpressing metastatic breast cancer patients (Franklin et al., 2004). Therefore, it still needs to develop another anti-HER2 antibody with superior efficacy in monotherapy.

CHAPTER 3

HER2 Antibody Improvements using CDR Random Mutagenesis, Phage Display and *in vitro* Screening

3.1 Introduction

HER2 is a member of the ErbB/HER (Human epidermal growth factor receptor) family which consists of EGFR, HER2, HER3 and HER4. HER2 has been implicated important roles in growth, differentiation and survival in cancer cells as well as in normal cells (Whenham et al., 2008). In contrast to other HER family members, HER2 does not require ligands for the receptor-receptor interactions (Nicolas et al., 2008). In cancer cells the HER2 protein can be expressed up to 100 times more than in normal cells (2 million versus 20,000 per cell, respectively) (Shepard et al., 1991). Such overexpression or amplification of HER2 promotes the formation of receptor homo- and heterodimers with other HER family members, leading to uncontrolled cell proliferation and tumor growth (Mayumi et al., 2006; Ono and Kuwano, 2006).

HER2 is a member of the ErbB/HER (human epidermal growth factor receptor) family which consists of EGFR, HER2, HER3 and HER4. HER2 has been implicated important roles in growth, differentiation and survival in cancer cells as well as in normal cells (Whenham et al., 2008).

Therefore, HER2 has been investigated as a promising therapeutic target for cancer. Particularly, targeted-therapy using anti-HER2 monoclonal antibodies such as Herceptin (Trastuzumab, hu4D5: binding to domain IV), Kadcyla (Trastuzumab-maytensinoid:

antibody-drug conjugate) and Perjeta (Pertuzumab: binding to domain II) has been used to treat HER2 positive cancers.

Herceptin (trastuzumab) launched by Genentech in October 1998 is a humanized version of murine monoclonal antibody, hu4D5. It binds extracellular domain (ECD) IV of HER2 receptor, subsequently inhibits its downstream PI3K-Akt signaling (Hudziak et al., 1989; Yakes et al., 2002; Sliwkowski et al., 1999) and induces cell cycle arrest via induction of cyclin-dependent kinase inhibitor p27/kip1 and apoptosis (Carter et al., 1992) in metastatic HER2 positive breast and gastric cancer cells, which in turn inhibits HER2-meidated tumor growth.

A combination of Herceptin with chemotherapy has shown significant improvements in cancer treatment. Disease-free survivals at 3 years were 75.4% and 87.1% with chemotherapy alone and in combination with Herceptin, respectively, in patients with HER2-overexpressing metastatic breast cancer (Romond et al., 2005). However, despite its proven clinical benefit, most patients who have an initial response to Herceptin develop resistance within one year of treatment initiation.

Accordingly, it is required to develop another anti-HER2 antibody having improved affinity, efficacy or the like. For this purpose, various approaches are as follows: screening a novel anti-HER2 antibody with unknown epitope, random mutagenesis strategies of Herceptin (hu4D5) variable region or Fc-engineering technologies

enhancing antibody effector function (e.g., antibody dependent cell–mediated cytotoxicity, ADCC) by increasing its binding to FcγIII on effector cells such as macrophages.

Among these approaches, for this purpose a popular strategy to improve the binding affinity and efficacy of the antibody is mutagenesis, and particularly, substitution of the residues at some positions of CDR-H and CDR-L would be considered. Based on this way, it is previously reported that substitution of residues in the CDRs of hu4D5 influences antibody affinity (Gerstner et al., 2002).

In the previous report, they constructed phage-displayed Fab libraries targeting 19 positions of hu4D5 including R50(V_H), W95(V_H), Y100a(V_H) and H91(V_L) known to be important to bind with HER2 molecule (Kelley et al., 1993) (Fig. 3-1). The libraries were divided into five groups by 5~7 residues, respectively. The binding affinity of a single mutant D98(V_H)W (K_D 0.11 nM) was increased by 3-fold compared to the parent antibody hu4D5, but the anti-cancer activity of the variant was not reported. They also suggested that further improvement in binding affinity might be found using alternative methods of binding selection or targeting more plastic or variable positions (Gerstner et al., 2002). However, there were no reports of success in screening variants superior to D98(V_H)W in binding affinity and functional activity such as anti-cancer activity until now.

The aim of this study was to investigate whether further modifications of the antibody that has been already affinity-maturated could improve its binding affinity and subsequent efficacy and to establish of antibody optimization technology for antibody improvement strategy, using hu4D5 as a model system.

Therefore, firstly, the CDR regions of Herceptin that already has high binding affinity to specific antigen HER2 were first changed by random mutagenesis, and the following screen was planned to select the variants with improved anti-cancer activity and binding affinity. In addition, since there was a possibility to increase those activities by mutating the framework part (or region) instead CDR regions (Ding et al., 2010; Kobayashi et al., 2010), it was planned to select new improved HER2-targeting therapeutic antibodies through error-prone random mutagenesis of the entire variable region from the selected variants and the well-established phage display technology.

Secondly, *in vitro* functional anti-tumor activity, binding affinity, target cross-reactivity (specificity), mechanism of signaling inhibition and *in vivo* anti-tumor activity of variants were evaluated, and, it was also speculated how to attribute the modification of hu4D5 to improvement in binding affinity using molecular modeling analysis. (Refer to Chapter 4.)

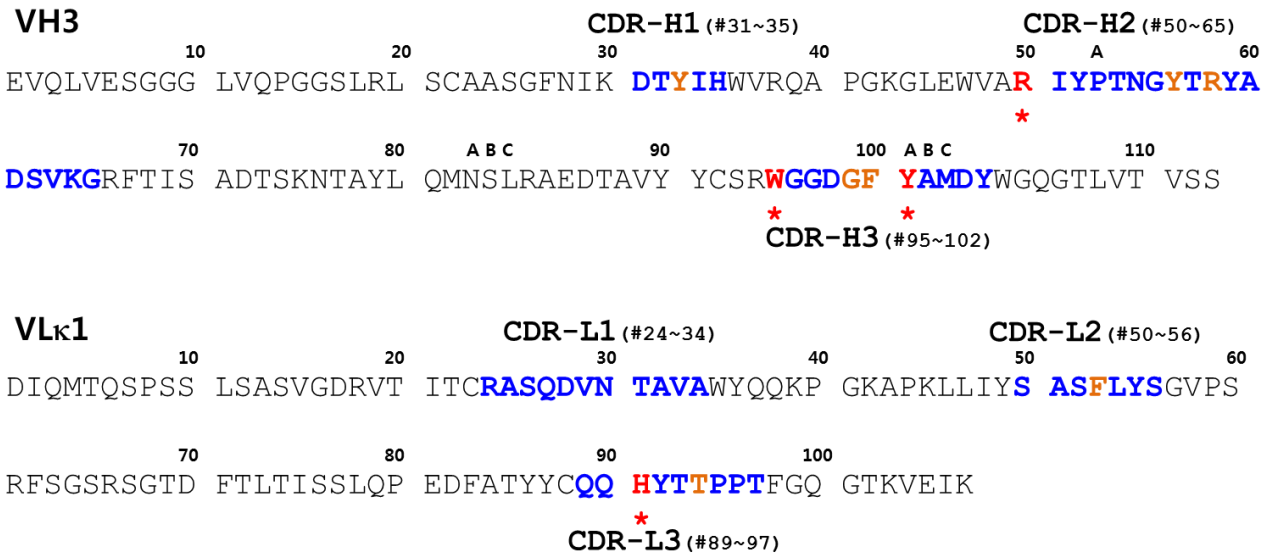

Fig. 3-1. Variable sequence of hu4D5 (Herceptin).

* Key residues: V_H R50, V_H W95, V_H Y100a, V_L H91 (Kelley et al., 1993; Gerstner et al., 2002)

CDR, complementarity-determining region; FR, framework

3.2 Materials and methods

3.2.1 Construction of scFv libraries

Phage-displayed scFv (a single chain variable fragment) libraries were constructed using a phagemid vector pCMTG (Oh et al., 2007) encoding the scFv-pIII fusion protein. The structure of the vector is schematically shown in Fig. 3-2A. The scFv comprising a light variable chain, a linker and a heavy variable chain in order was placed under the control of the lac promoter inducible by IPTG. The linker sequence is GGGGSGGGSGGSS.

A "stop template" version of the scFv display vector which was generated using stop codon TGA by overlapping PCR and was confirmed by sequencing was used as a PCR template to generate libraries to inhibit re-emerging and enrichment during screening process.

Libraries LN01 and LN02 randomized at four positions of the CDR-H3 (# 96, 97, 98 and 100) and at six positions of the CDR-H3 (# 98, 100, 100b, 100c, 101 and 102), respectively, were generated by degenerate PCR. The Phage-displayed LN01 and LN02 libraries were mixed and panning procedure was carried out. To generate library LN03 randomized at seven positions of CDR-L3, two sublibraries randomizing four positions on each (#89, 90, 92, 93 and #93, 95, 96, 97) were generated using degenerate PCR and

combined, and then panning procedure was carried out.

After sequence identification of isolated scFv through the panning process, heavy chain and light chain were constructed using dual vector system (pOptiVEC & pcDNA3.3, Invitrogen, USA) and transiently expressed in CHO-S cells as a full IgG1. After purification, functional anti-tumor activity of the antibody variants was evaluated in breast cancer cells, SK-BR-3 to select optimal heavy chains and light chains. The heavy chain variant selected from the LN01 or LN02 and light chain variant selected from the LN03 were cloned in dual expression vector system and transiently expressed in CHO-S cells as a full IgG1, resulting in "Combination Series C01" and "Combination Series C02", respectively. The purified combinatorial antibodies were evaluated based on anti-proliferative activities against SK-BR-3 cells.

The library LN04 was randomized at six position of the CDR-L2 (#50, 51, 52, 54, 55, 56) using the selected variants from "Combination Series" C01 and C02 as a template and were screened as described above. The LN05 library was constructed by error-prone PCR method for random mutagenesis of entire variable regions.

Degenerate PCR was performed using a Bio-Rad C1000 thermal cycler according to manufacturer's instructions (Ex Taq, Takara,

Japan). PCR condition was as follows: denaturation, 95°C for 20 sec; annealing, 57°C for 30 sec; extension, 72°C for 45 sec; 27 cycles. Error-prone PCR was conducted using 100 ng of template DNA with GeneMorpII Random mutagenesis kit (Stratagene, USA) under the 32-cycle condition of denaturing for 20 sec at 95°C, annealing for 30 sec at 57°C, and extension for 45 sec at 72°C. PCR scheme and primer sets used in this study are shown in Fig. 3-2 and Table 3-1, respectively.

Each PCR product was retrieved using Gel and PCR Clean-up system (Promega, USA), and then cleaved with a restriction endonuclease. Similarly, the pCMTG vector was also cleaved with the same restriction endonuclease and treated with shrimp alkaline phosphatase (USB, 70092Z). Then, the fragments were ligated overnight at 16°C using DNA ligation system (Promega, M8225).

The phagemid DNA libraries were introduced into *E. coli* XL1-blue-MRF' (Stratagene, USA) by electroporation (Sidhu et al., 2000), and the transformants were infected with 20 MOI (multiplicity of infection) and cultured overnight under the presence of Ex12 helper phages (Back et al., 2002) to encapsulate phagemid DNA, thereby generating phage particles displaying scFv fragments on its surface.

In summary, constructed libraries and candidate screening scheme in this study is shown in Fig. 3-3.

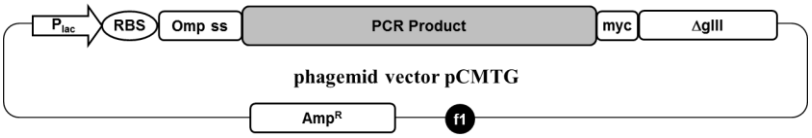
P lac
RBS
Omp ss
PCR Product
myc
ΔgIII
phagemid vector pCMTG
Amp R
f1

(A)

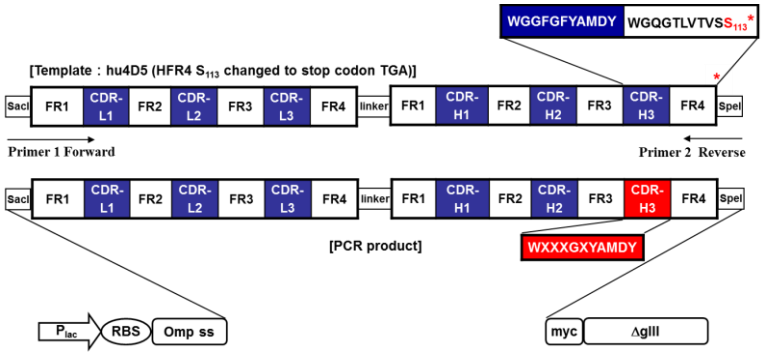
WGGFGFYAMDY
WGQGTLVTVSS 113 *
[Template : hu4D5 (HFR4 S 113 changed to stop codon TGA)]
SacI
FR1
CDR-L1
FR2
CDR-L2
FR3
CDR-L3
FR4
linker
CDR-H1
CDR-H2
CDR-H3
SpeI
Primer 1 Forward
Primer 2 Reverse
[PCR product]
WXXXGXYAMDY
P lac
RBS
Omp ss
myc
ΔgIII

(B)

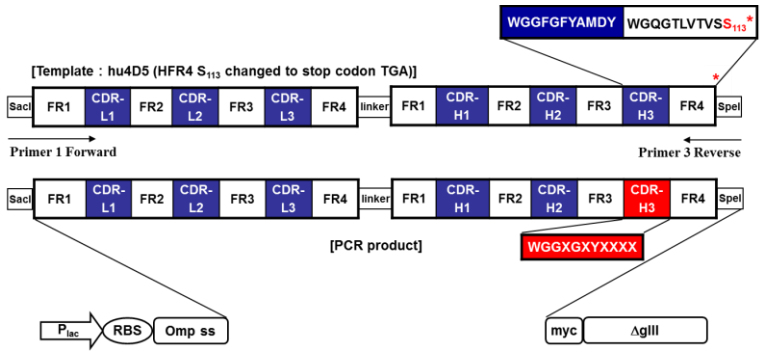
WGGFGFYAMDY
WGQGTLVTVSS 113 *
[Template : hu4D5 (HFR4 S 113 changed to stop codon TGA)]
SacI
FR1
CDR-L1
FR2
CDR-L2
FR3
CDR-L3
FR4
linker
CDR-H1
CDR-H2
CDR-H3
SpeI
Primer 1 Forward
Primer 3 Reverse
[PCR product]
WGGXGXYXXXX
P lac
RBS
Omp ss
myc
ΔgIII

(C)

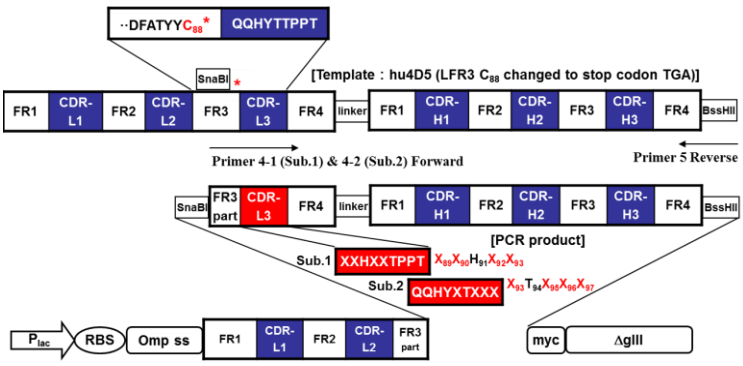
··DFATYY C 88 *
QQHYTTPPT
SnaBI
[Template : hu4D5 (LFR3 C 88 changed to stop codon TGA)]
FR1
CDR-L1
FR2
CDR-L2
FR3
CDR-L3
FR4
linker
CDR-H1
CDR-H2
CDR-H3
BssHII
Primer 4-1 (Sub.1) & 4-2 (Sub.2) Forward
Primer 5 Reverse
FR3 part
[PCR product]
Sub.1
XXHXXTPPT
X 89 X 90 H 91 X 92 X 93
Sub.2
QQHYXTXXX
X 93 T 94 X 95 X 96 X 97
P lac
RBS
Omp ss
myc
ΔgIII

(D)

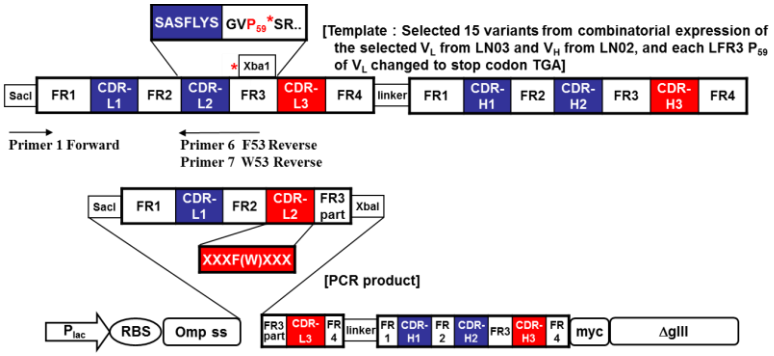

(E)

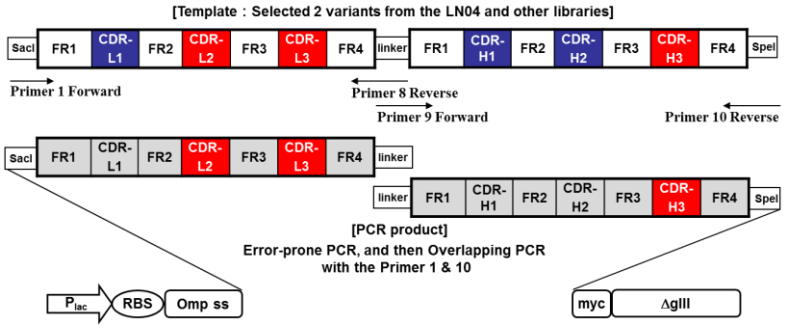

(F)

Fig. 3-2. Library construction map.

(A) Overall phagemid vector pCMTG (B) LN01

(C) LN02 (D) LN03 (E) LN04 (F) LN05

Table 3-1. PCR primer sequences used for the library construction.

No. of Library	PCR templates	PCR purpose & methods	No. of primer and direction	Primer Sequences
LN01	hu4D5 (HFR4 S_{113} changed to stop codon TGA)	Randomizing 4 positions of CDR-H3 (96,97,98,100) Random Degenerate	1. Forward	AATTgagctcGATATCCAGATGACCCAGAG
			2. Reverse	AATTACTAGTGCTACTCACGGTCACCAGAGTTC CCTGTCCCCAgtaatccatggcgtaMNNgccMNNMNN MNNCCATCTAGAGCAGTAGTAC
LN02		Randomizing 6 positions of CDR-H3 (98, 100, 100b, 100c, 101, 102) Random Degenerate	1. Forward	AATTgagctcGATATCCAGATGACCCAGAG
			3. Reverse	AATTACTAGTGCTACTCACGGTCACCAGAGTTC CCTGTCCCCAMNNMNNMNNMNNgtaMNNgcc MNNaccgccccatctagag
LN03	hu4D5 (LFR3 C_{88} changed to stop codon TGA)	Two sub-libraries : each randomizing 4 positions of CDR-L3 (89,90,92,93 and 93, 95, 96, 97) Random Degenerate	4-1. Forward	GACTTCGCTACGTACTACTGCNNKNNKcacNNK NNKactcctccgacaTTCGGACAAGGCAC
			4-2. Forward	GACTTCGCTACGTACTACTGCcaacagcactacNNK actNNKNNKNNKTTCGGACAAGGCAC
			5. Reverse	AATTGCGCGCtactcacggtc
LN04	Selected 15 variants from combinatorial expression of the selected V_L from LN03 and V_H from LN02 (LFR3 P_{59} changed to stop codon TGA)	Randomizing 6 positions of CDR-L2 (50, 51, 52, F53 or L53, 54, 55, 56) Random Degenerate	1. Forward	AATTgagctcGATATCCAGATGACCCAGAG
			6. Reverse (for F53)	tgaaTCTAGAtggcacaccMNNMNNMNNgaaMNN MNNMNNgtagatcagcagcttc
			7. Reverse (for W53)	tgaaTCTAGAtggcacaccMNNMNNMNNccaMNN MNNMNNgtagatcagcagcttc
LN05	Selected several number of variants from the LN04 and other libraries	Any positions of variable regions FR1-CDR1-FR2-CDR2-FR3-CDR3-FR4 Random Error-prone	1. Forward	AATTgagctcGATATCCAGATGACCCAGAG
			8. Reverse	GGAGCCTCCGCCACTACCTCCTCCTCCCTT GATCTCCACCTT
			9. Forward	GGTAGTGGCGGAGGCTCCGGTGGATCCAGC GAGGTCCAACTGGTC
			10. Reverse	AATTACTAGTGCTACTCACGGTCACCAGAG

* CDR, complementarity-determining region; FR, framework

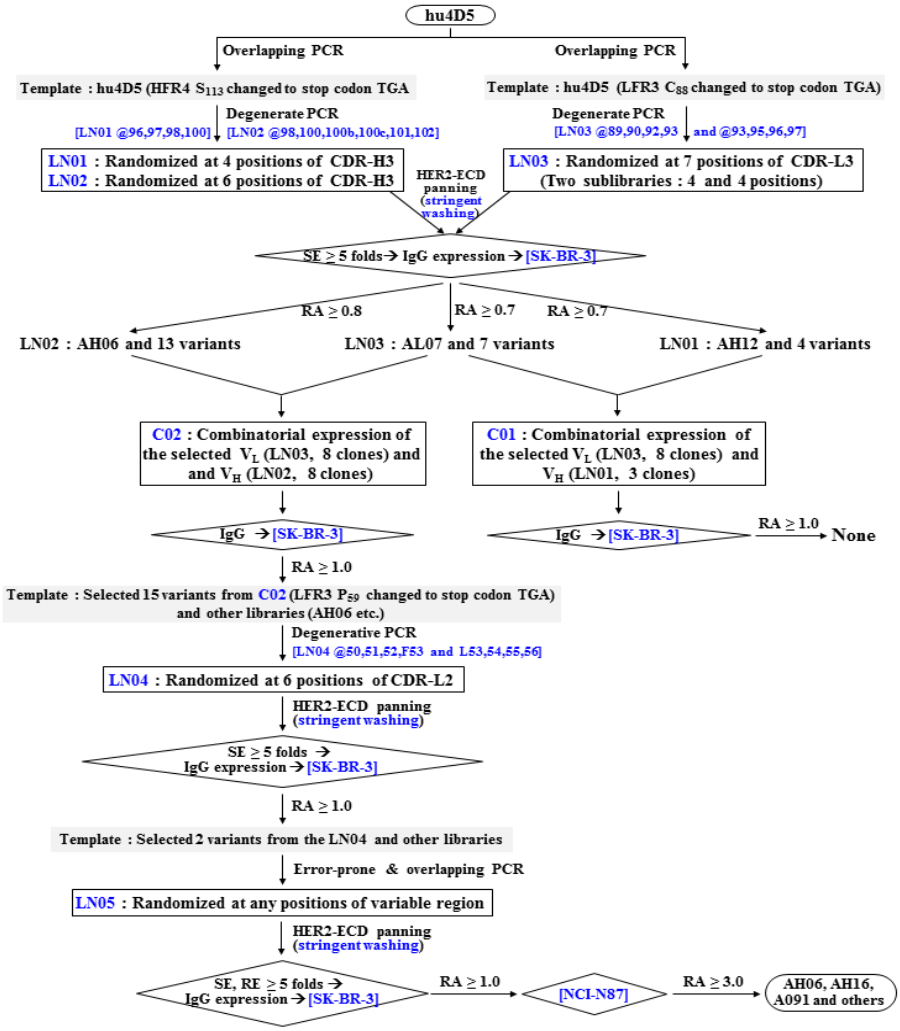

Fig. 3-3. Candidate screening flow scheme.

ELISA units and anti-proliferative activity against tumor cells were considered in selecting variants. The variants whose SE and RE values were 5 fold higher than those of negative blank were selected. And then further selection was preceded based on RA as indicated. SE, Screening ELISA unit of OD_{450}; RE, Relative ELISA unit of OD_{450}; RA (Relative activity), a ratio of IC_{50} of parent hu4D5 to the variant in anti-proliferative activity against breast tumor SK-BR-3 or gastric tumor NCI-N87 cells.

3.2.2 Selection of HER2-specific variants from scFv libraries

To screen out HER2-specific antibody from the libraries, Maxi-Sorp immunotubes (Nunc, 444202) were coated with human HER2-ECD (extracellular domain of *erb* B2 or p185HER2 fused with Fc, R&D systems, USA). After that, the libraries infected with Ex12 helper phage (IG therapy, Korea) were used at panning procedure as manufacturer's instruction. Maxi-Sorp immunotubes (Nunc, 444202) were coated overnight with 2 μg/ml of human HER2-ECD (extracellular domain of *erb* B2 or p185HER2 fused with Fc, R&D systems, USA) at 4°C, and blocked with 2% nonfat milk in TBS-T for 2 hours. Phages were cultured overnight and enriched, followed by resuspension of the enriched phage with 2% nonfat milk in TBS-T. The phage solutions were added to the coated immunotubes at a concentration of 10^{12} phage particles/ml, and incubated for 2 hours for binding with HER2-ECD.

In particular, the stringency of panning was controlled in washing step. That is, the plates were washed up to 20 times with TBS-T. After washing, 1.0~1.5 M ammonium thiocyanate was treated for 10 min., followed by washing with TBS-T. Then, bound phages were eluted with 0.1 M glycine (pH 2.2) for 10 minutes, and subsequently the eluted solution was neutralized with 1M Tris-HCl (pH 9.0). The eluent was propagated in *E. coli* TG1 cell (mid-log phase, OD_{600} 0.5).

3.2.3 Screening ELISA for screening of recombinant scFv

After three to five panning procedures, screening ELISA using soluble scFv-pIII fusion molecules prepared from *E. coli* clones was performed as described previously (Song et al., 2009). Screening ELISA was performed to isolate HER2-specific antibody variants. Individual clones were grown in a 96-well format in 200 μl of 2YT broth supplemented with 1 mM IPTG, and the culture supernatants were used in ELISA to detect phage-displayed scFv that bound to antigen-coated plates but not to IgG-coated plates.

To select HER2-specific antibody variants, ELISA was performed with human HER2-ECD or human IgG (Sigma) as coating antigens and anti-pⅢ antibody (MoBiTec, PSKAN3) as a detecting antibody. Consequently, clones expressing phage-displayed scFv that bound to antigen-coated plates but not to IgG-coated plates were selected. Maxi-Sorp 96-well microtiter plates were coated with 50 ng/50 μl/ml of recombinant HER2-ECD fused with Fc or human IgG. After overnight incubation at 4°C, the plates were washed three times with TBS-0.05% Tween 20 (TBS-T), and then blocked with 2% nonfat milk for 2 hours at 37˚C. The culture supernatants were treated for 2 hours, and then the plates were washed three times with TBS-T.

After washing with 200 μl of TBS-T at three times, the isolated antibody variants were added to Maxi-Sorp 96-well microtiter plates and then incubated with anti-pIII antibody (MoBiTec,

PSKAN3) for 1 hour, followed by incubation with the HRP-conjugated anti-mouse Fc specific antibody (Sigma, A0168) for 45 minutes. The plates were washed three times, TMB peroxidase substrate was added, and the absorbance was read at 450 nm using a microplate reader.

3.2.4 Relative ELISA for measurement or screening of relative scFv affinity by using ammonium thiocyanate elution

To assess relative binding of the soluble scFv fragment expressed in *E. coli*, ELISA was performed with thiocyanate solution (Johnsson et al., 1991). The procedure was similar to that described in Method 3.2.3., except the extra step treating the ammonium thiocyanate. In the next step of scFv incubation, 1 M ammonium thiocyanate buffer was treated for 15 min at room temperature, followed by washing step. The remaining steps were conducted in the same way as described in Method 3.2.3.

Phagemids extracted from the selected clones were analyzed by DNA sequencing, and then nucleotide sequences and amino acid sequences of CDR were identified through NCBI IgBLAST (http://www.ncbi.nlm.nih.gov/igblast/).

In summary, after antibody libraries constructed, the general screening scheme using phage display technology is shown in Fig. 3-4.

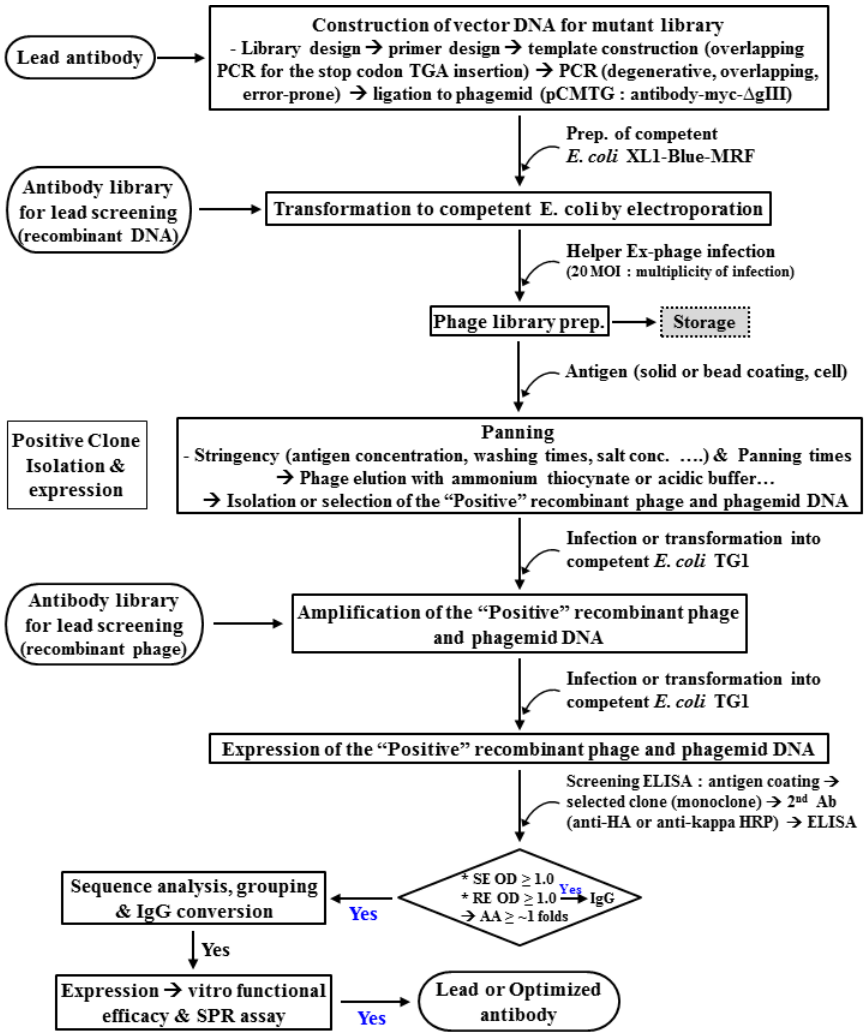

Fig. 3-4. Antibody screening flow scheme using phage display.

3.2.5 Cloning, transient expression and purification of the isolated variants

To access antitumor activity and binding affinity of the isolated variants, a mammalian expression vector system pOptiVEC (for heavy chain expression, Invitrogen, USA) and pcDNA3.3 (for light chain expression, Invitrogen, USA) were used to express the full-length IgG1 antibody. FreeStyle™ CHO-S cells (Invitrogen, USA) were transformed with the expression vector containing antibody gene according to manufacturer's protocol. Five days after the transfection, the culture media were harvested and the IgG form of antibody variant was purified using Mabselect (GE Healthcare, UK). Purified IgG1 form of the antibodies were expressed transiently in CHO-S cells, and then purified IgGs evaluated functional anti-tumor activity in breast cancer cells SK-BR-3 and finally in gastric cancer cells NCI-N87.

3.2.6 Anti-proliferative activity against tumor cell *in vitro*

Effects of the isolated antibody variants on cell proliferation were assessed using HER2-positive breast cancer cell line SK-BR-3 (HTB-30, ATCC ; McCoy's 5a media, Gibco BRL) and gastric cancer cell line NCI-N87 (CRL-5822, ATCC ; RPMI-1640, Gibco BRL). The cells were seeded at a concentration of 7.5 x 10^3 cells/well, cultured at

37°C with 5% CO_2 overnight, and treated with the serially diluted antibodies the next day. After 6 days of the treatment, viable cells were counted by WST-8 cell proliferation assay (Dojindo, Japan) as described previously (Wang et al., 2000). Twenty μl of the reconstituted WST-8 mixture was added into each well of the plate. After the cells were incubated at 37°C for 2 hours, the absorbance was measured at 450 nm in a microplate reader.

3.3 Results and Discussion

3.3.1 Construction of variants scFv libraries

Since the parent antibody hu4D5 had high affinity K_D value of 0.35 nM (Gerstner et al., 2002), it was difficult to select an antibody having improved affinity by general panning method. Thus, in order to increase the probability of the selection of high-affinity antibody, strategies and methods were used as follows.

It is concerned that tight-binding "contaminant (parent or template antibody, hu4D5)" scFv might be dominantly selected, since the parent antibody hu4D5 is a highly tight-binding antibody. Thus, the template for each library was a modified version of phagemid containing a stop codon (TGA) introduced at an upstream or downstream position where the amino acid was to be mutated by overlapping PCR method. A different position

introducing stop codon for each library is as follows: S113 position of HFR4 in CDR-H3 for the libraries LN01, and LN02, C88 position in CDR-L3 for the library LN03 (P59 position of LFR3 in CDR-L2 for the library LN04).

Thereafter, a random mutagenesis procedure was carried out as described in the following strategy. Mutagenic oligonucleotide primers (Table 3-1) with degenerate NNK codons at the positions to be diversified were used to simultaneously introduce CDR diversity and remove the stop codon, whereby an open reading frame that encoded a scFv library member fused to a homodimerizing c-myc and pIII was generated.

To maximize the probability of selecting variants having enhanced binding affinity and minimize the library size and number of construction, this study primarily excluded CDR-H1 and CDR-L1 consist of 5 and 10 residues, respectively. CDR2 and CDR3 thought to be important to binding and specificity with antigen were randomized intensively. However, the strategy for site-directed random mutagenesis of entire CDR residues including CDR-H3 (Kabat No. #95~102, 11 amino acid residues, $W_{95}G_{96}G_{97}D_{98}$ $G_{99}F_{100}$ Y_{100a} $A_{100b}M_{100c}D_{101}Y_{102}$), CDR-H2 (Kabat No. #50~65, 17 amino acid residues, $R_{50}I_{51}Y_{52}$ $P_{52a}T_{53}N_{54}$ $G_{55}Y_{56}T_{57}R_{58}Y_{59}A_{60}D_{61}$ $S_{62}V_{63}K_{64}G_{65}$), CDR-L3 (Kabat No. #89~97, 9 amino acid residues, $Q_{89}Q_{90}H_{91}Y_{92}$ $T_{93}T_{94}$ $P_{95}P_{96}T_{97}$), and CDR-L2 (Kabat No. #50~56, 7 amino acid residues, $S_{50}A_{51}S_{52}F_{53}$ $L_{54}Y_{55}S_{56}$) is practically impossible, since the

theoretical diversity of each library is 2 x 10^{14}, 6 x 10^{20}, 5 x 10^{11} and 1 x 10^{9} respectively, especially CDR-H2, which is too large to construct the libraries.

Therefore, CDR-H2 was excluded, and in order to design the library with a suitable size for efficient screening, CDR-H2 R50, CDR-L3 H91, CDR-H3 W95, CDR-H3 Y100a positions (Gerstner et al., 2002) previously reported as key residues to be most critical to antigen binding was excluded from randomization. W95 (59% or 82%), G99 (90% or 100%), Y100a (88% or 100%) in CDR-H3, T94 (45%) in CDR-L3 and F53 (67%) in CDR-L2 conserved with frequencies more than 45% after screening from random mutagenesis library was also excluded from randomization. Even though F100 in CDR-H3 was conserved with frequency 52% (Gerstner et al., 2002), F100 position thought to may have a role in antigen-antibody interface was designated as a target site for randomization library construction.

The F53 position in CDR-L2 was fixed F or W, because the position was conserved with F53 (67%) or W53 (55%) (Gerstner et al., 2002).

Since theoretical library size of CDR-H2 composed of 14 residues is 1.6 x 10^{18}, which is too large to construct the libraries, CDR-H2 was excluded from randomization library construction, except a key residue, R50 and relatively invariant residues, R50 (100%), Y56 (74%) and R58 (59%).

In conclusion, total 6 residues consisting of the key residues (CDR-L3 H91, CDR-H3 W95 and CDR-H3 Y100a) and relatively invariant residues (CDR-H3 G99, CDR-L2 F53, CDR3 T94) were excluded from randomization library construction. Libraries targeting CDR-H3, CDR-L3 and CDR-L2 except 6 residues described above were constructed using NNK codon (N=A, G, T or C; K=G or T) in several divided subgroups. According to mutagenesis strategy in a stepwise fashion, LN01, LN02 and LN03 libraries targeting CDR-H3 and CDR-L3 were constructed and actual diversity of each library was determined by counting the number of colonies, and were 9.7×10^7, 1.5×10^8 and 3.7×10^8, respectively (Table 3-2).

To verify that the randomized position of each library is appropriately changed by PCR, DNA sequences of the scFv region in the recombinant phagemid from $\geq$ 20 clones selected after PCR, ligation and transformation steps, were analyzed by sequencing analysis. In order to prevent parental contamination of libraries, it was determined prior to panning whether inserted stop codon was present and whether the library met the following criteria: $\leq$ 30% of the frame shift frequency and $\leq$ 10 % of duplicated sequences. PCR was carried out until the library met the above requirements.

At each step, variants selected by sequencing analysis of the approximately more than 100 clones obtained through panning were converted into the IgG format and expressed transiently in CHO-S cell. Finally, antitumor activity of the selected variants was

evaluated using cell growth inhibition assay.

Table 3-2. Randomized CDR positions and library diversity.

Library series	Theoretical diversity	Actual diversity	Randomized CDR positions		
			CDR-H3	CDR-L3	CDR-L2
LN01 (degenerate)	1.6×10^5	9.7×10^7	96, 97, 98, 100	-	-
LN02 (degenerate)	6.4×10^7	1.5×10^8	98, 100, 100b, 100c, 101, 102	-	-
LN03 (degenerate)	$2 \times 1.6 \times 10^5$	3.7×10^8	-	89, 90, 92, 93 and 93, 95, 96, 97	-
C01 [a] (combinatorial)	-	-	-		
C02 [b] (combinatorial)	-	-	-		
LN04 (degenerate)	$2 \times 6.4 \times 10^7$	1.3×10^8			50, 51, 52, F53 or L53*, 54, 55, 56
LN05 (error-prone)	-	2.4×10^8	FR1-CDR1-FR2-CDR2-FR3-CDR3-FR4		

a) Transient expression of antibodies from the combinatorial libraries LN01 (V_H) and LN03 (V_L) in CHO-S cells.

b) Transient expression of antibodies from the combinatorial libraries LN02 (V_H) and LN03 (V_L) in CHO-S cells.

* The original F53 (V_L) position of CDR-L2 was replaced to F (same as the original position) or W.

3.3.2 Selection of HER2-specific variants from scFv libraries

After making the libraries, screening process was performed using a series of panning with a HER2-ECD-Fc as an antigen to select variants with enhanced anticancer activity than hu4D5 in HER2-positive cancer cells (Fig. 3-3).

Therefore, high-stringency screening to select an antibody having higher affinity than the parent antibody hu4D5 was performed as follows. First, washing was carried out for up to 44 hours to select an antibody exhibiting enhanced off-rate (Chen et al., 1999). Second, pre-elution was performed with 0.1 M glycine (pH 2.2) before the final elution (Chen et al., 1999). Third, weakly bound antibodies were removed by treating ammonium thiocyanate before elution (Macdonald et al., 1988; Wang et al., 2000). The washing step was performed with 0.1 M glycine (pH2.2) and 1 M ammonium thiocyanate sequentially or in a different order during three to five rounds of panning. Fourth, the antibodies with high affinity were enriched during successive rounds of panning by decreasing the concentration of HER2 ECD-Fc, from 2.0 to 0.1 μg/ml.

In summary, it seemed that "tight binding variant antibodies" with high affinity were enriched by 4 methods during successive rounds of panning.

Since HER2 ECD-Fc was used as an antigen, non-specific antibody that binds to the Fc protein should be considered. Therefore, ratio

of the number of colonies from a negative antigen (human IgG or BSA) to that from HER2 ECD-Fc was determined, and if ratio of the number of colonies from a negative antigen (human IgG or BSA) was less than 1%, this study further proceeded with the screening. The enrichment factor is calculated from the input and output ratios. Enrichment factor is defined as: [output/input ratio of selection round N]/[output/input ratio of the first selection round].

Five, eighteen and ten kinds of antibody sequences were isolated in accordance with panning stringency from library LN01, LN02 and LN03 randomized at 4 residues and 6 residues of CDR-H3 and 7 residues of CDR-L3, respectively.

Because four variants from LN02 and one variant from LN03 were transiently expressed at extremely low levels in CHO-S cell, these four clones were not counted. The number of selected variants from CDR-H3 and CDR-L3 randomizing libraries was 5, 15 and 9, respectively (Table 3-3). These variants were expressed in CHO-S cells as an IgG format, and their proliferation inhibitory activity was assessed in SK-BR-3 cells.

Since the primary purpose of this study was to improve the biological activity of the antibody, the anti-proliferative activity ratio or folds of variants was calculated as IC_{50} of hu4D5 / IC_{50} of variant. IC_{50} of variants for anti-proliferative efficacy in SK-BR-3 cells was determined and compared with that of the parent hu4D5.

Table 3-3. Summary of library screening and list of isolated variants.

Library No.	Number and list of isolated variants	List of selected variants and ratio of anti-proliferative activity (IC_{50} : hu4D5/variants) against SK-BR-3 cell (in parentheses)
LN01 (Randomized at 4 positions of CDR-H3 from hu4D5)	5 AH01, AH11, AH12, AH18, AH19	AH01 (0.7), AH11 (0.7), AH12 (0.8) (Three variants whose ratio were more than 0.7 were used to the next step combinatorial expression experiment.)
LN02 (Randomized at 6 positions of CDR-H3 from hu4D5)	14 AH03, AH04, AH05, AH06, AH07, AH13, AH14, AH15, AH20, AH21, AH22, AH23, AH24, AH25	AH03 (1.0), AH04 (0.9), AH05 (1.1), **AH06 (1.3)**, AH07 (0.9), AH13 (0.9), AH20 (0.8), AH24 (0.8) (Eight variants whose ratio were more than 0.8 were used to the next step combinatorial expression experiment.)
LN03 (Randomized at 7 (4 and 4) positions of CDR-L3 from hu4D5 : Two sublibraries)	9 AL01, AL03, AL04, AL05, AL06, AL07, AL08, AL09, AL10	AL01 (0.7), AL04 (0.8), AL05 (0.8), AL06 (0.8), AL07 (0.9), AL08 (0.9), AL09 (0.8), AL10 (0.9) (Eight variants whose ratio were more than 0.7 were used to the next step combinatorial expression experiment.)
C01 (Combinatorial expression of the isolated V_H from LN01 and V_L from LN03)	23 (V_H 3 species x V_L 8 species = 24 combinations)	0 (None variants whose ratio were more than 1.0 were selected to be used as a template for Library LN04 preparation.)
C02 (Combinatorial expression of the isolated V_H from LN02 and V_L from LN03)	58 (V_H 8 species x V_L 8 species = 64 combinations)	A010 (1.0), A034 (1.0), A012 (1.0), A021 (1.0), A024 (1.0), A055 (1.0), A014 (1.0), A015 (1.0), A016 (1.0), A058 (1.1), A039 (1.0), A031 (1.0), A032 (1.1), A065 (1.0), A066 (1.0) (Fifteen variants whose ratio were more than 1.0 were selected to be used as a template for Library LN04 preparation.)
LN04 (Randomized at 6 positions of CDR-L2 of the selected 17 variants from the C02)	3 A083, A084, A085	A083 (1.0), A085 (1.0) (Two variants whose ratio were more than 1.0 were selected to be used as a template for Library LN05 preparation.)
LN05 (Randomized at any positions of variable region of selected 2 variants from the LN05 and others (AH06, AH16, 4D5 etc.))	25	**A091 (1.1)**, A094 (1.0), A099 (1.0), A100 (1.0), A101 (1.0), A103 (1.0), A107 (1.0) (7 variants)
Direct engraftment of changed residues of CDR-H3 from the Library LN01 and LN02	2 AH16, AH17	AH16 (1.1), AH17 (1.0)
Total	139	45

It was planned to select the variants as a candidate of biobetter antibody selected based on the anti-proliferative activity ratio in the SK-BR-3 cells (IC_{50} of hu4D5 / IC_{50} of the variant) of 1 or more (Fig. 3-3).

All 5, 9 and 13 variants isolated from each LN01, NL02 and NL03 did not meet the criteria, respectively, but only one AH06 isolated from the LN02 was the best, and the ratio of anti-proliferative activity was about 1.3 for SK-BR-3 cells (Table 3-3, Fig. 3-5).

Since the variants isolated from LN01 or LN02, and LN03 have changed only in each CDR-H3 or L3, a new and additional "combinatorial variants" can be made from shuffling of the variants changed V_L from LN03 and the variants changed V_H from LN01 or LN02.

Therefore, in order to confirm the possibility of the anti-cancer effect of the "combinatorial variants" is increased, this study selected 3, 8, and 8 variants met the criteria of activity ratio were more than 0.7, 0.8 and 0.7 from LN01, LN02, and LN03, respectively.

And two series of the "combinatorial expressions of heavy and light chain variants", C01 (CDR-H3 variants from LN01 and CDR-L3 variants from LN03) and C02 (CDR-H3 variants from LN02 and CDR-L3 variants from LN03) were generated by transient expression in CHO-S cells.

In case of LN02 randomized at six positions (98, 100, 100b, 100c, 101, 102) in CDR-H3, three variants meeting the criteria, anti-proliferative activity ratio 1.0 or more, including AH06, were selected. For the heavy chain and light chain shuffling or combination, "Combinatorial Expression Series" C02 step was implemented in combination with the selected variants from CDR-L3 randomizing library, in a similar manner.

All variants selected from LN03 targeting seven positions (89, 90, 92, 93, 95, 96, 97), dividing into two sublibraries, four residues on each (89, 90, 92, 93 and 93, 95, 96, 97) in CDR-L3 did not meet the criteria, but "Combinatorial Expression Series" C01 and C02 step was implemented using eight variants whose anti-proliferative activity ratio was more than 0.7 in combination with the selected variants from CDR-H3 randomizing library.

In order to check the possibility of the anti-cancer effect is improved through combination between the selected variants from CDR-H3 and CDR-L3 randomizing libraries, pOptiVEC (for heavy chain expression) and pcDNA3.3 (for light chain expression) vectors were constructed and expressed in CHO-S cell in combination to produce as IgG1 format combined with heavy and light chains.

In the Series C01, total 24 variants by the combination of three CDR-H3 variants from LN01 and 8 CDR-L3 variants from LN03 were expressed transiently in CHO-S cells. Twenty three variants were purified and their anti-proliferative activity against SK-BR-3 cells was assessed. However, there was no variants having the activity ratio of 1.0 or more (Fig. 3-5).

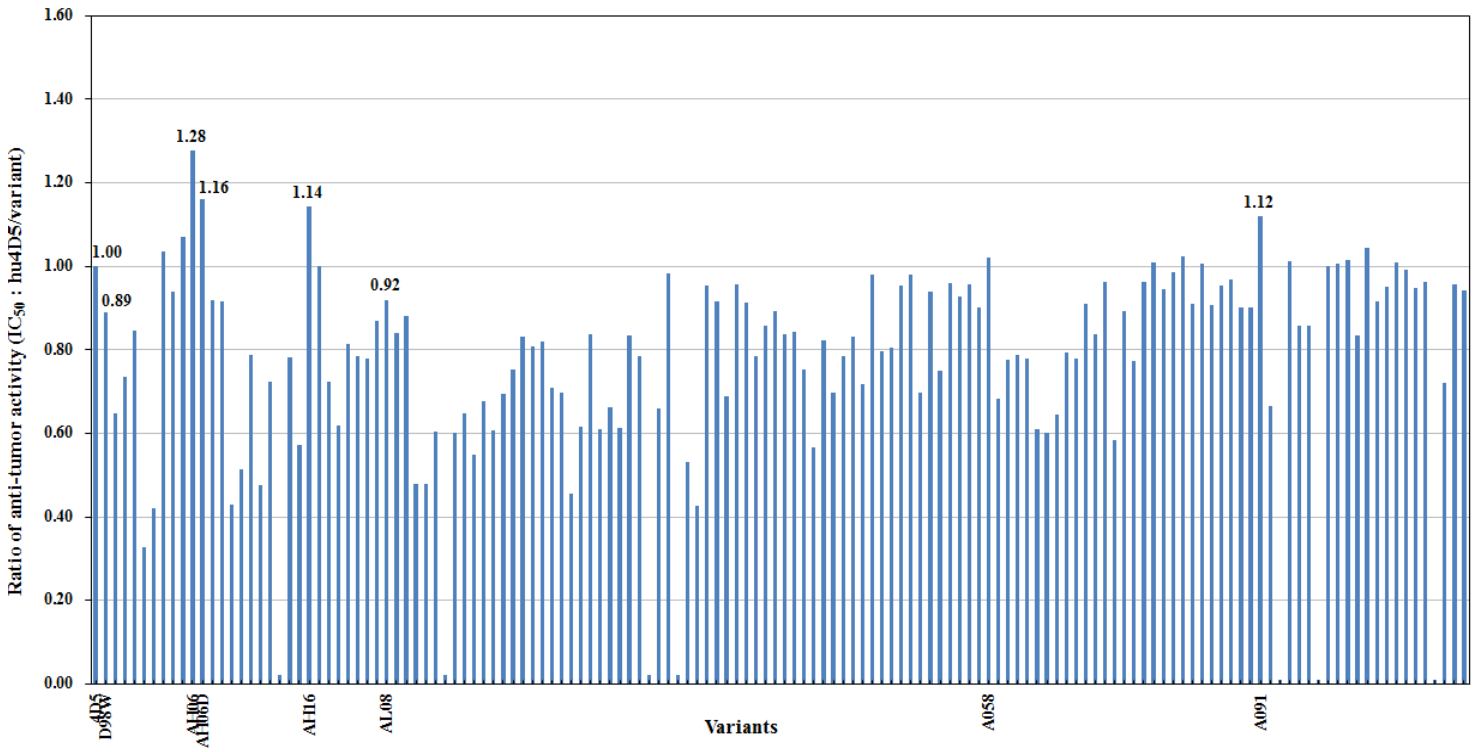

Fig. 3-5. Results of antibody libraries screening. Ratio of IC_{50} for *in vitro* anti-tumor efficacy in SK-BR-3 breast cancer cells (variant/hu4D5). The modified variant, AH06D, with substitution at D98 was artificially derived from the parental variant AH06 to evaluate the effect of position 98 in CDR-H3.

In C02, total 64 variants by the combination of eight CDR-H3 variants from LN02 and eight CDR-L3 variants from LN03 were expressed transiently in CHO-S cell. As a result of measuring the anti-proliferative activity of 58 kinds of IgG selected from C02 against SK-BR-3 cells, there were 15 variants having the activity ratio of 1.0 or more. Unfortunately, there was no variants having significantly enhanced anti-cancer activity than AH06 derived from LN02 (Fig. 3-5).

To examine the effect of randomization of CDR-L2, LN04 randomized at 6 positions (#50, 51, 52, F53 or L53, 54, 55, 56) of CDR-L2 was constructed using 15 variants selected from C02 as PCR templates. Two variants with the anti-proliferative activity ratio of 1.0 or more were obtained, but there was no variants having significantly enhanced anti-cancer activity than AH06 (Fig. 3-5).

Unlike LN01~LN04 series randomizing CDR-H3, L3 and L2 and screened for anticancer activity, LN05 targeting entire variable regions was constructed by error-prone PCR method using two variants (such as A083 and A085) selected from LN04, as PCR templates. As a result of cell proliferation inhibition assay in SK-BR-3 cells, there were 7 variants having activity ratio of 1.0 or more. Among them, A091 was shown to have relatively enhanced activity (Fig. 3-5).

In summary, 153 variants were obtained by the stringent panning procedure from the randomized libraries. After conversion into IgG1 format, the selected variants were expressed transiently in CHO-S cell and purified by Protein A affinity chromatograpy to produce antibody variants. The total 139 variants were well expressed as IgG form with structural stability, variants were selected based on the anti-proliferative activity ratio in the SK-BR-3 cells (IC_{50} of hu4D5 / IC_{50} of variant). Biological activity of the selected variants was preferentially measured in well-known breast cancer cell line SK-BR-3 since the final goal was to obtain improved antibodies in not only binding affinity but also biological activity (Table 3-3, Fig. 3-5).

And several variants such as AH06 selected in the screening variants whose ratio were more than 1.1 were further tested for anti-cancer activity against HER2-positive gastric cancer cell NCI-N87 and binding affinity using BIAcore™. Anticancer activity of the selected variants including AH06, AH16 and A091 were measured in another important HER2-positive gastric cancer cells, NCI-N87. Besides, binding affinity for HER2-ECD was precisely measured using BIAcore™ to see whether the binding was improved to some extent. (Refer to Chapter 4.).

3.3.3 Inhibitory effects of the variants on cell proliferation

Anti-proliferative effect of antibody variants from constructed library was examined against breast cancer SK-BR-3 cells. Most effective variants including AH06, AH16, A091 were finally selected (Table 3-4). The anti-proliferative effect of the selected variants was also assessed in another HER2 over-expressed gastric cancer NCI-N87 cells (Fig. 3-6). The efficacy *in vitro* of AH16 having approximately 2-fold higher binding affinity compared to hu4D5, which is similar to D98W, was similar to that of hu4D5. Also, other variants, AL07, AH12 and A082 showed the anti-proliferative activity similar to hu4D5 (data not shown).

The cell growth inhibitory activity against NCI-N87 of AH06 (IC_{50} 0.12 μg/ml = 0.81 nM) was increased 7.22 times compared to the parental antibody hu4D5 (IC_{50} 0.88 μg/ml = 5.88 nM) (Fig. 3-6). On the other hand, hu4D5 D98W was increased 4.3-fold in the K_D value against HER2, but anti-proliferative effect against SK-BR-3 and NCI-N87 was low compared to the parental hu4D5 (Table 3-4 and Fig. 3-6). Interestingly, although binding affinity of A091 was decreased 2-fold, anti-proliferative effect against NCI-N87 was improved 2.95-fold (IC_{50} 0.33 μg/ml = 1.99nM). These results show the functional biological activity of the antibody is not necessarily proportional to antigen-binding affinity.

Therefore, additional biological activity (or efficacy), such as binding affinity, cross-reactivity, specificity, signaling inhibitory

Table 3-4. Deduced sequences, anti-cancer activity and binding kinetics of representative variants (as IgG format) from each libraries at 25°C. Residues were numbered according to Kabat and colleagues.

Library	Variants	CDR-L2 (#50~56)	CDR-L3 (#89~97)	CDR-H3 (#95~102)	Other mutations	Relative anti-tumor activity : ratio of IC_{50} (hu4D5 / variant)		k_{on} ($10^5 M^{-1}s^{-1}$)	k_{off} ($10^{-4}s^{-1}$)	K_D (nM)	Relative affinity : ratio of K_D (hu4D5 / (variant)
						SK-BR-3	NCI-N87				
-	hu4D5	SASFLYS	QQHYTTPPT	WGGDGFYAMDY		1.0 (0.9~4.5nM)	1.0 (5.88nM)	2.4	1.2	0.48	1.0
-	D98W	--------	---------	---W-------	-	0.89	0.48	4.9	0.6	0.11	4.3
LN01	AH12	-------	---------	-H-V-M-----	-	0.84	ND	2.5	2.8	1.12	0.4
LN02	AH06	-------	---------	---W----FAL	-	1.28	7.22	7.7	0.5	0.06	7.4
*	modified AH06 D (W98D)	-------	---------	---------FAL	-	1.16	5.96	3.0	0.5	0.15	3.1
**	AH16	-------	---------	-NAK---SFVH	-	1.14	1.67	5.1	0.7	0.15	3.2
LN03	AL07	-------	----I-NI-	----------	-	0.87	ND	2.3	1.8	0.79	0.6
C02	A058	-------	----Q--AS	---W----FAL	-	1.02	2.79	2.2	2.3	1.05	0.5
LN05	A091	TTTWP--	--Y-N--V-	---W----FAL	V_L T73S, V_H P41R	1.12	2.95	6.5	7.1	1.10	0.5

* To evaluate effect of position 98 in CDR-H3, W98 in CDR-H3 of AH06 was substituted with D98. ** Direct engraftment of changed residues of CDR-H3 from the Libraries, LN01 and LN02. CDR, complementarity-determining region; FR, framework; dashes indicate sequence identical to that of hu4D5. Values for k_{on} and k_{off} are measured at 25°C by SPR on BIAcore. The relative affinity, reported as K_D (parent)/K_D (variant) indicates the fold increase in binding affinity versus the parental antibody hu4D5. ND : not-determined. Breast cancer cells (variant/hu4D5). The modified variant, AH06D, with substitution at D98 was artificially derived from the parental variant AH06 to evaluate the effect of position 98 in CDR-H3.

activity of AH06 showing increased anti-proliferative activity were investigated further. And also, the *in vivo* xenograft anti-cancer activity of AH16 and A091 which isolated earlier than AH06 was tested. (Refer to Chapter 4.)

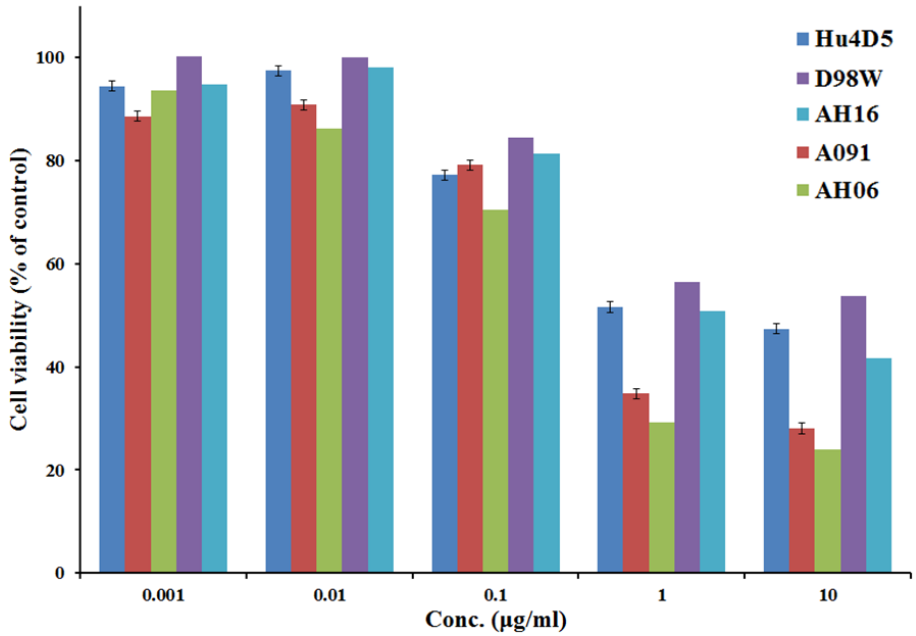

Fig. 3-6. Inhibitory effects of hu4D5 variants on NCI-N87 cell proliferation. The cells were treated with the indicated concentrations of variants for 6 days. Cell viability is expressed as a percentage relative to untreated control. Data represents the average SD of triplicate determinations. The cell growth inhibitory activity against NCI-N87 of AH06 (IC_{50} 0.12 μg/ml = 0.81 nM) was increased 7.22 times compared to the parental antibody hu4D5.

3.3.4 Influence of substituted residues on biological activity

The variant AH06 was derived from the library LN02, and has an unchanged light chain and a substituted heavy chain with the changes in D98W, M100cF, D101A, Y102L of CDR-H3 (Table 3-4). AH06 also showed substantially enhanced binding affinity. K_D value of AH06 was about 7.4-fold and 2.4-fold higher compared to those of the parent hu4D5 and D98W, the previously reported variant, respectively (Gerstner et al., 2002) And the variant AH06 had 7.2–fold enhanced anti-proliferative activity in comparison to hu4D5 (Table 3-4, Fig. 3-6). Even though A091 showed a strong growth inhibitory activity of about 3 times higher than hu4D5 in gastric cancer cell NCI-N87, binding affinity for HER2 was found rather decreased (Table 3-4). Thus, there was no direct correlation between the binding affinity and its biological activity in A091 variant.

The variant AH06 derived from the library LN02 has an unchanged light chain and a mutated heavy chain with the changes in D98W, M100cF, D101A, and Y102L of CDR-H3. The anti-proliferative activity ratio of C02, a combination of one heavy chain variant AH06 and eight light chain variants derived from the library LN03 randomizing CDR-L3 was all 1.0 or less , except for A058 (Table 3-3, Fig. 3-5). Therefore, a conclusion that the heavy chain with the changes in D98W, M100cF, D101A, and Y102L of CDR-H3 can form the optimal combination with the unmodified

light chain of hu4D5 was reached.

Since it was reported that D98W containing the substitution of Glu with Trp at position 98 in CDR-H3 has increased binding affinity constant (K_D) of about 3 times higher than hu4D5 (Gerstner et al., 2002), a modified version of AH06 (AH06 W98D), in which Trp was substituted with Glu at position 98, was constructed to evaluate whether the mutation has any impact.

The binding affinity of AH06 W98D was also 3.1 times higher compared to hu4D5 (Table 3-4), suggesting that the changed sequence of "F100c A101 L102" contributes to the improvement on its binding affinity of 3.1-fold for HER2-ECD molecule. The binding affinity of D98W was improved about 4.3-fold whereas AH06 showed a 7.4-fold higher binding affinity than hu4D5, which suggests W98 and the F100c A101 L102 sequence synergistically improve the binding affinity. (Refer to Molecular modeling analysis part of Chapter 4.)

3.3.5 Construction of variants scFv libraries

3.3.5.1 Strategic aspect

In order to increase the chance to find the variants having enhanced affinity than hu4D5, the differentiated strategy used for

library construction was randomization of M100c, D101 and Y102 positions considered as conserved in CDR-H3 rather than fixing. Resi B. Gerstner et al. (Gerstner et al., 2002) did not carry out the mutagenesis study out on this on all these positions, M100c, D101 and Y102. Besides, it was not reported whether the binding affinity is increased, decreased or unchanged by substitutions of several residues including these positions of hu4D5. Thus, these three positions were included in the random library construction.

Therefore, the libraries, LN01 and LN02 were constructed by randomizing eight positions of CDR-H3 such as G96, G97, D98, F100 and A100b. M100c, D101 and Y102 positions not attempted in the previous mutagenesis study were also included. The targeted positions were divided into LN01 and LN02 libraries with no more than six residues targeted in each. For CDR-L3, library LN03 was constructed by randomizing seven positions, except for a key residue, H91 and an invariant residue conserved with frequency 52%, T94 (Gerstner et al., 2002). In case of CDR-L2, library LN04 was constructed by randomizing six positions, except for F53 position. F53 or W53 was used at the 53 position. The screening process of each library was carried to the step-by-step (Fig. 3-3).

In summary, a series of processes for screening tighter binding variants having improved binding affinity compared to hu4D5 was performed as follows. Several libraries randomizing CDR-H3, CDR-L3 and CDR-L2 were constructed one by one. Among variants

obtained from each library by panning with HER2-ECD-Fc, some variants were selected using cell growth inhibition assay. Selected variant was used as a template required for library construction for the next step. By doing this, this study tried to Fig. out whether antitumor activity of the variants can be improved synergistically by combined changes in the two or more regions, not limited to any effect by that in the a certain region among CDR-H3, L3 and L2.

3.3.5.2 Analysis for appearance frequency of CDR residues

The variants selected by stringent panning with high selection pressure were analyzed to determine which residues were selected at randomized positions (Fig. 3-7).

3.3.5.2.1 Library LN01

Sequence pattern of five variants derived from LN01 randomized at four positions (#96, 97, 98 and 100), except for seven positions (#95, 99, 100a, 100b, 100c, 101, 102), corresponding to the first half of the CDR-H3 among 11 residues of CDR-H3 was analysed (Fig. 3-7 A). In consequence, parent-typeresidue was conserved with 60% frequency at both positions 97 and 100, whereas relatively diverse residues, different from the original residue were shown at

positions 96 and 98. Their anti-proliferative activity of 5 variants derived from LN01 was lower than parent hu4D5, indicating that randomization of four positions (#96, 97, 98 and 100) out of 11 residues of CDR-H3 is not effective for improvement of antitumor activity.

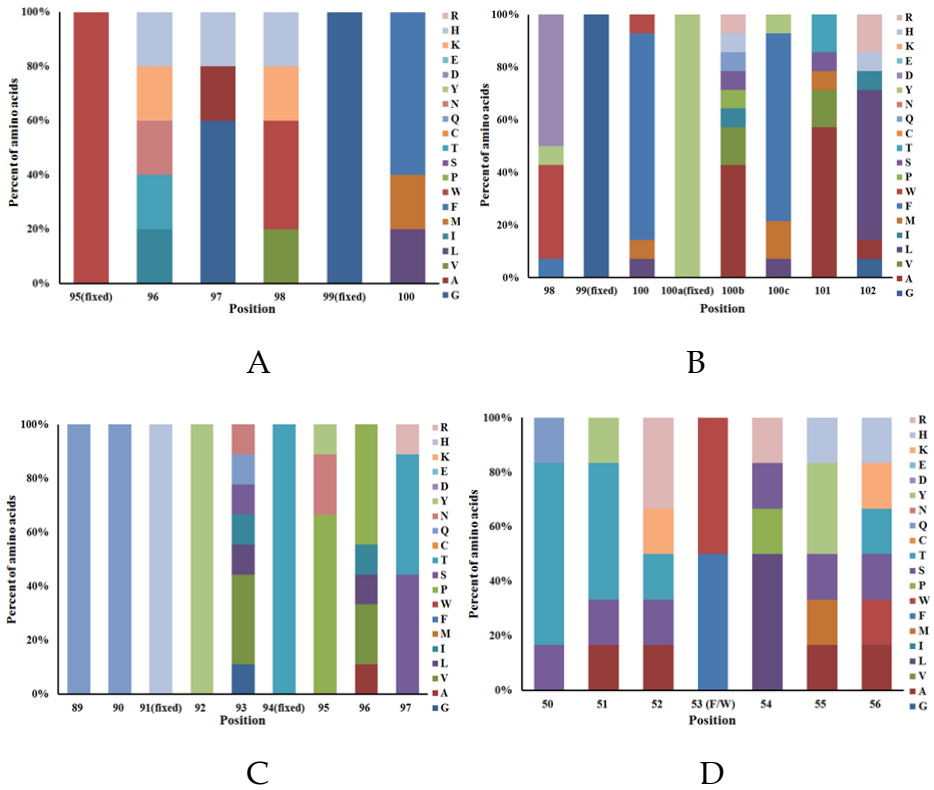

Fig. 3-7. Distribution of appeared amino acids at randomized positions of CDR. A. Library LN01 : 4 positions of CDR-H3, B. Library LN02 : 6 positions of CDR-H3, C. Library LN03 : 7 (4 and 4) positions of CDR-L3, D. Library LN04 : 6 positions of CDR-L2

3.3.5.2.2 Library LN02

Sequence pattern of five variants derived from LN02 randomized at seven positions (#95, 99, 100a, 100b, 100c, 101, 102), except for four positions (#96, 97, 98 and 100), corresponding to the second half of the CDR-H3 among 11 residues of CDR-H3 was analysed (Fig. 3-7 B). In consequence, parent-typeresidue were conserved with ≥ 40% frequency at #98, 100 and 100b position. At 98 position, the parent-type D occured in 50% of the selected clones and was replaced with W in 35.7% of selected clones.

Interestingly, at the neighboring #100c, 101 and 102 position, F, A and L occurred dominantly in selected clones. To conclude, the strategy for LN02 randomized at six residues was thought to be more successful than the strategy for LN01 randomized at four residues of 11 residues in CDR-H3 region since AH06 was derived from LN02.

The #98 and 100 positions were designated as random positions in both LN01 and LN02. Both libraries showed a similar amino acid residue and frequency at the #100 position, but not at the #98 position (Fig. 3-7 B). At the #98 position of LN01, variants were not survived under stringent panning procedure by the strategy to exclude four positions (#96, 97, 98 and 100) from randomization, corresponding to the second half of CDR-H3. At the #98 position of LN02, variants were not survived under stringent panning procedure by the strategy to exclude two positions (#96 and 97

position) from randomization, corresponding to the first half of CDR-H3.

It is difficult to explain the reside frequency observed at position 98 in LN01 and LN02. However, the interaction between fixed residues in the first half and the second half of CDR-H3 and the residue at position 98 could affect overall binding affinity, interaction between V_L and V_H, and stability of isolated variants. Therefore, it might be interpreted as the consequence by selection of variants survived under the stringent panning pressure.

In this study, the thermodynamic analysis of residue-residue interaction was attempted. Since it was practically impossible to analyze all of the isolated variants using computer modeling, AH06 having the best efficacy and its related variants were analyzed as a representative example. (Refer to Modeling part of Chapter 4.)

3.3.5.2.3 Library LN03

The sequence pattern of nine variants derived from LN03-1 and LN03-2 were analyzed (Fig. 3-7 C). The sub-library LN03-1 was randomized at four positions, #89, 90, 92 and 93, corresponding to the first half of the CDR-L3 and fixed at the #91 position known as a key residue and the positions #94, 95, 96 and 97 corresponding to the second half of the CDR-L3. The sub-library LN03-2 was randomized at four positions, #93, 95, 96 and 97, corresponding to

the second half of the CDR-L3 and fixed at the #91 position known as a key residue and the positions #89, 90, 92 and corresponding to the first half of the CDR-L3. All resulting residues at the #89, 90 and 92 positions in LN03-1 after randomization were identical to parental ones. How to explain the results?

It could be speculated that variants from the library LN03-1 randomized at the #89, 90, 92 and 93 positions, might not be survived under stringent panning procedure or/and under the strategy to fix four positions (#94, 95, 96 and 97 positions), corresponding to the second half of CDR-L3.

Sequencing analysis after library construction confirmed that the LN03-1 was practically randomized at the #89, 90, 92 and 93 position of CDR-L3 using degenerate PCR (data not shown). Therefore, it can be speculated that LN03-1 derived variants may be unable to be selected by high stringent panning, because the variant may have low binding affinity or strength not enough to tolerate the selection pressure without randomization in second half of the CDR-L3 (#94, 95, 96 and 97) although the first half of the CDR-L3 (#89, 90, 92 and 93) is changed.

Actually, AL04 was the sole variant thought to be derived from LN-03-1, which may be explained by that CDR-L3 sequence of AL04, "$Q_{89}Q_{90}H_{91}Y_{92}L_{93}T_{94}P_{95}P_{96}T_{97}$" results from the substitution only at the #93 position among randomized at four positions of LN03-1, T94, P95, P96 and T97.

Alternatively, AL04 could be interpreted as a variant derived from LN03-2 randomized at four positions, #93, 95, 96 and 97, corresponding to the second half of the CDR-L3 and fixed at four positions, #89, 90 and 92 corresponding to the first half of the CDR-L3. That is to say, AL04 substituted at the #93 position, but not at the #95, 96 and 97 positions was the only survivor under stringent panning procedure. However, it could not determine which of these two possibilities would be appropriate.

However, it is more than true that the variants randomized at the #89, 90 and 92 positions did not appear as if the positions had been designed to be fixed rather than randomized. Therefore, this indicates that randomization of the first half of the CDR-L3 is extremely limited in case of fixing the second half of the CDR-L3.

It can be speculated that the selection pattern by complicated interactions between the first half and second half of CDR-L3 might be caused by screening from the library LN03-1 fixing the 89, 90 and 92 positions, even though it was confirmed by sequencing to be sufficiently randomized at the positions. However, it was unable to confirm whether this speculation was appropriate, since this study could not actually get the basic quantitative data.

The screening pattern of variants unsubstituted in the 89, 90 and 92 positions despite the design as randomizing positions, like in a case of LN03-1, did not appear in the LN03-2. It could be

speculated that the variants randomized at the #93, 95, 96 and 97 positions are unaffected by residues at the #89, 90 and 93 positions and selected despite high selection pressure. Alternatively, it could mean that the first half "$Q_{89}Q_{90}H_{91}Y_{92}$" should need the second half "$T_{94}P_{95}P_{96}T_{97}$".

It also suggests that intact parental sequences of CDR-L3 are required for interactions between light and heavy chains or binding with antigen HER2. Alternatively, it suggests that the variants substituted in the second half of CDR-L3 could be selected only when the first half of CDR-L3 is intact.

Since the parental sequences were strongly conserved not only at a key residue position 91 but also 89, 90 and 92 positions, not conserved, corresponding to the first half of CDR-L3, these three positions as well as position 92 are likely to have important roles for binding with HER2 and/or stability of the antibody variant itself.

That is, it may be possible to infer that the four residues function as "one unit" and key residues, and have very important roles for binding and interaction of the antibody. If evidence supporting the hypothesis from quantitative analytical data and modeling analysis is provided, the four residues, #89, 90, 91 and 92 could be called "key regions", "key domain" or "key peptides"

There could be several possible interpretations about the

screening results with LN03, as above described. But the strategy randomizing the first half of CDR-L3, #89, 90, 91 and 92 positions, and the second half of CDR-L3, #93, 95, 96 and 97 positions was not efficient to original purpose for the improvement of antitumor activity, because the anti-proliferative activity ratio of selected 9 variants from LN03 was under 1.0 (≤ 1.0).

Because the isolated variants from LN03-1 appeared to unchanged despite randomization, it may be questionable whether there were problems with library construction methods, strategies and screening methods. As mentioned earlier, sequencing analysis for above 20 clones confirmed that there were no problems with library construction, therefore, it might be needed to double-check the strategies and screening methods. But, it was thought to be not a big problem as well, since we intended to further enhancement of antitumor activity and succeeded screening from LN02 library under stringent panning.

In case of CDR-L3 consisting of nine residues, the strategy randomizing six residues of the first half and six residues of the second half may be more efficient to select improved variants than the strategy randomizing four residues of the first half and four residues of the second half, used in this study.

The LN01 strategy randomizing four positions of the second half of the CDR-H3 consisting of 11 residues was not efficient to

improve antitumor activity, although the variants having diversely changed residues were selected from LN01. Variants showing more improved antitumor activity than AH06 variant derived from LN02 randomized at six positions were not isolated from LN01.

3.3.5.2.4 Library LN04

There were total 6 variants derived from LN04 library and sequenced in this study. Out of 6, 3 variants were expressed in CHO-S cells and their anticancer efficacy was evaluated (Table 3-3, Fig. 3-5). The other 3 variants, AL11, AL12 and AL16 were not expressed in CHO-S cells and should not be listed, however, they were counted as isolated variants in sequence analysis.

PCR templates of LN04 library targeting CDR-L2 were the variants derived from LN01, LN02, C01 and C02. The details were as follows: the LN01, LN02 and LN03-derived variants having not worse antitumor activity than hu4D5 (anti-proliferative activity ratio ≥ 0.7), the C01 and C02-derived variants having not worse antitumor activity than hu4D5 (anti-proliferative activity ratio ≥ 1.0). This was a major difference from the library LN01, LN02 and LN03 using parent antibody hu4D5 as a template.

Except for PCR template, library construction and panning strategy were carried out by same way. Six positions among seven

residues of CDR-L2 were randomized, except for fixing the #53 position with F53 or W53. As a result of screening, six variants were selected from LN04 library targeting CDR-L2. And the variants had F53 and W53 with 50% identical frequency, as designed, diverse residues appeared in the other randomized positions of LN04-derived variants (Fig. 3-7 D).

Judged from anti-proliferative activity ratio of LN04-derived variant (Fig. 3-5), the combining strategy CDR-H3 variants with CDR-L3 variants was not efficient to improve antitumor activity, since antitumor activity of the variants were lower than parent antibody, hu4D5.

3.3.5.2.5 Library LN05 (by error-prone PCR)

In order to increase the possibility of the anti-cancer effect, this study tried to randomize entire variable region including FR region, unlike a screening CDR randomization by degenerate PCR for some position in the construction library LN01, LN02, LN03 and LN04. So, the library LN05 was constructed using error-prone PCR method at low range of mutation frequency (4.5 mutations/kb). Performing 30 cycles of PCR using 500 ng of template DNA, it was confirmed the mutation frequency of 4~8 mutations/kb by sequencing analysis.

And the library LN05 had 2~7 substituted amino acids per scFv molecule, it generally corresponds to the mutation frequency of 4~8 mutations/kb since the size of V_L or V_H are approximately 330 bp and thus it is considered that a couple of amino acids are substituted in each chains. Sequence analysis of 17 variants selected from LN05, except variant not expressed or expressed at an extremely low level showed that 1~4 amino acids were substituted (Fig. 3-8).

With LN05 library screening method, A091 variant was selected by relative ELISA, target binding affinity and *in vitro* anticancer activity (Table 3-3, 3-4). AH06 derived from early library LN03 and its binding affinity was improved 10 times more than that of Hu4D5. Although random library was constantly constructed and kept performing screening processes to select the variants superior to AH06 from several series of library, the superior one to AH06 could not be obtained on the basis of anticancer activity and binding affinity.

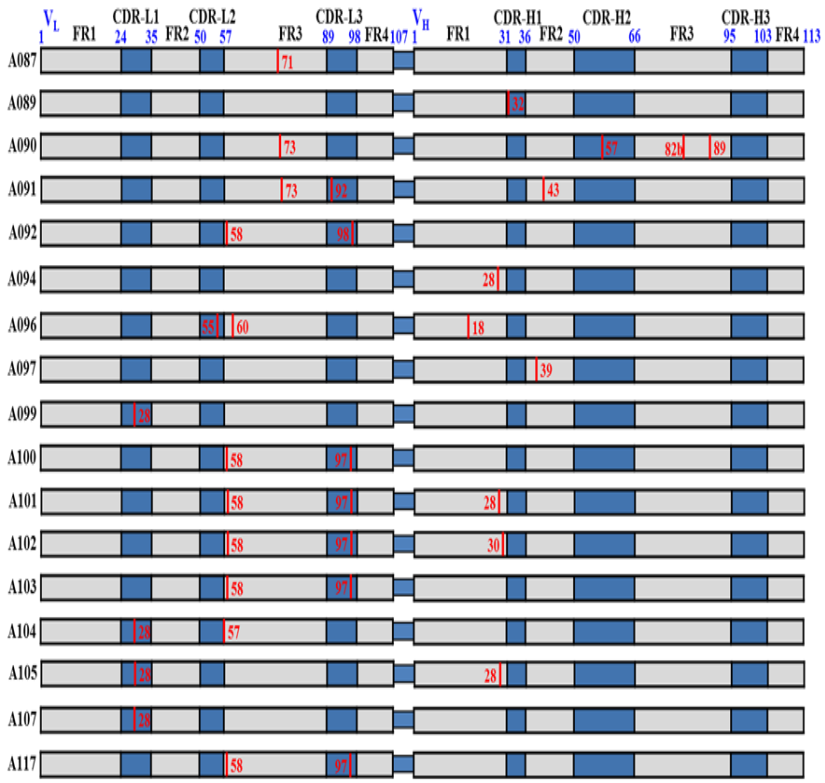

Fig. 3-8. Substituted positions in V_L-V_H region of the variants isolated from LN05. Out of total 31, 6 variants were not expressed, 3 variants exhibited low efficacy and 5 variants were not substituted, except those substituted at position 98 in CDR-H3.

3.3.6 Selection of HER2-specific variants: summary

After panning with 3~5 cycles with HER2 ECD-Fc as an antigen, from randomized scFv phage libraries LN01, LN02 and LN03, phage ELISA was performed to positive clones with more than 5-fold ELISA value ($OD_{450} \geq 0.5$) relative to negative blank. Also, relative phage ELISA using 1M ammonium thiocyanate (Macdonald et al., 1998; Wang et al., 2000) selected positive clones ($OD_{450} \geq 1.0$).

A mixture of such 16 variants selected form those libraries was used as a template to construct CDR-L2 randomized library LN04 as size as about 10^8 levels. From these libraries, variants were selected with the same method as libraries LN01, LN02, LN03.

To evaluate the anti-tumor activity of isolated variants against tumor cells, isolated variants were converted scFv variants into an IgG1 format, and transiently expressed in CHO-S cells. If the expression level of the IgG variant was less than 10~20% of that of hu4D5 or there was a problem with purity, e.g., aggregation and inappropriate assembly of heavy and light chains, the whole expression experiments were repeated several times to double check.

The deduced sequences analysis of representative variants, AH12, AH06, AL07, AH16, A058 and A091, selected from each library besides AH06 (Table 3-4) indicates that modification of libraries LN01 and LN03, except LN02, was not efficient to improve

biological functional activity compared to the parent hu4D5.

Changes of residues to W98, F100c, A101 and L102 in CDR-H3 region of AH06 variant played the most important role for improvement of the binding affinity compared to that of hu4D5. On the other hand, the anti-tumor activity of A058 which had the residues substituted with W98, F100c, A101, L102 in CDR-H3 (identical to AH06) and 3 residues substituted with Q93, A96 and S97 in CDR-L3 against SK-BR-3 was similar to that of hu4D5, however its HER2 binding affinity K_D was reduced to half that of hu4D5. Therefore, the data indicate that the modification of CDR-L3 is unable to contribute to largely the improvement of HER2 binding affinity.

A091 variant had 2 point-mutated residues V_L FR3 T73S, V_H FR2 P41R in extra CDR region by error-prone mutagenesis in addition to 4 substituted positions of CDR-H3 (as like AH06), 3 substituted positions of CDR-L3, and 5 substituted positions of CDR-L2. Anti-cancer activities of A091 was similar and increased to about 3 fold to that of hu4D4 against SK-BR-3 and NCI-N87, respectively, but, its HER2 binding affinity K_D was reduce to half that of hu4D5 (Table 3-4).

Taken together, substitution of other positions in CDR-L3 and CDR-L2 besides the positions substituted with W98, F100c, A101 and L102 in CDR-H3 did not largely influence anti-cancer activities

against SK-BR-3 cells, but negatively influenced their binding affinities.

However, only based on binding affinities of AH06, A091, A058, and others, it seems that it is unable to conclude that CDR-H3 is the only important determining region for improvement of antigen HER2 binding. Instead, judging from results of library construction and stringent panning, it is thought to may be more proper conclusions that possibilities for improvement of binding affinity potentially exist in CDR-H3 region of hu4D5, and this study just did evoke the potential to be appeared.

3.4 Conclusions

It was generated the variant AH06 whose binding affinity was enormously increased to 7.4-folds and also its anti-cancer activity against NCI-N87 cell was improved to about 7-folds compared to those of parent antibody hu4D5.

Namely, 139 variants were isolated from panning and screening procedures, and they were produced by transient expression in CHO-S cell, and purified as IgG solution whose purity and quantity were sufficient to screen and perform various evaluation. And the isolated variants were evaluated by anti-tumor activities

against breast cancer cell SK-BR-3 and gastric tumor cell NCI-N87 cell *in vitro*.

In summary, a series of antibody discovery steps were performed to screen the variants with improved biological activities by using antibody CDR mutagenesis and phage display technologies. Through this process, the upstream antibody engineering technology, such as antibody optimization, required to discover and improve biological efficacy of various therapeutic lead antibodies was able to be established and applied.

CHAPTER 4

Evaluations and Characterizations of HER2 Antibody Variants

4.1 Introduction

To be developed as a novel antibody drug having the clinical usefulness, the antibody should meet the standards or criteria as a novel drug, such as proper biological activity (efficacy) and reduced side effects. In addition, the convenience of drug administration for patient is also important, therefore, the pharmacokinetic properties of drug must be evaluated to choose the route of administration. These biological characteristics should be eventually tested and evaluated through the clinical trials process.

However, prior to clinical trials for the practical and actual evaluation, the values and feasibility as a clinically useful drug should be evaluated in terms of efficacy, safety and stability in animal model (Xu et al., 2015; Knezevic et al., 2015) through preclinical studies.

And also, before proceed to the preclinical test trials requiring huge costs for acquiring the data or information about efficacy, safety, stability and pharmacokinetics data of the drug, interim or discovery evaluation process is also necessary assess fundamental values as a novel drug whether it possesses effective biological activity and safety or not.

For example, *in vitro* activity and *in vivo* efficacy is necessary, and

thus, the evaluation of anti-proliferative activity against tumor cells harboring its specific antigen on the cell surface should be needed in case of anti-cancer antibodies. In addition, the physico-chemical binding affinity should be tested in order to interpret *in vitro* anti-proliferative activity. It is desirable to evaluate anti-cancer efficacy in animal models by reference to *in vitro* activity. Therefore, *in vivo* tumor xenograft model is widely used for efficacy assessment of anti-cancer antibody.

In addition, the action mechanism of anti-cancer antibody is well-known: the anti-cancer activities are exerted by not only inhibition of signaling mediated by the target antigen, but also effector functions such as ADCC (antibody-dependent cell cytotoxicity) (Baselga et al., 2001) and CDC (complement dependent cytotoxicity) (Kubota et al., 2009) through the IgG1 Fc region recognized by effector cells such as macrophages and natural killer cells. Therefore, it is recommended to perform the ADCC and/or CDC activity test. Herceptin is also known to induce ADCC to some extent (Barok et al., 2007).

In vitro specificity (cross-reactivity) test is needed to evaluate the safety of antibody. The antigenic specificity of antibody can be determined by binding assay with functionally similar antigens using ELISA.

When therapeutic protein such as antibody is administered into human body it might be able to act as a new foreign antigen itself and induce formation of anti-therapeutic protein antibody immunogenicity of therapeutic protein should be evaluated (Xu et al., 2015; Knezevic et al., 2015). The test for immunogenicity induction can be carried out *in silico* (Bryson et al., 2010). However, since the immunogenicity test in a big animal, monkey provides more reliable and predictable information, the result of *in silico* immunogenicity test prior to preclinical phase has a meaning only as a reference.

In this study, feasible items were evaluated among *in vitro* and *in vivo* activity and safety tests. Therefore, *in vitro* functional anti-tumor activity, binding affinity, target cross-reactivity (specificity), mechanism of signaling inhibition and *in vivo* anti-tumor activity of variants such as AH06 were evaluated, and, it was also speculated how to attribute the modification of hu4D5 to improvement in binding affinity using molecular modeling analysis.

4.2 Materials and Methods

4.2.1 SPR assay for affinity measurement of variants

The SPR (surface plasmon resonance) biosensor (BIAcore™-2000) was used to detect antibodies against HER2-ECD. After immobilization of HER2-ECD molecule onto the surface of a M5 sensor chip (GE Healthcare, USA), antigens were immobilized on the surface of a M5 sensor chip using an amino coupling method as described previously (Johnsson et al., 1991), at a level of approximately 90~130 response units.

HER2-ECD was covalently coupled by activation of the biosensor chip using N-ethyl-N'-(3-dimethylaminopropyl)carbodiimide and N-hydroxy-succinimide. HER2-ECD was diluted to approximately 30 μg/ml in 10 mM sodium-acetate, pH 4.8, and injected at 5 μl/min flow rate to achieve approximately 90~130 response units of coupled proteins.

A solution of 1 M ethanolamine was injected as a blocking agent. For kinetic measurements, 5-fold, serially diluted antibodies were injected with increasing concentrations (from 0.032 nM, 0.16 nM, 0.8 nM, 4 nM, 20 nM to 100 nM) at flow rate of 10 μl /min for 5 min, followed by injecting a running buffer for 30 min to monitor dissociation. Equilibrium dissociation constants, K_D values from surface plasmon resonance measurements were calculated as k_{off}/k_{on}.

4.2.2 Domain specificity analysis of variants to HER2-ECD antigen (indirect ELISA)

To determine HER2 domain specificity of isolated variants, ELISA was performed with recombinant ΔHER2-ECD (HER2-ECD, which is a partially deleted form of domain IV consisting of 562 amino acids from residue 22 to residue 584 of HER2) (Genentech Patent US6949245, 2005) fused with Fc or HER2-ECD fused with Fc (R&D system, USA) as coating antigens. Maxi-Sorp 96-well microtiter plates (Corning, USA) were coated with 0.5 μg/ml of recombinant ΔHER2-ECD fused with Fc or HER2-ECD fused with Fc (R&D system, USA).

After overnight incubation at 4°C, the plates were washed with TBS-T and blocked with 5% nonfat milk. After the plates were treated with the isolated antibody variants, and then incubated with HRP-conjugated anti-human kappa chain (Sigma, USA). TMB peroxidase substrate was added and incubated for 20 min., and the absorbance was read at 450 nm using a microplate reader. ELISA analysis was performed using methods as described previously (Yoon et al., 2006).

4.2.3 Cross-reactivity analysis of variants to other receptor tyrosine kinases (indirect ELISA)

To analyze cross-reactivity of the antibodies to receptor tyrosine kinases other than HER2, Maxi-Sorp 96-well microtiter plates were coated with 1 μg/ml of Fc-fused ECD of PDGFRβ, VEGFR2, IGF-IR, FGFR3 (IIIc), EGFR, HER3 or HER4 (R&D systems, USA), or 2 μg/ml of HGFR/c-Met ECD-Fc (R&D systems, USA). After overnight incubation at 4°C, the plates were incubated with 30 nM of the isolated antibody variants at 37°C for 2 hours.

After washing with TBS-T, the plates were treated with anti-goat IgG-peroxidase antibody (Sigma, A5420) or anti-mouse IgG-peroxidase antibody (Sigma, A9044) at 37°C for 1 hour. TMB substrate solution was added and incubated for 20 minutes, and the absorbance was read at 450 nm using a microplate reader. ELISA analysis was performed using methods as described previously (Yoon et al., 2006).

4.2.4 Inhibitory effect of variants to HER2 signaling (immunoblot)

The ability of isolated antibody variants to inhibit signaling activation was assessed in HER2 positive gastric cancer cells, NCI-N87 (CRL-5822, ATCC). The cells were seed at a concentration of 2

x 10^5 cells/ml into a 100-mm cell culture dish and treated with 10 μg/ml of antibodies for 16 hours to analyze pAkt and 72 hours to analysis p27, and lysed by adding RIPA buffer (1.0% NP-40, 0.5% deoxycholic acid, 0.1% SDS, 50 mM Tris-HCl, pH8.0) with 1 mM EDTA, 1mM PMSF, protease inhibitor cocktail (Thermo, USA) and phosphatase inhibitor cocktail (Thermo, USA). Western blot analysis was performed using methods as described previously (O'Brien et al., 2010).

Harvested cells were centrifuged at 15,000 rpm for 30 minutes at 4°C and the supernatant was isolated. Protein concentration was determined using the Bradford method. 20 μg of protein samples were separated by SDS–PAGE, and transferred onto PVDF membrane, and then blocked with 5% nonfat milk for 1 hour, and incubated overnight at 4°C with specific primary antibodies. Subsequently, the membrane was washed and incubated with HRP-conjugated goat anti-rabbit IgG (Jackson ImmunoResearch, Europe). The membrane was reacted with an enhanced chemiluminescence kit (Amersham Biosciences, USA), and captured chemiluminescence images using LAS-3000 (Fuji, Japan).

4.2.5 Antitumor efficacy of variants *in vivo* xenograft model

BT-474 (HER2 positive breast cancer) cells were inoculated in the concentration of 5 x 10^7 cells/mouse (200 μl) to 5-week old female athymic nude mouse (Balb/c), subcutaneously, after implanting 17 β-estradiol and norgestrel pellets 24 hours prior to inoculation (Liang et al., 2010). After reaching 80~100 mm^3 in tumor size, antibodies were administered at the dose of 20 mg/kg for 4 weeks, twice a week, intraperitoneally. After completion of the test, the tumor tissue for all test groups were removed and measured by the weight and volume.

Anti-cancer activity was estimated as the percentage of inhibition rate (IR %) of tumor volume compared the tumor volume of experimental group with the tumor volume of control (vehicle) group.

$$* \text{Tumor volume } (mm^3) = (\text{length} \times \text{width}^2) \times 0.5$$

$$* \text{IR\%} = (1 - TVt/TVc) \times 100$$

(wherein, TVt is average tumor volumes of the experimental group, and TVc is average tumor volumes of the control (vehicle) group.)

4.2.6 Computing the stability and analyzing antibody-antigen interaction

To analyze molecular interactions between the antibody and a HER2, the structural information of HER2 and hu4D5 was referred from the PDB (code: 1N8Z; web site: http://www.rcsb.org/pdb/home/home.do). To investigate effects of mutations in the antibody variable regions on stability, force field and charges were estimated using CHARMm module and Momany-Rone, respectively (Discovery Studio 3.5, Accelrys Inc, USA, http://accelrys.com/). Data of intraprotein interaction was obtained from Protein Interactions Calculator (http://pic.mbu.iisc.ernet.in/) and the binding energy between the antibody and HER2 molecule was calculated by the equation 1, as undermentioned.

All the experiments were carried out on a 3.40 GHz Intel Core i7 Quard-Core processor. Molecular modeling was performed using the Macromolecules modules on Discovery Studio 3.5 (Accelrys Inc.), and CHARMm (ver. 36.2) was used for energy minimization.

Equation 1. Binding energy of antibody and antigen HER2

$$\Delta G^{\text{HER2:V}_H/\text{V}_L \text{ binding energy}} = \Delta G^{\text{HER2/V}_H/\text{V}_L \text{ energy}} - (\Delta G^{\text{HER2 energy}} + \Delta G^{\text{V}_H/\text{V}_L \text{ energy}})$$

4.3 Results and Discussions

4.3.1 Affinity determination of variants by SPR

Binding affinities (K_D) of selected variants to HER2 antigen were calculated from association rate constants (k_{on}) and dissociation rate constants (k_{off}) measured using BIAcore ™-T200 as k_{off}/k_{on}. As shown in Table 3-4 and Fig. 4-1, the K_D value of parental antibody hu4D5 to antigen HER2 was 0.48 nM, and that of the D98W (in CDR-H3) variant modified from hu4D5 to antigen HER2 was 0.11 nM, similar as described (Gerstner et al., 2002).

Although binding affinities (K_D) of most variants (AH16 A091, and etc.) were similar or decreased to that of parent hu4D5, on the other hand, the K_D of AH06 was 60 pM and sharply showed improvement to 7.4-folds to that of parent hu4D5 (Fig. 4-1). This result indicates that the binding affinity of AH06 is remarkably increased.

To investigate the effect of the other three changed residues, F100c, A101 and L102 in CDR-H3 of AH06 on the binding affinity to HER2, the "modified AH06 W98D" by substituting W at only one position Kabat #98 with D in CDR-H3 was additionally generated. As a result, the K_D of the "modified AH06 W98D" was increased up to 3.1-fold compared to that of hu4D5 (Table 3-4).

Therefore, it was able to conclude that residues substitutions at positions Kabat #98, 100c, 101, and 102 in CDR-H3 region from D98,

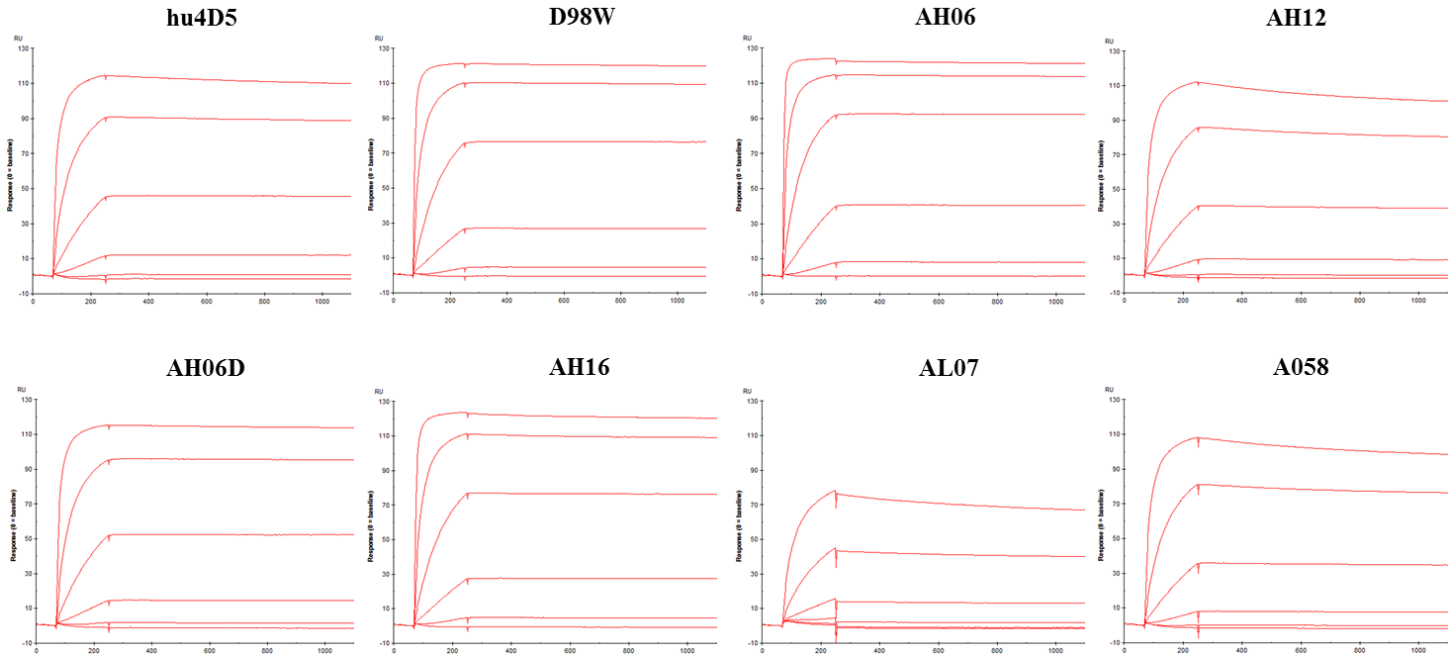

Fig. 4-1. SPR binding analysis of isolated variants to immobilized human HER2-ECD. Antibody variants were injected at six different concentrations ranging from 100 nM, 20 nM, 4 nM, 0.8 nM, 0.16 nM, and to 0.032 nM over a surface on which 100 RU of HER2-ECD had been coupled. The parameters solved for each run are shown in Table 3-4 (Chapter 3). The K_D of AH06 was 60 pM and sharply showed a 7.4-fold increase compared with that of parent hu4D5 (K_D 0.48 nM).

M100c, D101 and Y102 of hu4D5 to W98, F100c, A101 and L102 of AH06 contribute to a considerable synergistic improvement of binding affinity to HER2.

4.3.2 Domain specificity of variants against HER2 molecule

To determine antigen binding epitope or domain on HER2, binding ELISA with a comparative antibody 2C4 (R&D system, USA) capable of binding to domain II of HER2 and the antigen ΔHER2-ECD-Fc (amino acid residues #22~584, R&D system) truncated in a part of domain IV and full HER2-ECD-Fc was analyzed. Since hu4D5 is known to bind to intact domain IV, and it cannot bind to domain IV-truncated antigen ΔHER2-ECD (Genentech Patent US6949245, 2005). On the other hand, the comparative test antibody 2C4 can bind to both antigens ΔHER2-ECD and intact HER2-ECD and thus can be used for the comparative analysis.

While antibody 2C4 could bind to both antigens ΔHER2-ECD and intact HER2-ECD, antibodies hu4D5, AH16 and A091 could not bind to ΔHER2-ECD. The binding ELISA indicates that variants AH06 and A091 is capable binding to domain IV of HER2 antigen, specifically, as similar to hu4D5 (Fig. 4-2.).

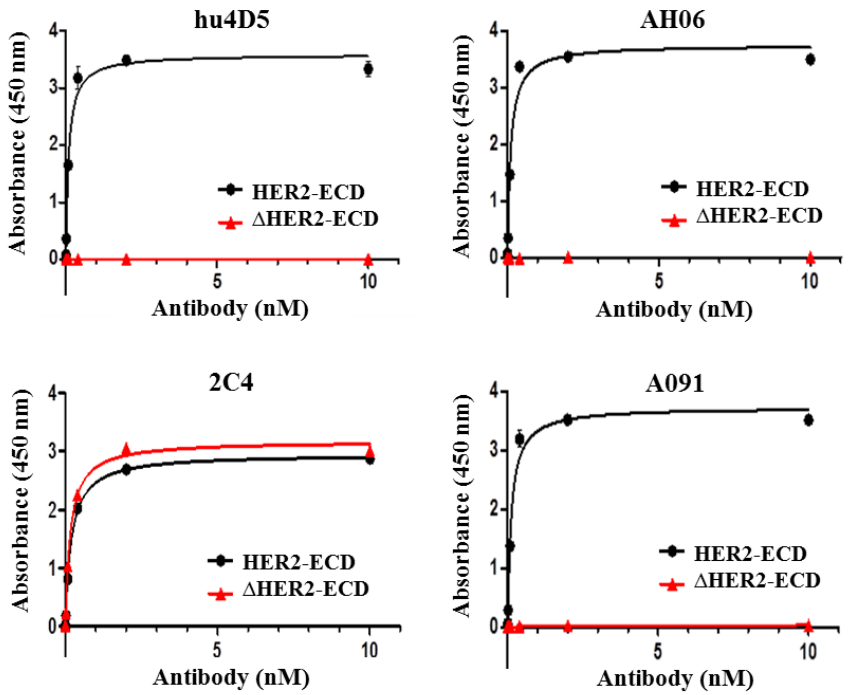

Fig. 4-2. Domain specificity of the AH06 against HER2 molecule. AH06 is capable binding to domain IV of HER2 antigen, specifically, as similar to hu4D5. Indirect ELISA was performed with recombinant ΔHER2-ECD or HER2-ECD fused with Fc as coating antigens. The ΔHER2-ECD, which is a partially deleted form of domain IV consisting of 562 amino acids from residue 22 to residue 584 of HER2 molecule were expressed in CHO-S cells and purified. The data are the average of duplicate determinations.

4.3.3 Cross-reactivity of variants to other receptor tyrosine kinases

Antigenic cross-specificity or cross-reactivity of AH06 and A091 was tested by using ELISA with HER family antigens (EGFR, HER2, HER3, HER4) and other receptor tyrosine kinases (RTK, such as PDGFRβ, VEGFR2, IGF1R, FGFR3 and HGFR). The variants AH06 and A091 were not capable of binding to any other RTKs (EGFR, HER2, HER3, HER4, PDGFRβ, VEGFR2, IGF1R, FGFR3 and HGFR) except only HER2 (Fig. 4-3 A and B) and were specific to only HER2 antigen.

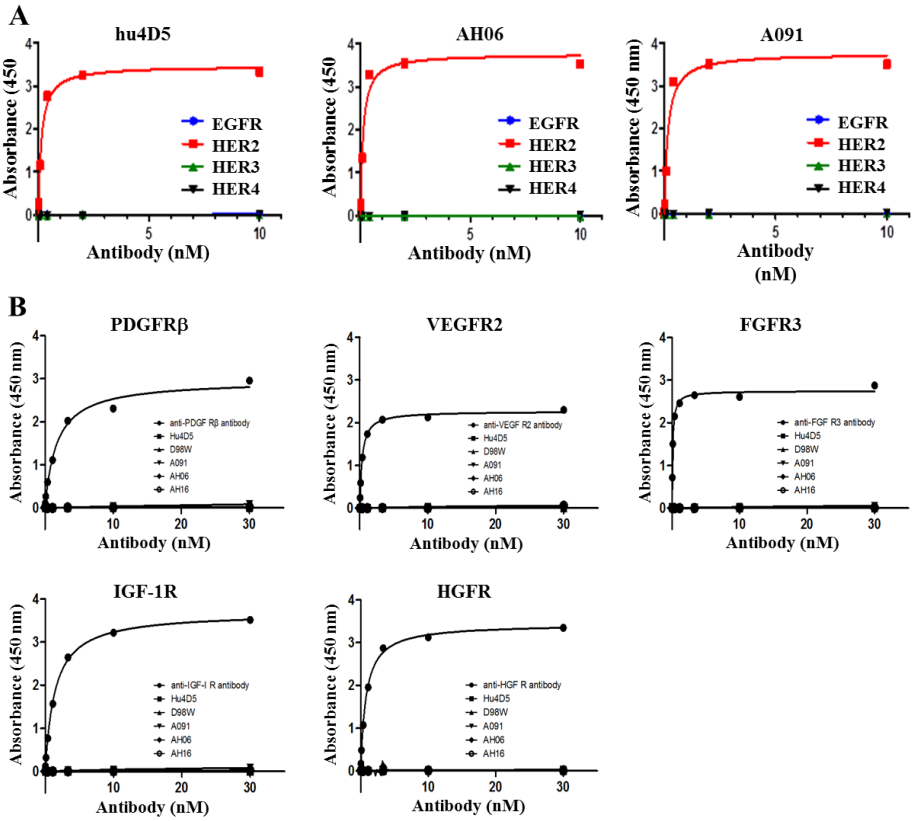

Fig. 4-3 A, B. Cross-reactivity of the isolated variants to HER family (A) and receptor tyrosine kinase family (B). AH06 was not capable of binding to any other RTKs (EGFR, HER2, HER3, HER4, PDGFRβ, VEGFR2, IGF1R, FGFR3 and HGFR) except only HER2 and were specific to only HER2 antigen.

Indirect ELISA was performed with recombinant EGFR, HER2, HER3, HER4, PDGFRβ, VEGFR2, IGF1R, FGFR3 and HGFR as coating antigens, followed by treatment of the antibody variants and the antibodies binding to each coated receptor as positive controls. The data are the average of triplicate determinations.

4.3.4 Effect of variants on downstream signaling of HER2

To determine the inhibitory mechanism of HER2 signaling by hu4D5 and AH06 variant, antibodies were treated in gastric cancer cell line NCI-N87. Protein levels including HER2, phosphorylated HER2 (pHER2), Akt, phosphorylated Akt (pAkt) and P27 were examined by Western blot analysis (Fig. 4-4). Phosphorylation of HER2 and AKT were inhibited without a change in protein expression of HER2 and Akt by treatment of hu4D5 as well as AH06.

On the other hand, the expression level of the cyclin-dependent kinase inhibitor p27 was increased much more when cells were treated with AH06. These results suggest that AH06 antibody inhibits activation of the PI3K-Akt signaling pathways via HER2 and induces cell death by increasing the expression of the p27 similarly to the parent hu4D5. Thus, cell-context dependent induction of p27 might contribute to cellular susceptibility to AH06.

Through the inhibition of signal transduction, the isolated antibody AH06 had a powerful anti-tumor effect in the *in vitro*, suggesting that it might be used as an effective therapeutic agent to target HER2.

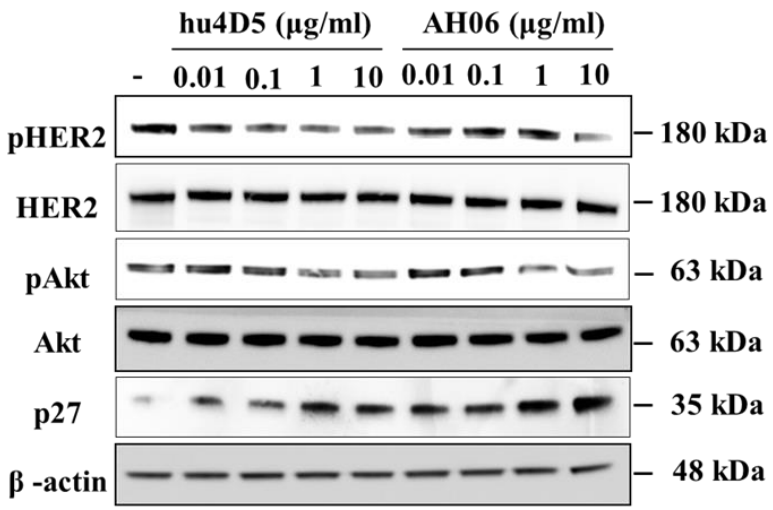

Fig. 4-4. Effects of hu4D5 and AH06 on HER2 signaling.

Protein levels of HER2, pHER2, Akt, pAkt and p27 were detected by western blot, after 10 μg/ml of AH06 treatment to NCI-N87 gastric cancer cells. β-actin was also tested as a loading control.

* Incubation time: HER2 (5 days), pHER2 (30 min), Akt/pAkt (16 hr), p27 (72 hr)

4.3.5 Antitumor efficacy of variants *in vivo* xenograft model

To elucidate *in vivo* antitumor efficacy of antibody, *in vivo* xenograft was performed using breast cancer cells BT-474. Tumor volume was significantly decreased ($p < 0.05$) from days 7 to 42 after administration of Herceptin (hu4D5) when compared with the vehicle group. AH16 and A091 significantly reduced ($p < 0.05$) tumor volume from days 24 to 42 and days 21 to 42, respectively, when compared with the vehicle control group (Fig. 4-5 A).

Tumor weight was significantly reduced only in A091 group. Therefore, A091 caused tumor growth inhibition equivalent to that of hu4D5, as well as showed the stronger efficacy in terms of relative tumor weight than the other groups (Fig. 4-5 B).

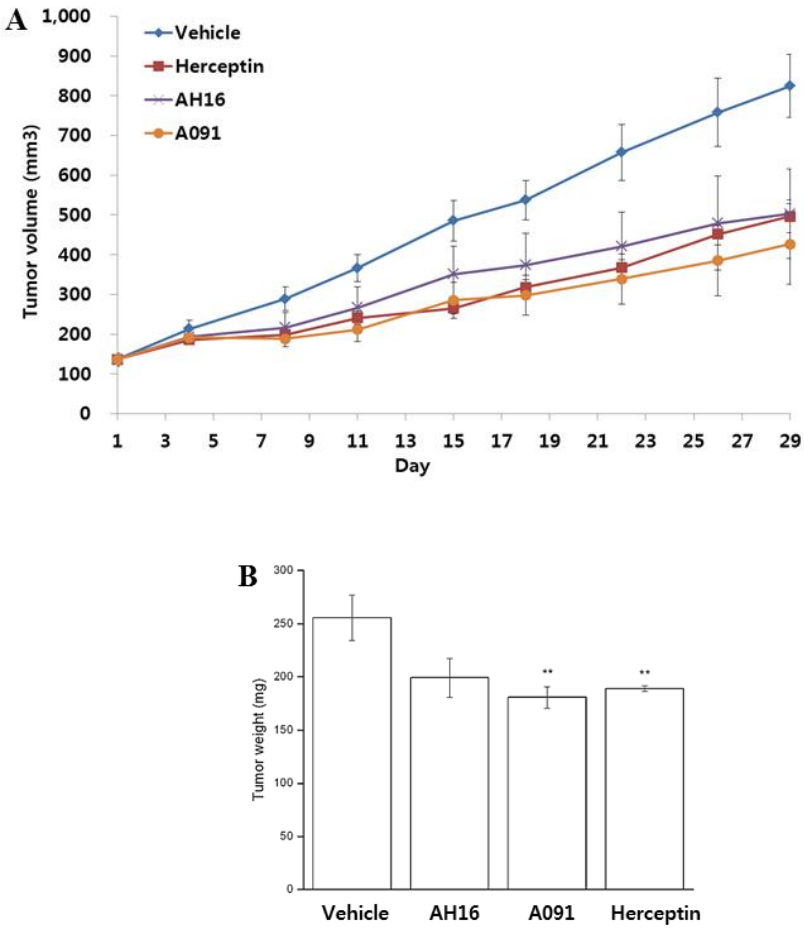

Fig. 4-5. Antitumor efficacy of antibody *in vivo* BT-474 xenograft model.

A. Antitumor efficacy of antibody in tumor volume.

B. Antitumor efficacy of antibody in tumor weight.

4.3.6 Computing and analyzing antibody-antigen interaction

4.3.6.1 Binding analysis with binding energies and affinities

To analyze binding modes and binding energies of 4 changed residues (W98, F100c, A101 and L102) of AH06 to its antigen HER2, molecular modeling methodology and the Equation 1 was used. The parent hu4D5 and a modified version of AH06 (AH06 D98), wherein W (Trp) was replaced with D (Asp) at 98 position in the CDR-H3 of AH06, were selected as references.

Binding free energy was calculated using the Molecular Dynamics (CHARMM forcefield), but not the docking simulations considering protein-protein (HER2 and variants) interaction, and the binding structures between HER2 and variants (or hu4D5) were simulated based on PDB (code: 1N8Z). The binding free energy between HER2 and variants (or hu4D5) was calculated from the Equation 1.

The relationship between the binding affinity and binding free energy is generally $\Delta G = -RT \ln(K_D)$ (Lee and Olson, 2006). Therefore, binding affinity is able to be calculated with binding free energy as follows. $K_D = e^{(-\Delta G/RT)}$ (R: ideal gas constant, T: absolute temperature)

The K_D values of variants listed in Table 4-1B were experimental data obtained by SPR analysis (BIAcore™ T200), and the ΔG values

listed in Table 4-1A and B were theoretical ones calculated from the Equation 1. Such comparison was carried out to see a correlation between binding affinity and binding free energy.

Based on the calculation of binding energy, the association between binding energy and binding affinity depending on residues in CDR-H3 of AH06, hu4D5 and the "modified AH06" was analyzed.

The residues W98, F100c, A101 and L102 in CDR-H3 of AH06 were replace with D98, M100c, D101 and Y102, respectively, in that of hu4D5. AH06 had more a higher binding affinity for HER2 as well as lower binding energy, compared to hu4D5 (Table 4-1), suggesting that AH06 could bind to HER2 more stable than hu4D5.

Next, it was investigated which ones among the 4 residues (W98, F100c, A101 and L102) of AH06, different from those of hu4D5, contributed to the improvements in terms of binding affinity and binding energy.

Firstly, the only residual difference between AH06 and "modified AH06" is in position 98, W98 and D98, respectively. The binding affinity of AH06 to HER2 was stronger than that of "modified AH06" and the binding energy of AH06 was to some extent lower than that of "modified AH06" (Table 4-1).

Table 4-1. Binding energies and affinities of AH06 and hu4D5.

A. Binding energy

	$\Delta G^{HER2/VH/VL}$ energy	ΔG^{HER2} energy	$\Delta G^{VH/VL}$ energy	$\Delta G^{HER2:VH/VL}$ binding energy
hu4D5	-19716.1	-12050.6	-7374.3	-291.2
modified AH06	-19394.5	-12050.5	-7052.0	-292.0
AH06	-19432.8	-12050.7	-7065.2	-316.9

B. Binding affinity (Biacore)

Antibody	K_a (1/Ms)	K_d (1/s)	K_D (M)	ΔG (kcal/mol)
hu4D5	2.4×10^{5}	1.2×10^{-4}	0.48×10^{-9}	-291.2
modified AH06	3.0×10^{5}	0.5×10^{-4}	0.15×10^{-9}	-292.0
AH06	7.7×10^{5}	0.5×10^{-4}	0.06×10^{-9}	-316.9

hu4D5: CDR-H3 D98, M100c, D101, Y102,

modified AH06: CDR-H3 D98, F100c, A101, L102

AH06: CDR-H3 W98, F100c, A101, L102

Since 3 residues, F100c, A101 and L102, of CDR-H3 are present in both AH06 and "modified AH06", it could be concluded that differences in binding affinity and binding energy of two antibodies are only determined by the residue W or D at position #98. The substitution with W at position 98 increased the binding affinity and decreased the binding energy, suggesting that W98 plays a significant role in binding to HER2.

Secondly, to evaluate roles of residues at the positions #100c, 101 and 102 of CDR-H3, hu4D5 having M100c, D101 and Y102 residues was compared with the "modified AH06" having F100c, A101 and L102 residues. The binding affinity of "modified AH06" was about 2-fold higher than that of hu4D5, however, unexpectedly there was no significant improvement in the binding energy of "modified AH06" compared to that of hu4D5 (Table 4-1).

The analysis of binding affinity and binding energy of CDR-H3 variants indicates that the 3 residues F100c, A101 and L102 of AH06 can enhance binding affinity to HER2 (by additional hydrophobic interactions) about 3-fold, however, what exerts more influence is W98 of CDR-H3.

Although this study did not calculate the binding energy of the "modified hu4D5 D98W" variant which the residue D at the position #98 of CDR-H3 of hu4D5 was substituted with W, the binding affinity of the "modified hu4D5 D98W" was about 3-fold to that of hu4D5 (Table 3-4), these results suggested that those

residues W98 and F100c, A101 and L102 of CDR-H3 of AH06 exerted synergistic effects on binding affinity to HER2 and binding energy.

4.3.6.2 Simulation of binding mode using molecular modeling analysis

To elucidate the experimental data, the binding modes of hu4D5 and AH06 to HER2 using molecular modeling was simulated and analyzed. The residues F100c, A101 and L102 of CDR-H3 of AH06 were located in the region of V_H-V_L interface. Since these 3 residues were located several Ås apart from the HER2 residues (Fig. 4-6 A), it is unlikely that the residues directly interact with HER2 antigen. Therefore, they may indirectly contribute to improvement of binding affinity by influencing interaction between light and heavy chains of the antibody, rather than direct interaction with HER2 molecule.

It was simulated that there could be a direct hydrophobic interactions between the aromatic ring group of tryptophan residue (W98) of AH06 and the aliphatic group of isoleucine (I613) residue located in the domain IV of HER2 as well as the heavy and light chain hydrophobic interactions between the phenyl ring of F100c in CDR-H3 and the hydrophobic groups that is consist of Y36, P44

and F98 located in V_L (Fig. 4-6 B). On the other hand, there was no significant interaction between the residue (D98) of hu4D5 and the aliphatic group of isoleucine (I613) residue located in the domain IV of HER2 (Fig. 4-6 C, D).

In summary, computer modeling and simulation provided possible explanations for which residues influence improvement of binding affinity to HER2 and how they interact with other residues of antibody itself and with HER2.

In addition, as Resi B. Gerstner et al. mentioned (Gerstner et al., 2002), a clear role of W98 of CDR-H3 in HER2 binding is unclear. Here, this study provide a possible explanation for that using modeling analysis regarding improvement of binding affinity of AH06.

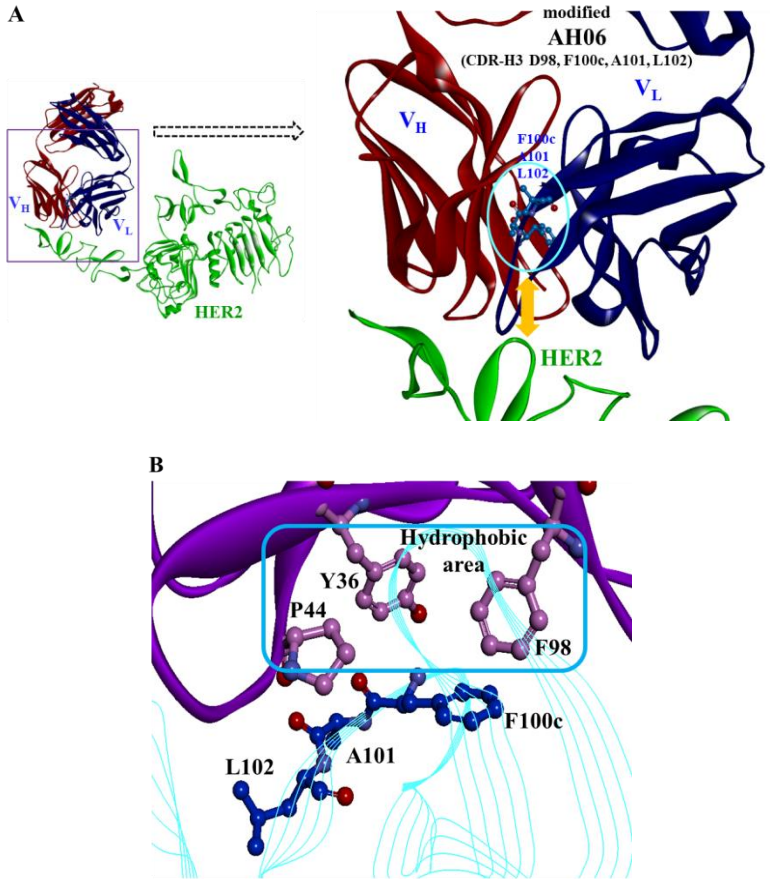

Fig. 4-6. Molecular interaction models of AH06 and hu4D5 complex with HER2. (A) A distance between three residues, F100c, A101 and L102 of modified AH06 (blue circle) and HER2 molecule (green). The residues F100c, A101 and L102 of CDR-H3 of AH06 were located in the region of V_H-V_L interface. The V_H domain and V_L domain are colored with red and blue, respectively. (B) Molecular interactions between V_H and V_L. The V_H domain and V_L domain are colored with pink and light blue. The residues F100c, A101 and L102 of CDR-H3 and Y36, P44 and F98 of V_L were located in the region of V_H-V_L interface. It was simulated that there could be a direct hydrophobic interaction between the phenyl ring of F100c in CDR-H3 and the hydrophobic groups that is consist of Y36, P44 and F98 located in V_L.

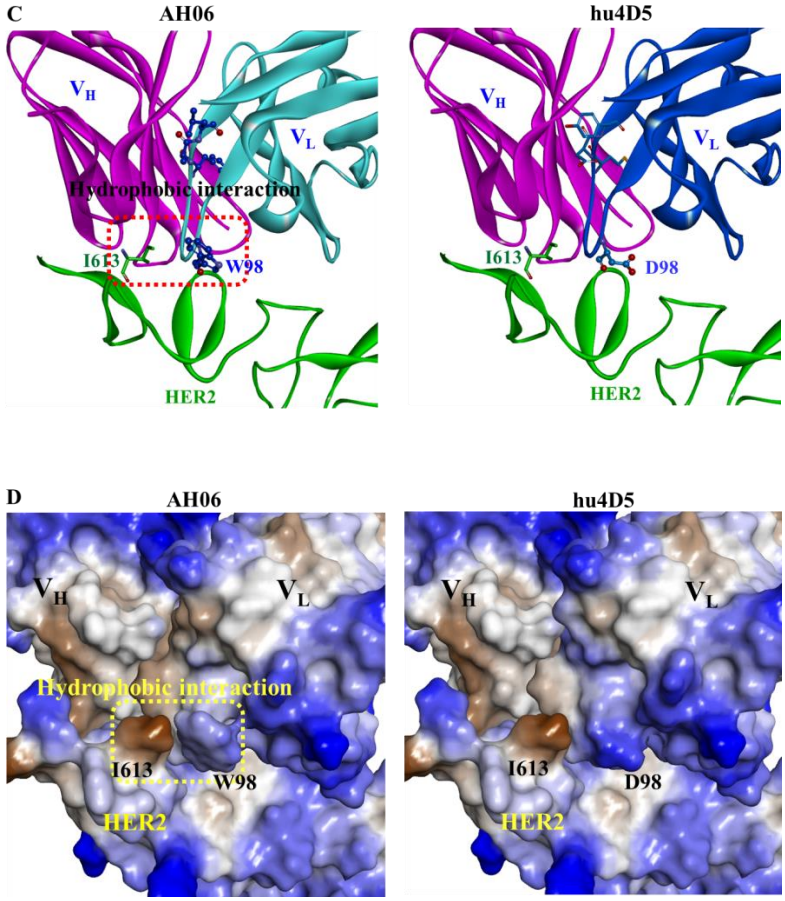

Fig. 4-6. Molecular interaction models of AH06 and hu4D5 complex with HER2 (continued). (C) Ribbon model: The mutated region of variants is presented as a red square. (D) Surface model: The mutated region of variants is presented as a yellow square. Brown, hydrophobic; Blue, hydrophilic. It was simulated that there could be a direct hydrophobic interaction between the aromatic ring group of tryptophan residue (W98) of AH06 and the aliphatic group of isoleucine (I613) residue located in the domain IV of HER2 as well as the heavy and light chain hydrophobic interactions by the residues F100c, A101 and L102 of CDR-H3.

4.4 Conclusions

AH06 was the best candidate as a biobetter antibody that has an increase by 7.4-fold in binding affinity (K_D: 60 pM) to HER2 compared to hu4D5, respectively.

AH06 specifically bound to domain IV of HER2 and did not have cross-reactivity with other receptor tyrosine kinases (RTK) such as HER1 (EGFR), HER3 and HER4, PDGFRβ, VEGFR2, IGF1R, FGFR3 and HGFR. And also, AH06 decreased the level of phosphorylation of HER2 and AKT to a similar extent, but most of all, highly increased the overall level of p27 in gastric cancer cell NCI-N82 as compared to hu4D5, suggesting that AH06 could be a potentially more efficient therapeutic agent than parent hu4D5.

To address how the binding affinity of AH06 to HER2 was enormously increased, binding energy calculation and molecular modeling stimulation were performed. As a result, it was indicated that the substitution of residues of CDR-H3 to W98, F100c, A101 and L102 could stabilize binding of the antibody to HER2 and that there could be the direct hydrophobic interactions between the aromatic ring of W98 within AH06 and the aliphatic group of I613 within antigen HER2 domain IV. And the substitution of the residues F100c, A101 and L102 of CDR-H3 within AH06 could result in the inter-chain hydrophobic interactions (not strong as that of W98) between the phenyl ring of F100c in CDR-H3 and the

hydrophobic groups that consist of Y36, P44 and F98 located in V_L. Therefore, such two kinds of interactions exerted such interactions could have synergistic effects on improvement of binding affinity of AH06 to HER2.

CHAPTER 5

Bioprocess Development of HER2 Antibody Variant

5.1 Introduction

In order to release active antibodies to pharmaceutical market, it is required to establish a high-producing cell line and mass animal cell culture technology for achievement of the maximum cell growth and production. Thus, it is also required to develop screening system for selection of high-producing (expression) cell clones, study various media and additives, and optimize the production process.

Among the variant such as AH06, AH16, and A091 discovered through the upstream antibody engineering technology and screening process (Refer to Chapter 3), firstly discovered AH16 (IgG1) [Heavy chain, total 451 amino acid residues; V_H, Kabat No. #1~113 (120 amino acid residues); C_H1~3, #114~444 (331 amino acid residues); Light chain, total 214 amino acid residues; V_L, Kabat No. #1~107 (107 amino acid residues); C_L, #108~214 (107 amino acid residues); N-glycosylation at the position, N294] was chosen as a model antibody to establish and set-up the downstream bioprocess required to produce the antibody, and a series of bioprocess such as stable cell line development, culture media and additive screening, and purification process were performed (Fig. 5-1).

Therefore, as the first step, the development of stable cell line using suspension type of DHFR-deficient CHO DG44 cell is needed

to produce the antibody.

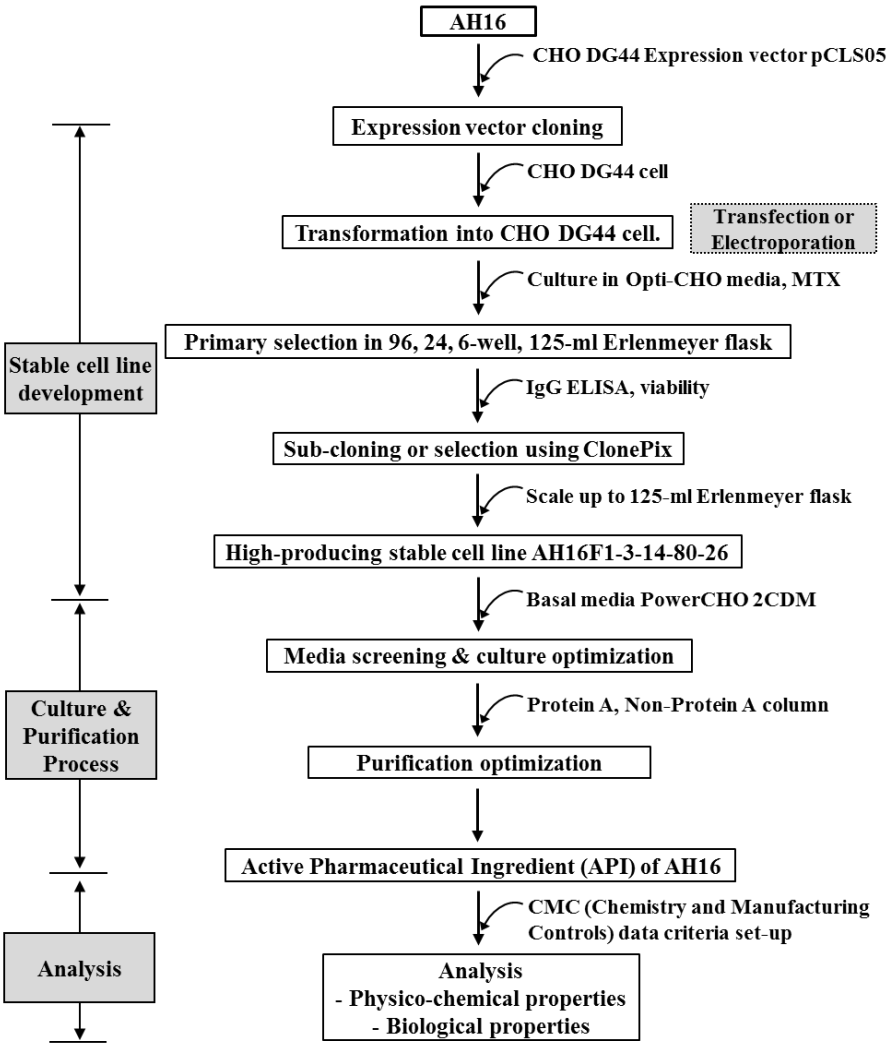

Fig. 5-1. Bioprocess flow scheme for AH16 production and analysis.

In addition, selection and optimization of basal media and additives is also needed. In order to increase or maximize the antibody productivity, many companies such as BD Bioscience and SAFC have their own basal culture media and additives self-developed through the culture media library or media formulation. In general, carbon sources, concentrated amino acids, vitamins, salts and minerals are included in supplement solutions, whereas lipids, hydrolysates and growth factors substances chemically undefined are not included.

In the study on increment of productivity by screening of the media additives, there are a number of possible combinations of additives available, and so, the statistical analysis tools such as Design-of-Experiment (DOE) are used to easily design and analyze media combinations and the result (Parampalli et al., 2007). To increase the productivity of anti-cancer antibody AH16-F1, the media and additive optimization is required through the screening of culture media and their additives for the AH16-producing stable cell line. Therefore, to determine the optimal media and additives, screening with 5 commercial basal media and 10 supplements (additives) was performed.

As next step, in order to purify AH16 from the culture fluids and optimize the purification process, after testing resins from the

major manufacturers under the same conditions, the proper Protein A resin was selected based on purity, yield, quantity of leached Protein A, prices and ease of CIP (cleaning-in-place). Next step, SP Sepharose HP resin was used for capturing step to establish a non-Protein A-based process. The sulfopropyl (SP) functional group is a strong cation exchanger in the resin. Using this cation exchange chromatography, we tried to purify the target protein AH16 can be efficiently separated from impurities such as HCP and HCD.

The study on analysis and evaluation for characterization of API (active pharmaceutical ingredient) and establishing the physico-chemical and biological criteria of the novel antibody as API produced through the bioprocess and clinically used is very important and absolutely necessary as a mean of quality management to monitor and control clinical efficacy and side effects. Therefore, API of AH16 produced through the bioprocess was characterized and analyzed.

5.2 Materials and Methods

5.2.1 Construction of expression vector

An expression vector named pCLS05 (Korean Patent Application No. 10-2011-0056685) was invented in order to produce a Herceptin variants, AH16 from CHO DG44 cell. Heavy and light chain genes were inserted in the multiple-cloning site (MCS) of the vector and expressed under the control of a CMV promoter. Also, a scaffold attachment region was introduced between the heavy chain and DHFR.

5.2.2 Transfection of CHO DG44 cells using pCLS05AH16F1 vector

CHO DG44 cells were purchased from Life Technology (USA) (Cat. No. 12609-012, Lot No. 363938) and used as a parental cell line for AH16 drug substance production. CHO DG44 is a stable aneuploid cell line established from a Chinese Hamster's ovary (Tjio and Puck, 1958) and dihydrofolate reductase (DHFR)-deficient (Urlaub et al., 1983; Kaufman et al., 1985; Werner et al., 1998).

Transfection of CHO DG44 cells was performed as following methods using an electroporation. Approximately 24 hours before transfection, DG44 cells were inoculated at 3 x 10^5 cells/ml in an

125-ml flask containing 30 ml DG44 medium. The flasks were place on an orbital shaker platform rotating at 110 rpm at 37°C, in a humidified 5% CO_2. At that time, cells were measured using tryphan blue and maintained at least 95% cell viability for high transfection efficiency.

On the day of transfection, DG44 cells were diluted at 1 x 10^7 cells/ml in 0.5 ml CD OptiCHO. Thirty μg pCLS05AH16F1 were added into the cells. The DNA and cells were mixed gently and transferred to a sterile electroporation cuvette. Transfection was performed using the Gene Pulser Xcell electroporation system (Bio-Rad, USA). The condition was 150 voltages and 950 μF capacitance. The transfected cells were transferred to a T75 flask containing DG44 medium and cultured for 3 days.

5.2.3 Selection of stable transformants producing AH16

After 3 days of transfection, transformants were measured cell viability and added 10 ml of the OptiCHO media every 2~3 days. The cells were maintained by adding 10ml of the OptiCHO media every 2~3 days, and the cell viability was assessed. When the cell culture media in the T75 Flask reached 40 ml, it was replaced with 20 ml of fresh media. This procedure was repeated until cell viability reached between 90~100%.

5.2.4 Selection of single colonies using ClonePix

After selection, stable pool were inoculated at 5 x 10^6 cells in the 6-well plate containing CloneMedi-CHO DHFR semi-solid media. The cells were cultured for 2 weeks and isolated single colonies using ClonePix. The picking condition was described on Table 5-1.

Table 5-1. ClonePix picking condition.

Name	Expression
Edge Excluded	IF Edge Excluded = True
Too Big	IF Total Area >= 0.7
Too Small	IF Total Area <= 0.05
Irregular 1	IF Compactness <= 0.45
Irregular 2	IF Axis Ratio <= 0.45
Proximity	IF Proximity <= 0.4
Low FITC	IF [FITC 1s] Exterior Mean Intensity <= 1,470.970 AND [FITC 1s] Interior Mean Intensity <= 210
Accept	Anything else

5.2.5 Scale-up of culture for selecting clones

In order to select the top 20% of clones in terms of AH16 expression, a quantitative ELISA was performed with the cell culture supernatants. The selected cell clones were transferred to a

24-well plate and cultured. When the cells were cultured to 90% confluent in the well, the productivity was estimated by ELISA. The top 15% of the clones with AH16 expression were selected and inoculated at 2 x 10^5 cells/ml in 125 ml Erlenmeyer flask containing 30 ml CD FortiCHO media with 500 μg/ml Geneticin, 4 mM L-glutamine. The flasks were place on an orbital shaker platform rotating at 110 rpm at 37°C, in a humidified 5% CO_2.

After 3 passages, both of cell growth and productivity were measured. In order to select clones for MTX amplification, specific growth rate (μ) and specific product rate (q) (Derek et al., 2007) were calculated.

The specific growth rate (μ) and the specific productivity (q) were calculated as follows.

Specific growth rate (μ) = (ln X_2 - ln X_1)/day

(wherein, X_1 is viable cell density at seeding time and, X_2 is viable cell density at sampling time, and D (day) is time of sampling.)

Specific productivity rate (q) = PCD (pg/cell/day)

= ΔTiter/ΔIVC x 10^6

(wherein, ΔIVCD (integral viable cell density) (unit: cells x day/ml) = (X_2 - X_1)/(ln X_2 - ln X_1) x day.

ΔTiter means productivity of products. X_1 is viable cell density at seeding time and, X_2 is viable cell density at sampling time)

5.2.6 MTX amplification

After clonal selection, the cells were diluted at 3 x 10^5 cells/ml in a 125-ml Flask containing 30 ml CD Opti CHO media with 20 nM MTX and 500 μg/ml Geneticin. Flasks were placed on an orbital shaker platform rotating at 110 rpm at 37°C, in a humidified 5% CO_2. The cell culture media were exchanged every 3 days until cell viability is between 90~100% and the media volume was kept above 30 ml.

Once the first round of MTX selection resulted in higher levels of protein expression and better viability, the stable cells were inoculated at a final concentration of 2 x 10^5 cells/ml in a 125-ml flask containing 30 ml of CD Opti CHO media with 500 μg/ml Geneticin and 8 mM L-glutamine, and the culture media were harvested for ELISA determination of product titer after 11 days of incubation.

Based on productivity and quality, additional amplifications were performed after gene amplification using 20 nM MTX. The cells selected in the first round of amplification were inoculated at 3 x 10^5 cells/ml in growth media with 80 nM MTX. The media were exchanged every 3~4 days until cells viability were 90%.

After recovery, the cells were diluted at 2 x 10^5 cells/ml in CD Opti CHO media with 500 μg/ml Geneticin, 8 mM L-glutamine and maintained for 12 days to measure clonal productivity by

using IgG ELISA. The second amplification with 80nM MTX was terminated and followed additional amplifications with increasing MTX concentrations (160 nM, 320 nM). To estimate an output of the cells, ELISA was performed after all round of amplification.

After MTX amplification, the subcloning and scale up process were performed as described previously. Considering specific growth rate (μ) and specific product rate (q), the final clone was selected as a producer stable cell line.

5.2.7 Quantification of antibody AH16F1 by ELISA

The wells of microtiter plates were coated with goat anti-human IgG-Fc antibody diluted at a 1:200 ratio in coating buffer. After saturation with 1% BSA, both of sample diluted in PBS and Human reference Serum diluted in PBS were added to the well. After washing, goat anti-Human IgG-Fc-HRP antibody (Bethyl, A80-104P, 1 mg/ml) diluted at a 1:100,000 ratio in 1% BSA/TBST was added and kept. Finally, TMB solution was added into the well and the color was developed in dark. The reaction was stopped by adding 2 N of sulfuric acid, and absorbance was measured at 450 nm using an ELISA reader.

5.2.8. Comparison of 5 commercial media for the screening of basal medium

Five commercial basal media 3 chemically defined (CD) media family, CD FortiCHO (Invitrogen Cat. A11483-01) and Power CHO2CDM (Lonza Cat. BE12771Q), ProCHO 5 (Lonza Cat. BE12-766Q), and 2 serum-free media family, SFM4CHO (HyClone, Cat. SH30548.02) and UltaCHO (Lonza, Cat. 12-724Q) were used to screen the optimal basal medium for the AH16-producing stable cell line.

5.2.9 Cell culture and assessment for media screening

AH16F1-3-14-80-26 cell line expressed AH16 was inoculated at the final concentration of 2 x 10^5 cells/ml in a 125-ml Erlenmeyer flask containing 25 ml of growth medium supplemented with 4 mM glutamine.

Evaluations for the selection of basal medium were based on the cell survival and productivity. After 7 days of cell culture, the cell number and survival rate were measured by trypan blue staining, the culture fluid was collected and the concentration of antibody in the resulting filtrate was measured by IgG ELISA method.

5.2.10 Measurement for the effect of a single additive

Ten kinds of a single additive, HYPEP 5603, HYPEP 7504, HYPEP 1510, HYPEP 4601, Cotten CNE 50M, TC yeastolate, Soytone, Sheff-CHO Plus ACF, Cell Boost6 and Cell Boost5 were tested to screen basal additives. The 10x concentrates of each additive were prepared in PowerCHO 2CDM media, and they were diluted to 1X concentration and used in main culture experiment (Table 5-2).

To compare the effects of 10 additives for cell culture, each 10 kinds of media additives and the control group (e.g., no additives were added to basal medium, either PowerCHO 2CDM or FortiCHO in a 125-ml Erlenmeyer flask, resulting in total 22 experimental groups. Four mM of glutamine was added to each basal medium, and the AH16 producing stable cell was inoculated to be a concentration of 2 x 10^5 cells/ml to in a total volume of 25 ml.

Evaluations for the selection of basal medium were based on the cell survival and productivity. Seven and 10 days after the cell culture started, the cell number and survival rate were measured by trypan blue staining, and the concentration of antibody was measured by IgG ELISA method, as described above.

Table 5-2. Concentrates of media additives for AH16F1-3-14-80-26 cells.

Additives (Abbreviation)	Conc. of 10X concentrates (g/L)	Test conc. (g/L)
HYPEP 5603 (5603)	50	5
Soytone (SOY)	50	5
HYPEP 7504 (7504)	50	5
Cotten CNE 50M (CNE)	50	5
Sheff-CHO Plus ACF (Plus PF)	50	5
HYPEP 1510 (1510)	50	5
HYPEP 4601 (4601)	50	5
TC yeastolate (TC)	50	5
Cell Boost5 (C.B 5)	50	3.5
Cell Boost6 (C.B 6)	50	3.5

5.2.11 Determination of a ratio for the composition of media additives

To test the mixture ratio of 3 kinds of single additives (HYPEP 4601, Sheff-CHO Cell Boost5 ACF and Plus) selected from the culture test earlier, it was designed as Table 5-3.

According to the design of the additives mixture ratio (as Table 5-3), each 10 combinations were added to basal medium, either PowerCHO 2CDM or FortiCHO in a 125-ml Erlenmeyer flask, resulting in total 20 experimental groups. The AH16 producing stable cell was inoculated to be a concentration of 2 x 10^5 cells/ml

in a total volume of 25 ml.

Evaluations for the selection of media additives were based on the cell survival and productivity. After 7, 10 and 12 days of the cell culture, the cell number and survival rate were measured by trypan blue staining, and the concentration of antibody was measured by IgG ELISA method as described above.

Ten cultured fluids of 12-day in PowerCHO 2CDM media were filtered with 0.2 μm filter, and the concentrations of the antibody IgG was measured by using Protein A-HPLC. And the optimal mixture ratio of additives was determined using the JMP program for mixture analysis based on the measured antibody concentrations.

Table 5-3. Mixture ratio of media additives for AH16F1-3-14-80-26 cells.

Flask No.	HYPEP 4601 (g/L)	Sheff-CHO Plus ACF (g/L)	Cell Boost5 (g/L)
1	5	0	0
2	0	5	0
3	0	0	3.5
4	2.5	2.5	0
5	0	2.5	1.75
6	2.5	0	1.75
7	1.7	1.7	1.2
8	2	2	0.7
9	2	1	1.4
10	1	2	1.4

5.2.12 Determination of schedule for addition of media additives mixtures

The schedule test for addition of additives was performed in the conditions as follows (Flask No. 1: Only once at 3 days after seeding; Flask No. 2: Three times at 3, 6, 9 days after seeding; Flask No. 3: Three times at 4, 7, 10 days after). Four mM of glutamine was added to the PowerCHO 2CDM basal media, the recombinant human albumin was added at a final concentration of 250 mg/L on 7 days after culture. The AH16-producing stable cells were inoculated to be a concentration of 2 x 10^5 cells/ml in a total volume of 100 ml in a 500-ml Erlenmeyer flask. After 3 days of culture, the cell concentration, survival rate and metabolism analysis were periodically checked, and the glucose concentration of the culture was maintained to more than 2 g/L by adding glucose stock solution when the glucose concentration was lower than 3 g/L.

5.2.13 Samples for purification, resins, column, equipment, and reagents (Protein A process)

Samples for purification were 80 ml of the perfusion culture fluid of an AH16-F1 cell line, and the lists of resins, column, equipment, instruments and reagents were as follows.

- Resins used for Protein A resin screening test: MabSelect Xtra (GE), MabSelect Sure (GE), MabSelect Sure LX (GE), ProSep Ultra Plus (Merck Millipore), Absolute High Cap Protein A (Novasep), Protein A ceramic Hyper D_F (Pall).

  The resins were prepared in a 5 × 50 (1 ml) column using column packing ATOLL's service.
- Columns used for Protein A-based process study: MabSelect Xtra (GE) 5 ml prepacked column, Q Sepharose FF (GE) 5 ml prepacked column, SP Sepharose HP (GE) 5 ml prepacked column.
- Equipments and instruments: AKTA purifier(GE), AKTA Avant 150 (GE), conductivity meter(IsTek), pH meter (Mettler), stirrer (corning), balance (Mettler)
- Reagents: 10X PBS pH7.4 (Gibco), citric acid (Sigma), sodium citrate (Sigma), Trizma base (Merck), sodium hydroxide (Merck), sodium di-hydrogen phosphate monohydrate (Merck), ethanol (Merck), di-sodium hydrogen phosphate dihydrate (Merck), sodium chloride (Merck)

5.2.14 Small-scale purification using Protein A and non-Protein A resin (column)

Since a pre-run procedure is generally recommended, each column was pre-run prior to the sample loading, as the real process.

The same purification method was applied to 6 proteins A columns. A flow rate was 1 ml/min and steps for purification were as follows.

Step 1. Equilibration: 10 CV (column volume: packed resin volume) of 1X PBS (pH 7.4) was applied to equilibrate the column.

Step 2. Sample loading: Using the AH16-F1 stable cell line, loading perfusion culture fluid 80 ml.

Step 3. Washing unbound proteins: The column was washed with 20 CV of PBS (pH 7.4) to remove non-specifically bound compounds.

Step 4. Gradient elution: [A buffer: 1X PBS pH 7.4 /B buffer: 100 mM citrate pH 3.0] A gradient of B buffer to A buffer in 10 CV was applied to elute the target protein in fractions. 3.5 ml, corresponding to one-fourth volume of the elution fraction, of 1M Tris-HCl, pH 9.0 was added to each collection tube prior to elution to immediately neutralize the elution fractions.

Step 5. Hold: 5 CV of 100 mM citrate (pH 3.0) was applied to the column in order to elute any remaining residual target protein. If elution peak tailing appeared, put holding step and prevent loss of samples, but in this experiment peak tailing was not observed.

Step 6. Re-equilibration/CIP/storage: 10 CV of PBS, pH 7.4 was applied in order to re-equilibrate the column, and CIP

was performed as described in the manual. The column was filled with the storage buffer and stored at 4°C.

5.2.15 Analysis of intermediates and final purified products

Purity of the sample during the purification steps was analyzed by SDS-PAGE, SEC-HPLC, and UV absorption spectrometry (at 280 nm). For SDS-PAGE analysis, NuPAGE 3~12% Bis-Tris gel (1.0 mm, 10 well; Invitrogen) was used. After loading 10 μg of proteins onto each well, the gel was run for 60 minutes at 150 V (constant voltage) under reducing and non-reducing conditions.

Absorbance of the protein was measured at 280 nm using Gen5 2.00 (BioTek, USA), and the protein concentration was calculated using the mass extinction coefficient for IgG.

5.2.16 Structural analysis and identification tests

The "Specifications and Analytical Procedures" and its analytical test items for characterization and analysis of AH16 API were summarized in Table 5-4.

Table 5-4. The "Specifications and Analytical Procedures" items and methods.

Test item	Purpose	Test methods and Equipment	References
1. Appearance	-	N.A.	
2. pH	measurement	General test for "measurement of pH"	(Korean Pharmacopoeia)
3. Endotoxin	measurement	LAL (Limulus Amebocyte Lysate) test - Endosafe®-PTSTM Kit (Charles river, PTS 100)	(USPC, 2005; Yamamoto et al., 2000)
4. Identification test (Structure analysis & identification)			
1) Peptide mapping	N-term, C-term identification	Peptide mapping analysis - HPLC (Waters, e2695) - Column (Grace Vydac, 218 GK54 C_{18})	(Anneli and Basant, 1994)
2) Capillary isoelectric focusing (c-IEF)	Isoform distribution	c-IEF (Beckman Coulter, PA 800 plus)	(Beckman Coulter, 2011)
3) SDS-PAGE	Identification	SDS-PAGE - XCell SureLock Mini-Cell (Invitrogen, E10001)	
5. Purity test			
1) Capillary electrophoresis (CE)-SDS	Purity analysis	CE-SDS Capillary Electrophoresis (Beckman Coulter, PA 800 plus)	(Beckman Coulter, 2011)
2) Size exclusion (SE)-HPLC	Purity analysis	SE-HPLC (Waters, e2695) - Column (TOSOH, TSK-GEL G3000SW_{XL})	

3) Cation exchange (CEX)-HPLC	Purity analysis	CEX-HPLC (Waters, e2695) - Column (Dionex, ProPac WCX-10 Analytical)	(Harris et al., 2001; Moorhouse et al., 1997)
4) Host cell protein (HCP)	Host cell derived peptide analysis	ELISA (BioTek, Microplate reader)	
5) Host cell DNA (HCD)	Host cell derived DNA analysis	ELISA (Molecular Devices, FlexStation 3 Benchtop)	
6. Contents test	Quantity of the active ingredient	UV absorbance at 280 nm (Molecular Devices, SpectraMax Plus384)	(Korean Pharmacopoeia, UV absorbance determination)
7. Potency test (*in vitro* assay)			
1) NCI-N87	Anti-proliferative activity	WST-8	(Gong et. al, 2004)
2) BT-474	Anti-proliferative activity	WST-8	(Gong et. al, 2004)

5.3 Results and Discussion

5.3.1 Construction of the AH16 expression vector

An expression vector named pCLS05AH16F1 was invented in order to produce HER2 antibody AH16, a biobetter of Herceptin. In order to enhance productivity, two copies of CSP-B 5' SAR were inserted into the vector consisting of a CMV promoter, a dhfr gene, a neomycin resistance gene, a pUC origin and an ampicillin resistance gene. The dhfr gene makes the cells transfected have resistance to MTX in culture medium and then helps the cells survive and the target gene within the vector be amplified in chromosomes.

To ensure that an accurate manufacturing of the pCLS05AH16F1, enzyme mapping was performed by using enzymes such as Bam HI, Nhe I and Spe I (Fig. 5-2).

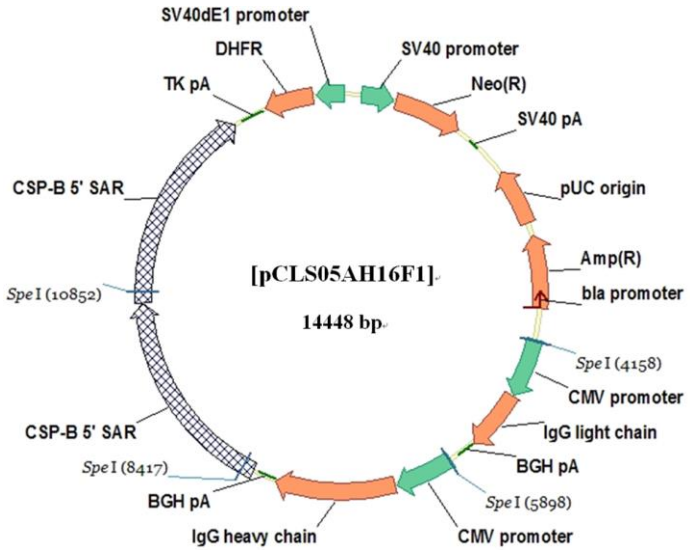

Fig. 5-2. Expression vector map of pCLS05AH16F1.

5.3.2 Selection of single colonies using ClonePix

After isolation of stable clones, the cells were diluted to 5 x 10^6 cells/well in the 6-well plate containing CloneMedi-CHO DHFR semi-solid media. After 2 weeks, the cultured cells were observed under a microscope and picked using ClonePix. Sixty eight clones were picked up among the 14,812 clones based on FITC level. The results were summarized in Table 5-5 and Fig. 5-3.

Table 5-5. Summary of clone picking.

Name	Count	Expression
Edge Excluded	6,207	IF Edge Excluded = True
Too Big	0	IF Total Area >= 0.7
Too Small	8,235	IF Total Area <= 0.05
Irregular 1	196	IF Compactness <= 0.45
Irregular 2	57	IF Axis Ratio <= 0.45
Proximity	36	IF Proximity <= 0.4
Low FITC	13	IF [FITC 1s] Exterior Mean Intensity <= 1,470.970 AND [FITC 1s] Interior Mean Intensity <= 210
Accept	68	Anything else
Sum	14,812	

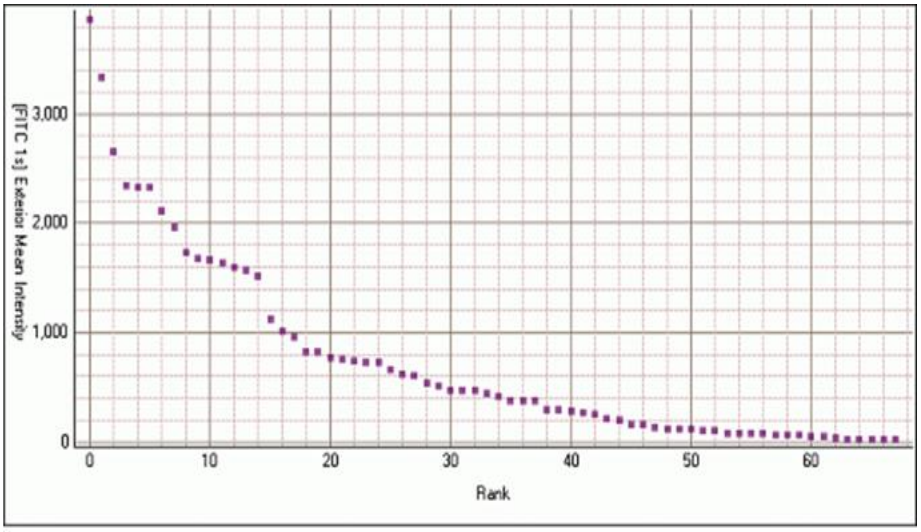

Fig. 5-3. Ranking plot in ClonePix.

5.3.3 Selection of amplified clones using MTX

The picked 68 clones were cultured for 2 weeks and the growth media were added. To estimate productivity of the clones, ELISA was performed. As a result (Table 5-6), the top 20% of clones were transferred to 24-well plates and cultured. When the cells in the well reached 90% confluent, ELISA was performed with the cell culture media to determine productivity (Table 5-7). Based on the productivity, the top 15% of the clones were selected and cultured in 6-well plates.

When the cells were cultured to 90% confluent in the well, the media were collected for ELISA determination of productivity. High expressed 15% clone were selected in the group (Table 5-8), they were inoculated at 3 x 10^5 cells/ml in 125-ml flasks containing 30 ml CD FortiCHO media with 500 μg/ml Geneticin, 4 mM L-glutamine. The cells were incubated at 37°C, in 5% CO, with orbital shaking at 110 rpm and the specific growth (μ) and productivity (q) (Table 5-9) were measured. AH16F1-3-11 and AH16F1-3-14 clones were selected based on both μ and q values.

Table 5-6. ELISA for IgG from cell culture supernatants in 96-well plates.

Sample ranking	Conc. (μg/ml)	FITC Exterior Mean Intensity	Well confluency	Sample ranking	Conc. (μg/ml)	FITC Exterior Mean Intensity	Well confluency
14	**1.70**	1566.59	90 %	7	0.18	2107.69	10 %
3	**0.94**	2651.42	90 %	30	0.15	512.566	90 %
2	**0.93**	3329.29	80 %	49	0.15	121.207	50 %
24	0.89	733.195	10 %	48	0.13	125.539	90 %
4	0.88	2343.42	90 %	22	0.11	760.974	40 %
9	0.79	1731.36	5 %	58	0.10	66.481	20 %
13	0.76	1600.74	10 %	46	0.10	162.931	10 %
20	0.67	819.171	20 %	43	0.10	258.918	10 %
5	0.60	2335.93	40 %	6	0.09	2331.56	10 %
11	**0.56**	1668.25	5 %	36	0.09	379.492	5 %
29	0.46	533.723	30 %	34	0.09	442.091	5 %
17	0.41	1019.13	20 %	62	0.08	43.032	5 %
47	0.38	162.618	30 %	45	0.06	193.188	5 %
31	0.32	471.043	10 %	63	0.06	42.36	10 %
10	0.26	1680.49	30 %	35	0.06	409.971	20 %
21	0.24	765.695	90 %	55	0.05	79.435	10 %
28	0.22	604.682	20 %	57	0.05	75.473	10 %
12	0.22	1643.07	10 %	23	0.04	741.56	30 %
15	0.21	1519.55	20 %	53	0.03	100.423	50 %
19	0.19	826.292	20 %	68	0.02	24.119	20 %
32	0.19	467.444	40 %	41	0.02	276.487	90 %
59	0.19	59.919	80 %	42	0.02	268.561	5 %
52	0.19	109.98	90 %	26	0.02	653.685	10 %

Table 5-7. ELISA for IgG from cell culture supernatants in 24-well plates.

Sample	IgG conc. (μg/ml)	Well confluency (%)	Sample	IgG conc. (μg/ml)	Well confluency (%)
AH16F1-3-11	129.75	100	AH16F1-3-39	6.24	90
AH16F1-3-14	106.70	100	AH16F1-3-21	5.23	10
AH16F1-3-20	46.24	50	AH16F1-3-3	4.69	50
AH16F1-3-1	35.99	80	AH16F1-3-2	3.70	30
AH16F1-3-31	20.21	60	AH16F1-3-12	3.43	50
AH16F1-3-30	15.94	60	AH16F1-3-22	3.01	20
AH16F1-3-59	13.42	90	AH16F1-3-32	2.67	30
AH16F1-3-24	12.64	50	AH16F1-3-34	1.66	80
AH16F1-3-44	11.30	90	AH16F1-3-4	1.59	40
AH16F1-3-9	11.29	80	AH16F1-3-42	0	20
AH16F1-3-5	10.44	10	AH16F1-3-68	0	20
AH16F1-3-48	10.17	90	AH16F1-3-5	0	10
AH16F1-3-49	10.10	90	AH16F1-3-21	0	10
AH16F1-3-16	9.97	100	AH16F1-3-22	0	10
AH16F1-3-52	9.41	40	AH16F1-3-30	0	20
AH16F1-3-53	8.08	40	AH16F1-3-32	0	10
AH16F1-3-13	8.06	80	AH16F1-3-41	0	100
AH16F1-3-10	6.86	90	AH16F1-3-53	0	10

Table 5-8. ELISA for IgG from cell culture supernatants in 6-well plates.

Sample	IgG conc. (μg/ml)	Well confluency (%)
AH16F1-3-11	105.50	100
AH16F1-3-14	102.20	100
AH16F1-3-3	92.49	100
AH16F1-3-59	48.28	100
AH16F1-3-48	32.67	100
AH16F1-3-49	27.22	100
AH16F1-3-52	20.40	100
AH16F1-3-4	18.85	100

Table 5-9. ELISA for IgG from cell culture supernatants in 125-ml Erlenmeyer flasks.

Sample	IgG conc. (μg/ml)	Cell conc. (cells/ml)		μ	q (pg/cell/day)
		Day 0	Day 12		Δtiter/ΔIVC
AH16F1-3-11	150.0	$3.0x10^5$	$4.3x10^6$	0.24	9.08
AH16F1-3-14	183.3	$3.0x10^5$	$5.0x10^6$	0.23	9.14

5.3.4 MTX amplification

AH16F1-3-14-11 and AH16F1-3-14 clones were diluted at 3 x 10^5

cells/ml in 125-ml Flasks containing 30 ml of CD Opti CHO media with 500 μg/ml Geneticin and 20 nM or 80 nM MTX. The flasks were placed on an orbital shaker platform rotating at 110 rpm at 37°C, in a humidified 5% CO_2. After MTX amplification, the media were harvested and ELISA was performed for comparison of productivity. AH16F1-3-14 with 80nM MTX showed a higher production (Table 5-10). Therefore, AH16F1-3-14-80 clone was selected for further subcloning.

Table 5-10. Comparison of antibody productivity of clones amplified with MTX (IgG conc.: μg/ml).

Clone no.	0 nM	20 nM	80 nM
AH16F1-3-11	150.5	162.9	101.9
AH16F1-3-14	183.75	-	198.4

5.3.5 Selection of single clone using ClonePix

After selection, AH16F1-3-14-80 cells were inoculated at 1 x 10^3 cells per well in 6-well plates containing CloneMedi-CHO DHFR semi-solid media. The cells were cultivated for 2 weeks and single colonies were isolated using ClonePix. Eighty cells were picked up among 18,373 cells based on FITC level (data not shown).

5.3.6 Selection of stable clone AH16F1-3-14-80-23

Eighty clones were cultured in 96-well plates containing the growth media for 2 weeks. In order to measure the antibody titers in 96-well plates, ELISA was performed with the media (Fig. 5-4). The clones were scaled up from 24-well to 6-well plates and 125-ml flasks. Each of the steps, the productivity was measured using IgG ELISA (Fig. 5-5, 6, 7). After comparing antibody titers, 4 top producing antibody clones (AH16F1-3-14-80-13, 15, 17 and 26) were selected. Both of the specific growth (μ) and the specific productivity (q) were measured to select the final clone among the 4 clones (Fig. 5-8, 9). Based on the result, AH16F1-3-14-80-26 was finally selected as a stable cell line (Table 5-11 and Fig. 5-10).

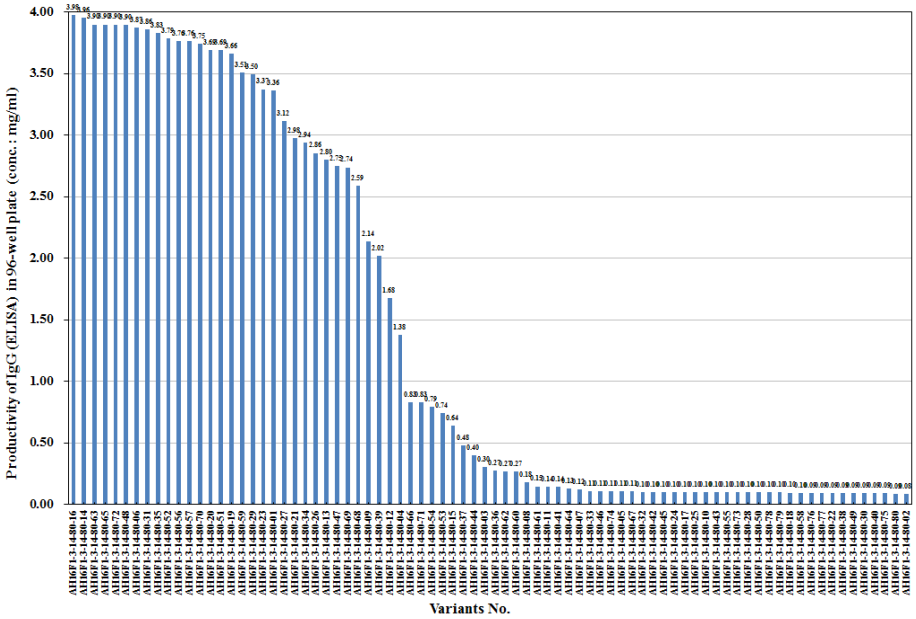

Fig. 5-4. AH16F1 antibody titers in 96well plates.

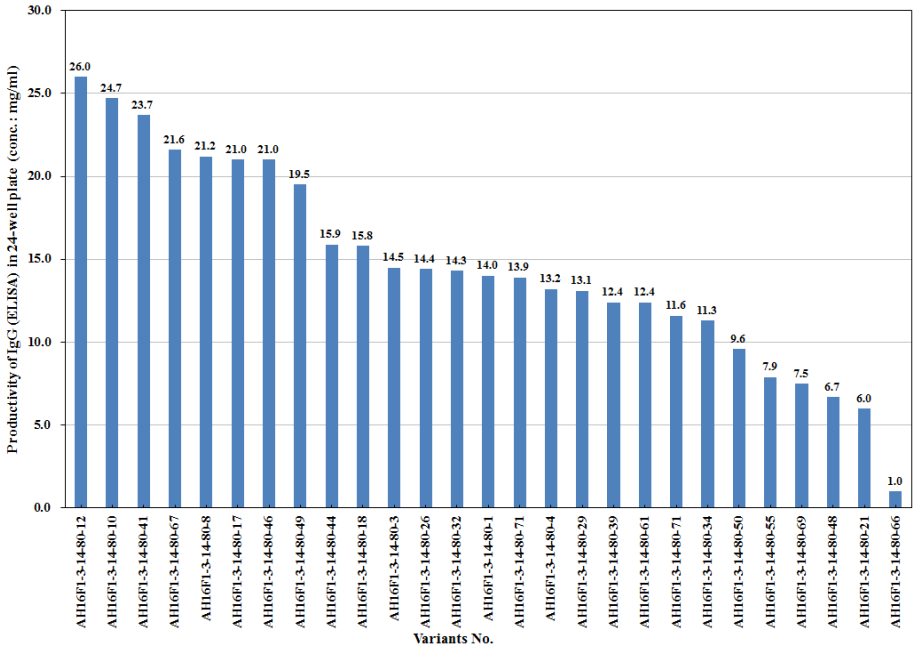

Fig. 5-5. AH16F1 antibody titers in 24-well plates.

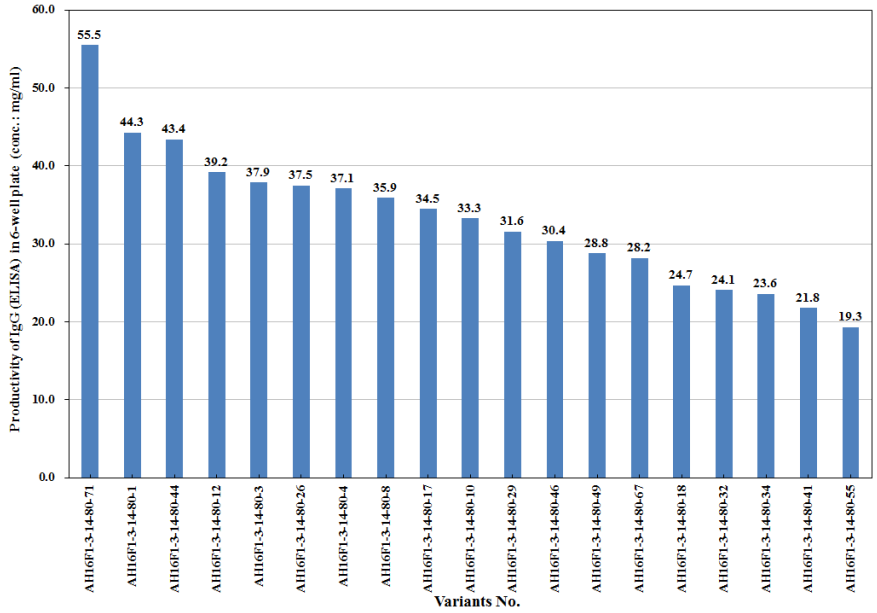

Fig. 5-6. AH16F1 antibody titers in 6-well plates.

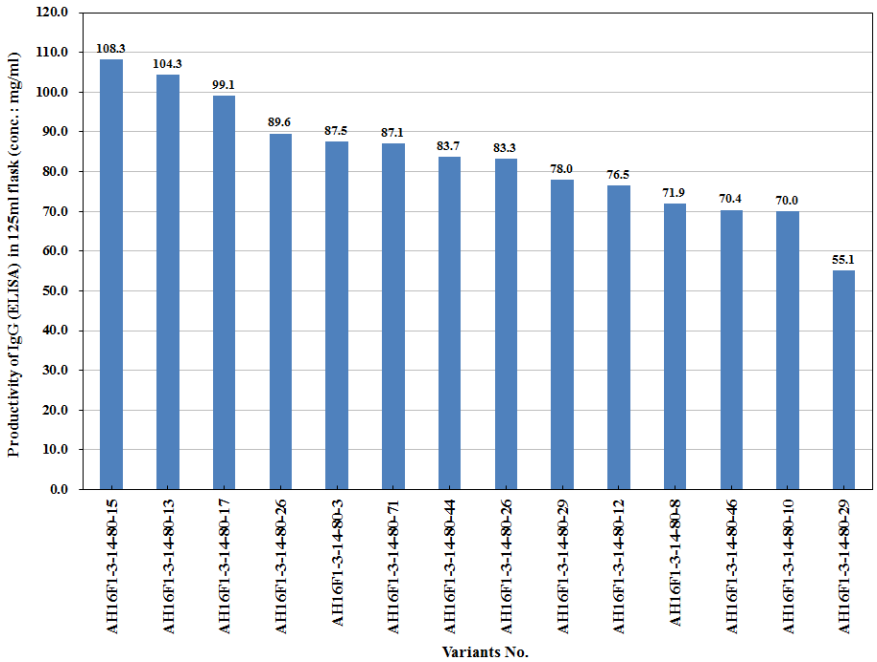

Fig. 5-7. AH16F1 antibody titers after 7 days of culture in 125-ml flasks.

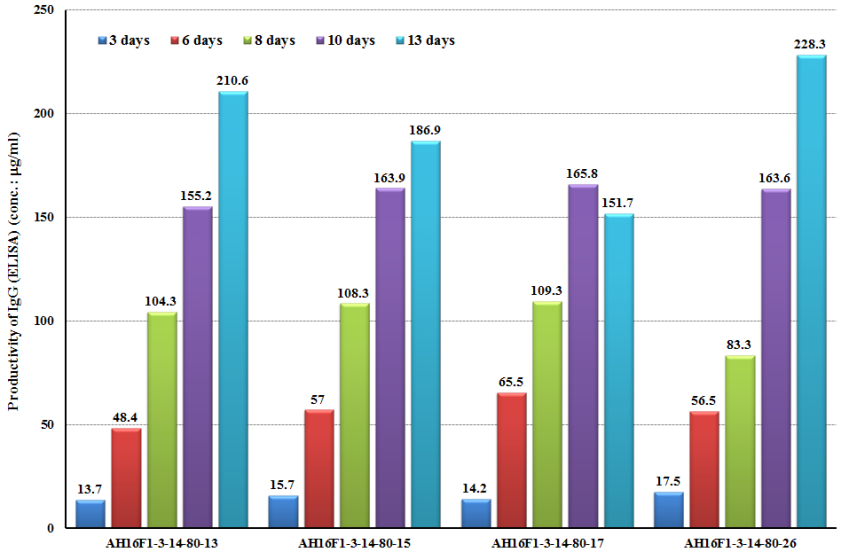

Fig. 5-8. Comparison of antibody productivity of 4 each clones.

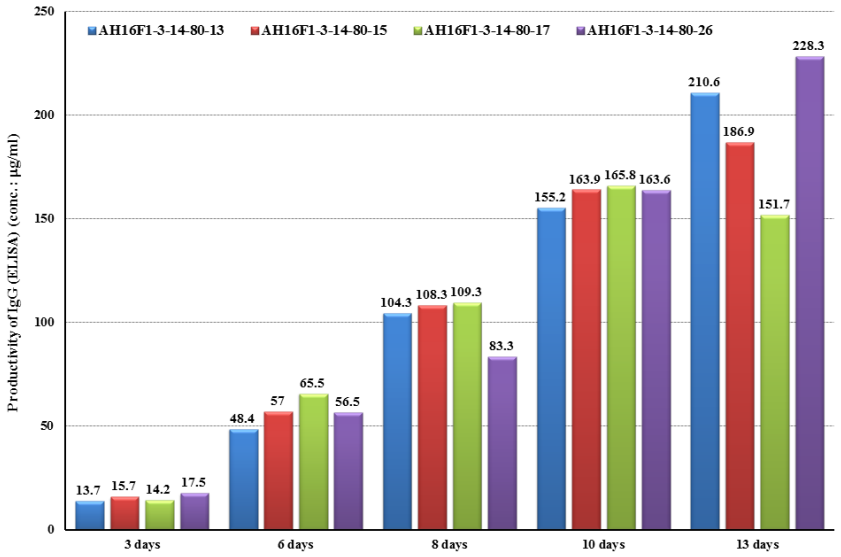

Fig. 5-9. Comparison of antibody productivity of 4 clones for each days.

Table 5-11. Comparison of specific growth rate (μ) and specific productivity rate (q, pcd) of selected 4 clones.

Clones	μ	q (pg/cell*day)
AH16F1-3-14-80-13	0.42	10.11
AH16F1-3-14-80-15	0.37	13.40
AH16F1-3-14-80-17	0.42	14.99
AH16F1-3-14-80-26	0.35	19.29

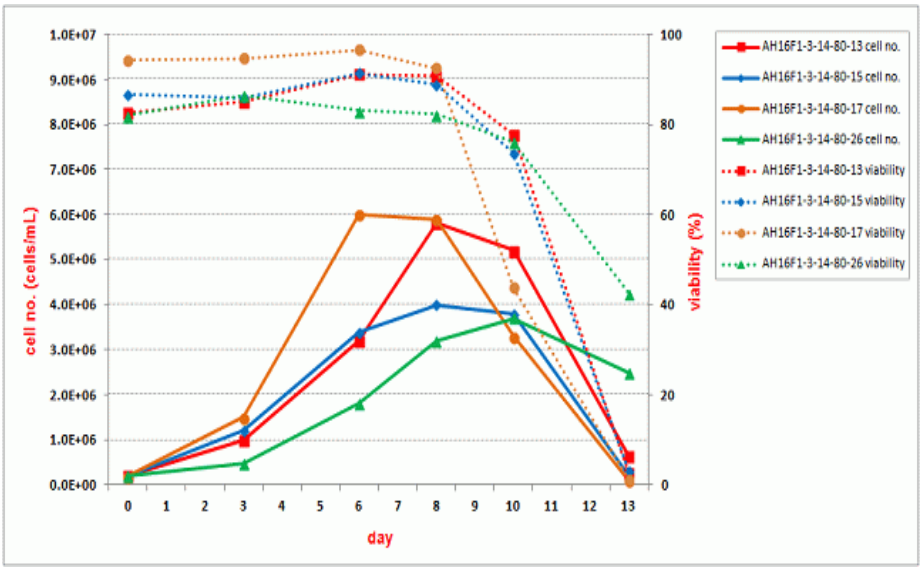

Fig. 5-10. Cell density and viability of the selected 4 clones during culture: Comparison of viability and the number of cells during culture, specific growth rate (μ) of selected 4 clones.

5.3.7 Assessment of the stability of the cell line producing AH16 over passages

To assess stability of the selected "stable cell line", AH1F1-3-14-80-26 expressed AH16F1, the productivity and growth rate were measured through long-term culture (15 passages) as described above.

The ELISA was performed for measuring antibody titers after 10, 11 and 12 days of culture. In the same way as above, the antibody titers ranged from 180 μg/ml to 245 μg/ml through 15 passages. The stably maintained antibody titer indicated the long-term stability of the cell clone (Fig. 5-11).

To determine the growth curve (or stability) of the stable cell clone AH16F1-3-14-80-26 during cell passages, both of viability and concentration of the cells were measured using trypan blue. By the results, the growth curve and survival rates at passage number 1, 5, 10, and 15 were very similar (Fig. 5-12).

Also, the antibody production at the 10, 11, and 12 days of 1~15 passages were consistently maintained to 180~220 μg/ml. Therefore, the antibody production and growth rate had been consistently maintained, which verified stability of the clone. Therefore, the AH1F1-3-14-80-26 clone can be suitable for large-scale manufacturing for production of the clinical antibody product.

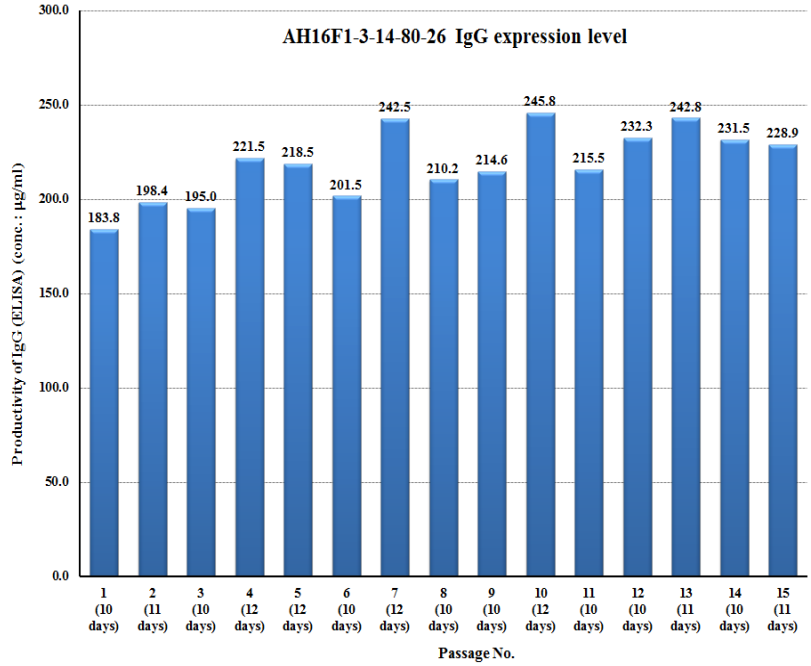

Fig. 5-11. IgG productivity of the stable cell line AH16F1-3-14-80-26 clone during cell passages.

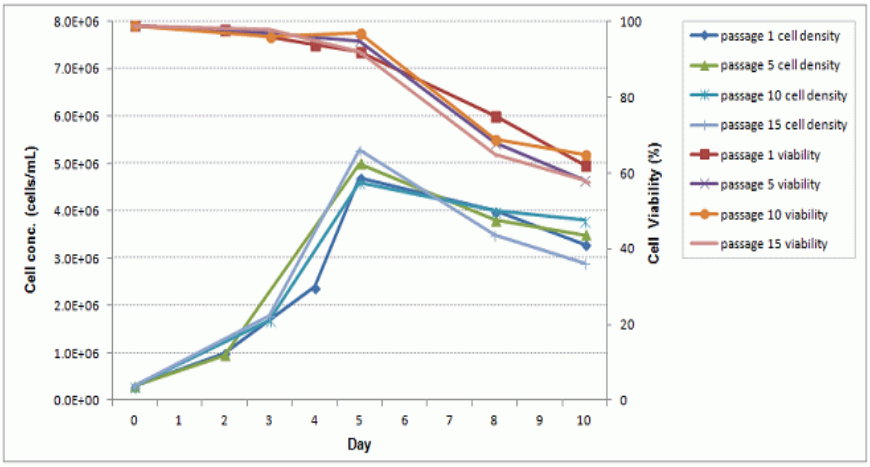

Fig. 5-12. The growth and viability curves of the stable cell clone AH16F1-3-14-80-26.

5.3.8 Selection of the basal media for the culture of the stable cell AH16F1-3-14-80-26

Based on IgG productivity at 7 days of culture, the PowerCHO 2CDM was selected as a basal medium among 5 basal media as shown in Fig. 5-13. However, other tests such as determination of mixture ratio of additives were compared to the results from using the basal media CD FortiCHO.

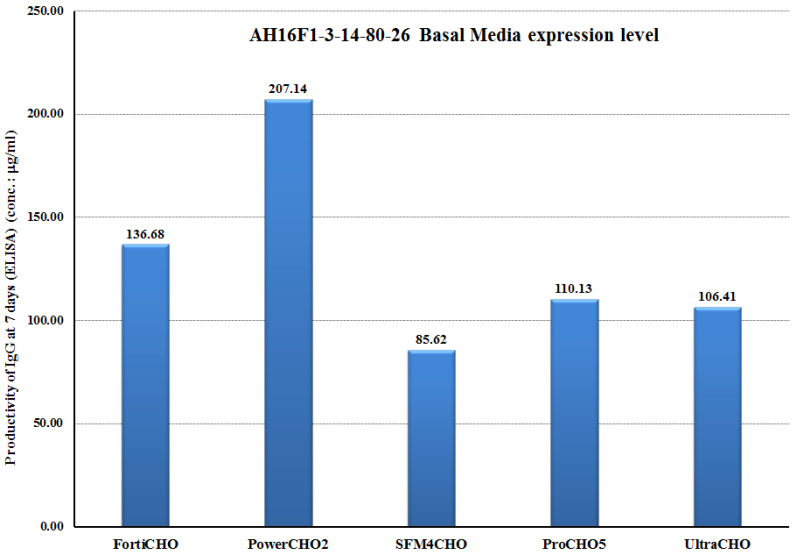

Fig. 5-13. AH16 expression levels in basal media.

5.3.9 Effects of single additives for AH16 production in basal media PowerCHO 2CDM

Cell growth, survival rate and AH16 productivity were assessed through the screening of 10 additives in basal media PowerCHO 2CDM, the additives Cell Boost5 (abbreviated as C.B 5) in PowerCHO 2CDM media showed the best performance in the maintenance of cell growth and viability of the stable cell line AH16F1-3-14-80-26 clone as well as in the production of the AH16 antibody (data not shown).

5.3.10 Productivity of media additives mixture in basal media PowerCHO 2CDM at 12 days

AH16 productivity of 12 days was determined using Protein A-HPLC to screen media additives mixture in basal media PowerCHO 2CDM. The additives mixture combination No. 2 (abbreviated as Combi. 2 : HYPEP 4601 zero g/L, Sheff-CHO Plus ACF 5 g/L, Cell Boost5 zero g/L) and No.5 (abbreviated as Combi. 5 : HYPEP 4601 zero g/L, Sheff-CHO Plus ACF 2.5 g/L, Cell Boost5 1.75 g/L) showed better outcomes (Table 5-12).

Table 5-12. IgG productivity related to the ratio of media complex additives in basal media PowerCHO 2CDM .

Combination No.	Protein conc. (μg/ml)
1	398
2	598
3	372
4	533
5	585
6	370
7	541
8	555
9	559
10	546

5.3.11 Determination of the ratio for combination of additives in basal media PowerCHO2

AH16 productivity of 10 arbitrarily designed media additives mixture combination in basal media PowerCHO 2CDM is as shown in Table 5-12. However, the best optimal combination ratio that was not designed yet, the best optimal combination ratio was calculated by statistical analysis program JMP (SAS Co., USA) using the productivity data measured by Protein A-HPLC at 12 days.

The best optimal combination ratio of 3 media additives was determined as HYPEP 4601 : Sheff-CHO Plus : Cell Boost5 = 0.0024 : 0.7290 : 0.2685. So, it could be converted as HYPEP 4601 : Sheff-CHO Plus ACF : Cell Boost5 = 0.0012 g/L : 3.6 g/L : 1.3 g/L in the actual concentration of 5 g/L additives mixture (Fig. 5-14).

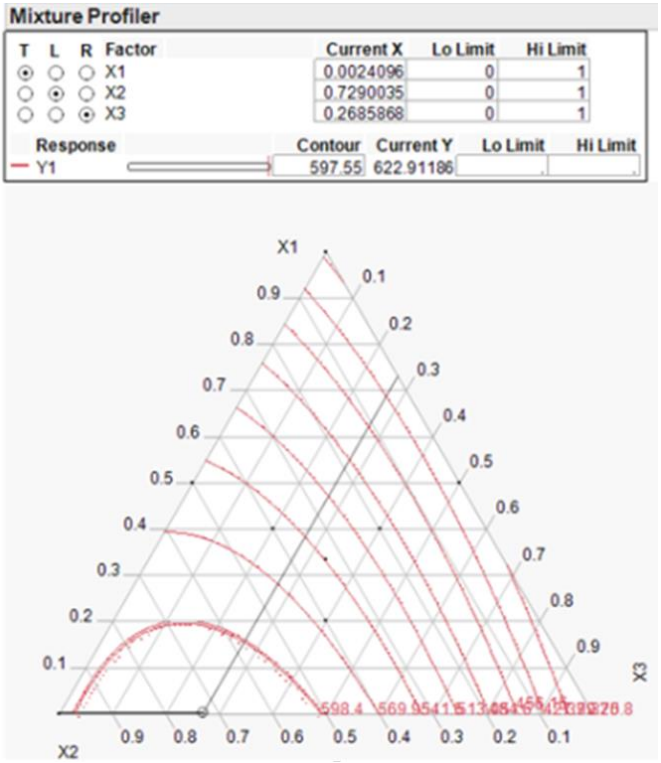

Fig. 5-14. The optimal ratio of media complex additives by JMP analysis.

5.3.12 The schedule determination for addition time

The productivity of AH16 was obtained to approximately 1.3g/L in the flask culture when the optimized combination mixture of 3 additives (HYPEP 4601, Sheff-CHO Plus ACF, Cell Boost5) calculated by JMP analysis was added at 3, 6, and 9 days of culture and when the glucose concentration in culture was kept to more than 2 g/L (Fig. 5-15).

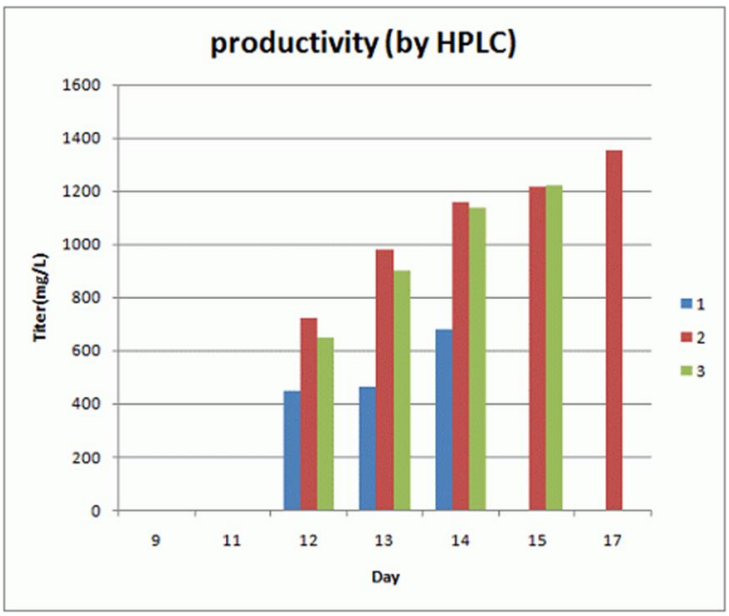

Fig. 5-15. IgG productivity depending on the addition of the media complex additives at 3, 6, 9 days after inoculation of AH16-producing stable cells in PowerCHO 2CDM. (1, at 3 days; 2, at 6 days; 3, at 9 days)

5.3.13 Summary of Protein A resin selection on a small scale

To select a more appropriate Protein A resin, 6 kinds of Protein A column were compared with purity and ligand leaching, MabSelect Sure and MabSelect Sure LX of GE healthcare showed the best performance (Table 5-13).

Table 5-13. Comparison summary of Protein A-based resins.

No.	Protein A resin	Purity (%)	Leached ligand (PPM)	Yields (%)	CIP (NaOH durability or endurance)
1	MabSelect Xtra	97.3 (4)	19.2 (2)	88.2 (1)	Medium
2	MabSelect Sure	98.3 (1)	8.1 (1)	81.7 (4)	High
3	MabSelect Sure LX	98.2 (2)	19.8 (3)	81.3 (6)	High
4	Prosep Ultra Plus	96.3 (6)	70.8 (5)	83.2 (2)	Low
5	Absolute High Cap	96.6 (5)	67.5 (4)	83.0 (3)	Medium
6	Protein A Ceramic HyperD_F	97.4 (3)	968.4 (6)	81.6 (5)	Medium

* The number in parentheses is ranking.

5.3.14 Evaluation of process yield and purity in Protein A-based small-scale purification study

The process was validated with culture fluids from three different cell lines. The products purified using MabSelect Sure column were diluted and loaded onto the second (Q Sepharose FF) and the third (SP Sepharose HP) columns connected in series. After loading, the second column was removed and purification was performed. The average yield and purity through 3 step purification processes were of 93.8% and 99.9%, respectively (Table 5-14), indicating a very effective purification process was developed.

Table 5-14. Protein A-based purification process and evaluation of yield and purity.

Protein A based 3 step purification process								
Sample	Before purification (Culture filtrate)			Purified sample			Yields (%)	Purity (%) **
	Conc. (mg/ml)	Vol. (ml)	IgG amount (mg) *	Conc. (mg/ml)	Vol. (ml)	IgG amount (mg) *		
Hu 1-8-80-9	0.194	40	7.8	0.479	15	7.2	92.6	99.93
Hu 1-8-80-28	0.305	40	12.2	0.764	15	11.5	93.9	99.86
Hu 1-8-80-29	0.384	40	15.4	0.972	15	14.6	94.9	99.89

* IgG amount (mg): estimated by Protein A HPLC

** Purity (%): analyzed by SEC-HPLC

5.3.15 Analysis of non-protein A-based small-scale purification process

Non-protein A-based purification process using SP Sepharose HP column was evaluated by SEC-HPLC (purity was 97.5%, data not shown) and the final yield. The final yield in the first step (capture) using SP Sepharose HP column was 99.4% (Table 5-15).

In general, it is known that non-protein A-based purification is inferior to protein A-based process on the yield and purity, but in this study, the first step (capture) in purification processes was able to be established with high purity and high efficiency.

Table 5-15. Analysis of small-scale non-protein A-based purification processes.

	A_{280}	LC quantification (μg/ml)	Volume (ml)	IgG quantity (mg)
Loading	0.575	119.2	250.0	29.8
Flow through	0.663	ND	1,921.0	ND
Elution peak 1	0.844	548.8	54.0	29.6
Elution peak 2	0.070	1.3	50.0	0.064
Strip	0.011	0.3	20.0	0.007
Yields	99.4%			

ND: not determined

5.3.16 Determination of molecular mass of AH16 using Q-TOF MS

The average molecular mass of AH16 was analyzed by Q-TOF mass spectrometer. In general, protein appears in multiple charge states in mass spectrometry, +40~+66 multi-charged mass ions were observed in total ion chromatogram (TIC) of AH16 (Fig. 5-16). The multiple charged ions were deconvoluted using MaxEnt to determine a molecular weight of AH16.

Mass ions having from +43 to +74 charges were analyzed by deconvolution using MaxEnt (maximum entropy) analysis tool (MaxEnt Solutions Ltd, UK) (Ferrige et al., 1991), and the expected molecular structure was predicted and the molecular weight of AH16 was calculated (Fig. 5-17). The molecular weight of AH16 was estimated as 148,408.92~148,921.42 Da, and it was about 2,535.20~3,047.70 Da larger than that of the predicted molecular weight (145,873.72 Da). And the difference seemed to be attributed to glycosylation of AH16.

Deconvolution of a multiple-charged mass spectrum confirmed the molecular weight of AH16 is 148,408.92 ~ 148,921.42 Da (Fig. 5-17). Major structure of AH16 protein was "glycosylation G0F N(2)-Lysine C-term (2)" (two glycosylated sites lacking galactose, called G0F, and two c-term lysine residues)

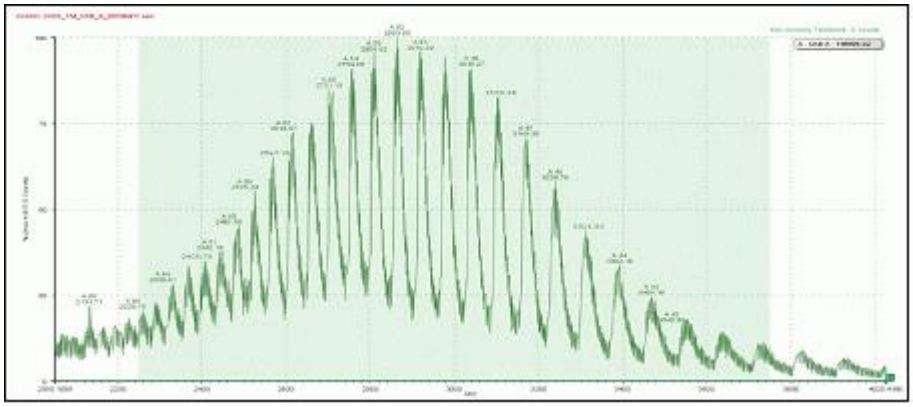

Fig. 5-16. Total ion chromatogram of AH16. Molecular weight (total mass) of AH16 by the total ion chromatogram (TIC).

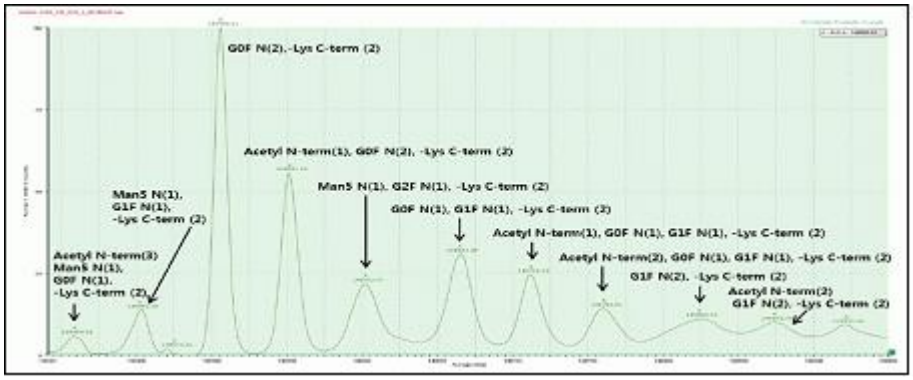

Fig. 5-17. Total mass deconvolution analysis of AH16.

5.3.17 Amino acids composition analysis of AH16

Amino acid composition analysis was performed and composition ratios of most amino acids were similar to theoretical values (Table

5-16). However, the composition ratio of tyrosine was less than the expected value due to oxidation during acid hydrolysis, and recovery yield of other amino acids were more than 90% and very similar to theoretical value.

Table 5-16. Amino acid composition of AH16.

Amino acid	Theoretical values (moles)	Estimated values (moles)	Yields (%)
Ala	72	72	100.0
Asx*	108	108.3	100.3
Glx*	124	124.3	100.2
Gly	84	84.1	100.1
Leu	98	97.1	99.1
Lys	92	90.6	98.5
Pro	94	93.6	99.6
Phe	46	45.6	99.1
Thr	110	109	99.1
Ile	28	27.7	98.9
Val	122	120.1	98.4
His	28	27.2	97.1
Ser	162	157.3	97.1
Arg	40	38.7	96.8
Met	8	7.3	91.3
Tyr	60	49.3	82.2

- Asx*: sum of Asn and Asp. - Glx*: sum of Gln and Glu.

5.3.18 N-Glycosylation structure analysis of AH16 using NP-HPLC

By results of identification of N-glycosylation sugar chain structure at Asn297 site of AH16 heavy chain, there are approximately 12 different peaks in the retention time range of 60~100 min. And N-glycosylation sugar chain structure was analyzed by comparing glucose unit (GU) value corresponding retention time of each peak (Fig. 5-18). N-glycosylation sugar chain structure at Asn297 of AH16 had 99% more bi-antennary sugar chain structure, and was predicted to have 62.6% fucosylated form (G0F) lacking galactose (Tab. 5-17), and the main peak was observed at retention time of 72.455 min.

It was predicted that the structures attached one galactose (G1F), and two galactose resides (G2F) were 26.4% and 3.91%, respectively. The fucosylated form of N-glycosylation sugar chain of AH16 was 93.5%, and the sialylated form of that was about 1.76%.

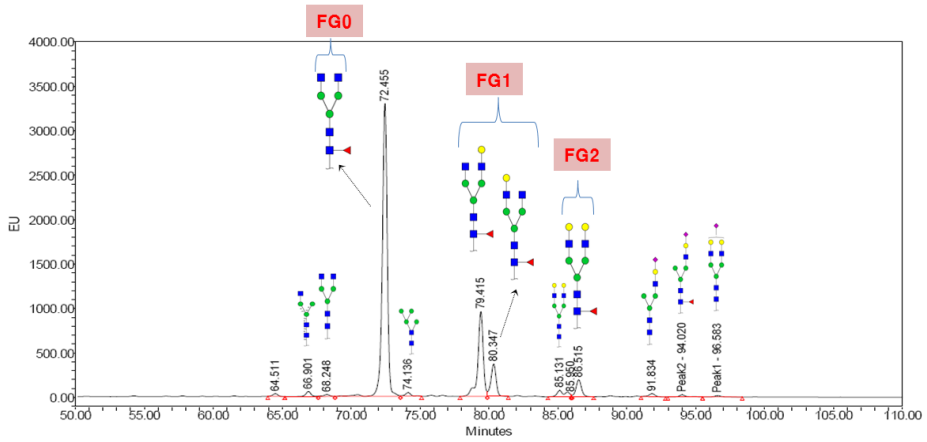

Fig. 5-18. N-glycosylation profiles of AH16.

◆ Sialic acid, ● Galactose, ■ N-acetylglucosamine,
● Mannose, ▲ Fucose

(After labeling with 2-aminobenzamide fluorescent dye derivatives, N-glycosylation of AH16 was analyzed using normal phase (NP) HPLC. The resulting 12 peaks were assigned glucose unit (GU) values by comparison with a 2-aminobenzamide (AB)-labelled dextran ladder (glucose homopolymer) (Routier et al. 1998; Melmer et al., 2010). The N-glycan of AH16 had predominantly the bi-antennary complex structure having 5 ~ 8 GU.)

Table 5-17. N-glycosylation pattern and ratio of AH16.

%	FG0	FG1	FG2	Sialylated type	High-mannose type	Fucosylated type
AH16	62.6	26.4	3.91	1.76	0.88	93.5

5.3.19 Physico-chemical properties : c-IEF analysis of AH16

The isomer heterogeneity and pI value of AH16 were measured. The pI value was in the range of 8.0~9.0, and 10 different isomers (isoform 1~10) were observed with a major peak at pI 8.60 (Fig. 5-19). There were approximately 2 basic (pI 8.68~8.72) and 7 acidic forms (pI 8.28~8.52) of AH16 observed. The isomers are related to the heterogeneity of glycoproteins commonly observed.

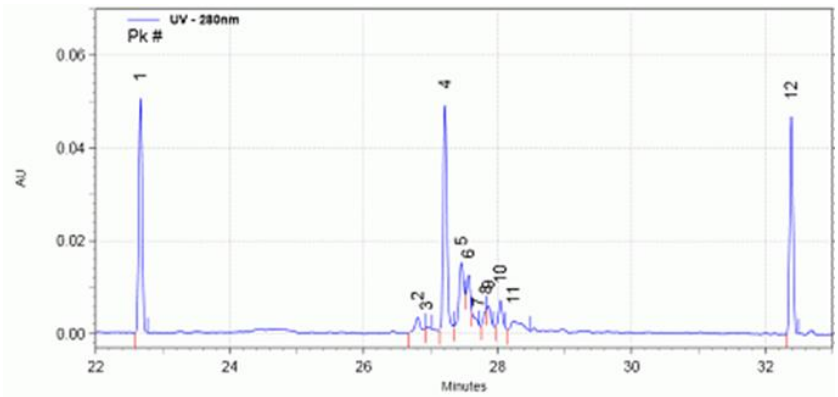

Fig. 5-19. c-IEF profile of AH16.

Peak 1, pI marker 10.0; Peak 2 ~ 11, AH16; Peak 12, pI marker 7.0

5.3.20 Purity analysis : SDS-PAGE of AH16

The purity and molecular weight of AH16 were determined using SDS-PAGE under reducing and non-reducing conditions. The main

peak was observed in the proximity of the intact 160 kDa IgG form under non-reducing conditions, and the heavy chain and light chain were identified as 50~60 kDa and 20~30 kDa under reducing conditions, respectively (Fig. 5-20).

Minor bands (shown in Fig. 5-20 A, B, C) were originated from the whole IgG and generated by the separation of heavy chain and light chain under denaturing conditions in SDS-PAGE analysis, but not under native conditions.

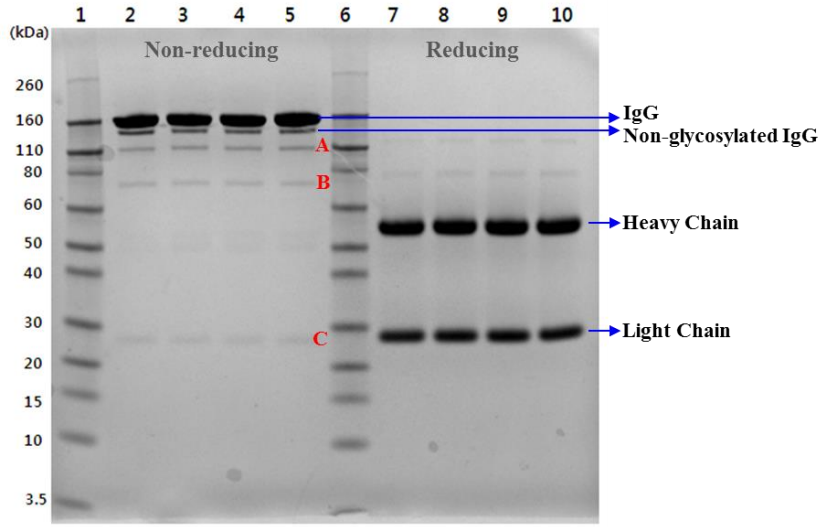

Fig. 5-20. Purity analysis: SDS-PAGE of AH16.

Lane 1, 6: Standard molecular weight marker

Lane 2, 7: AH16 (standard); Lane 3, 8: AH16 DS batch 1

Lane 4, 9: AH16 DS batch 2; Lane 5, 10: AH16 DS batch 3

A, 2HC + 1 LC; B, 1HC + 1 LC; C, LC

5.3.21 Specifications and Analytical Procedures of AH16 for quality control

Based on several experimental results, 12 different test items of AH16 standards API for quality control, their criteria (Table 5-18), and structural, physico-chemical, biological and immunological characteristics are shown in Table 5-19.

Table 5-18. Results of the Specifications and Analytical Procedures for AH16 (DS-16002, 1 batch only).

Test items	Acceptance criteria	Results
1. Appearance	Colorless and transparent solution	Adequate
2. pH	5.7 ~ 6.7	6.2
3. Endotoxin	< 10.00 EU/mg	< 5.92 EU/mg
4. Identification test		
1) Peptide mapping	Similar chromatogram with the standard	N.A.*
2) cIEF	1) Position within ± 0.2 standard pI 2) pI: 8.0 ~ 9.0	N.A.*
3) SDS-PAGE	1) Non-reducing conditions: Position of main band is identical to the Standard 2) Reducing conditions: Positions of Heavy Chain and Light Chain bands are identical to the Standard	N.A.*

5. Purity test		
1) CE-SDS	1) Non-reducing conditions: LMWI* is 10.0% or less. 2) Reducing conditions: NGHC** is 2.0% or less.	1) LMWI: 8.9% 2) NGHC: 1.4%
2) SE-HPLC	1) The amount of total impurities: 2.0% or less 2) The amount of single impurities: 1.0% or less	1) 0.8% 2) 0.6%, 0.2%
3) CEX-HPLC	1) Acidic form: 55.0% or less 2) Basic form: 5.0 % or less	1) 41.8% 2) 0.0%
4) HCP	100.0 ppm or less	14.7 ppm
5) HCD	0.20 ppm or less	0.12 ppm
6. Contents	1.00 ~ 5.00 mg/ml	2.75 mg/ml
7. Potency test (*in vitro* assay)		
1) NCI-N87	80~125% of the potency marked	N.A.*
2) BT-474	80~125% of the potency marked	N.A.*

*: Not Available, **: Low Molecular Weight Impurities,

***: Non-glycosylation heavy chain

Table 5-19. Summary of characteristics for AH16 API.

Category	Analysis item	Methods & Equipments	Results
Structure analysis and identifi-cation test	MW identification	Q-TOF MS (Waters, Xevo TQ-S)	148,408.92 ~ 148,921.42 Da
	Amino acid composition	UPLC (Waters, ACQUITY) - Column (Waters, AccQ-Tag Ultra)	Suitable for the theoretical value
	Amino acid sequence	Peptide Mapping - Protein Sequencer (Applied Biosystems, 140C Microgradient System) - UPLC (Waters, ACQUITY) - Column (Waters, BEH300 C18) - Q-TOF MS (Waters, Xevo TQ-S)	1) N-terminal - HC: NH3-EVQLVESGGG - LC: NH3-DIQMTQSPSS 2) C-terminal - HC: SLSLSPG-COOH - LC: SFNRGEC-COOH
	Higher-order structure analysis	CD (Chirascan™ CD Spectrometer, Applied Photophysics Ltd.)	Contents of β-strand and β-turn are 60.4%
	Glycosylation pattern analysis	NP- HPLC (Waters, e2695) - Column (TOSOH, TSKgel Amide-80)	FG0: 62.6% FG1: 26.4% FG2: 3.91%
	Monosaccha-rides composition	HPAEC-PAD - HPIC (ion chromatography) (Thermo scientific, ICS 5000) - Column (Dionex , Carbopac PA10)	3 kinds of neutral sugar 1 kind of amino sugar 1 kinds of acidic sugar
	Glycosylation rate	CE-SDS Capillary Electrophoresis (Beckman Coulter, PA 800 plus)	non-glycosylation heavy chain peak: 1.4%

Physico-chemical property	C-terminal deformed Body analysis	CEX-HPLC (Waters, e2695) - Column (Dionex, ProPac WCX-10 Analytical)	C-terminal deformed body percentages: 6.4%
	Isoform distribution	c-IEF (Beckman Coulter, PA 800 plus)	pI values of ten isoforms are within 8.0 ~ 9.0 ranges
	Aggregation	SE-HPLC (Waters, e2695) - Column (TOSOH, TSK-GEL G3000SW$_{XL}$)	Monomer contents: 99.2%
	Fragmentation	CE-SDS PAGE Capillary Electrophoresis (Beckman Coulter, PA 800 plus)	6 kinds of heterogeneity form. Contents of total low-molecular weight: 8.90%
Immuno-logical property	Binding affinity of antibody	SPR (GE Healthcare, BIAcore T200)	HER2 (K_D): 3.52±0.25 x 10^{-10} M
	Cross-reactivity to various antigens	ELISA	No cross-reactivity to 5 kinds of antigens (PDGF Rβ, VEGF R2/KDR/Flk-1, IGF-IR, HGF R/c-Met, FGF R3)
	Cross-reactivity to structurally similar antigens	ELISA	No cross-reactivity to 3 kinds of antigens (EGFR, HER3, HER4)
	Antigen determinants (epitope)	ELISA	Specific to domain IV of HER2 extracellular domain
Biological property	ADCC	Cell based assay	40.1% cell lysis at 1 ng/ml
	Binding to human	SPR (GE Healthcare, BIAcore T200)	FcγRIIIa (V type, K_D) : 1.07±0.30 x 10^{-8} M

	FcγRIIIa		FcγRIIIa (F type, K_D) : 2.24±0.10 x 10^{-8} M
	Binding to human FcRn	SPR (GE Healthcare, BIAcore T200)	8.51±1.01 x 10^{-8} M
	Binding to human C1q	ELISA	No binding
	Apoptosis induction	FACS (GE Healthcare, Canto)	BT-474: 17.7 % NCI-N87: 44.1 %
	Cell proliferation assay	WST-8	NCI-N87 (IC_{50}): 4.3nM BT-474 (IC_{50}): 15.9nM SK-BR-3 (IC_{50}): 3.1nM MDA-MB-453: 40% inhibition at 6.7nM MCF-7: no inhibition
Impurities	HCD		0.12 ppm
	HCP		14.7 ppm
Contents	UV absorbance		2.75 mg/ml

5.4 Conclusions

The expression vector for producing AH16 was constructed, and the AH16 producing AH16F1-3-14-80-26 clone whose antibody growth rate and productivity had been consistently maintained during 1~15 passages was finally screened as a stable producer cell line.

One basal media and 3 additives were selected, and the final productivity of AH16 using the optimized media mixture was approximately 1.3g/L in flask culture.

The three chromatography steps using Protein A resin column (1st step) and two steps of ion-exchange chromatography provided the yield of 93.8% and the purity of 99.9%. And non-Protein A-based cation-exchange chromatography was used as the first capturing step to purify AH16 efficiently separated from the impurities such as HCP (host cell protein) and HCD (host cell DNA), and provided the yield of 99% and the purity of 97.5%.

Analysis of physico-chemical, biological and immunological characteristics of AH16 verified that it meets the standards set based on the “Specifications and Analytical Procedures”.

Through this study, the downstream bioprocess technology required to produce antibody were able to be established and applied.

CHAPTER 6

Overall Discussions and Recommendations

6.1 Overall Discussions

The major findings in this study and the significance thereof are comprehensively summarized as follows.

Firstly, in terms of results, the variants such as AH06 having highly improved anti-cancer activities than the reference antibody were successfully generated using CDR random mutagenesis and phage display technology.

Secondly, in terms of technologies, upstream antibody engineering technologies (mutagenesis, phage display, maturation) and downstream bioprocess technologies essential for new antibody development were established.

Thirdly, in terms of research strategy, mutagenesis was performed on CDRs including residues influencing heavy and light inter-chain interactions as well as residues that function as direct antigen binding, which is distinctive from the preceding research (Gerstner et al., 2002). Another distinctive point is that it was possible to reduce enormous size of library constructions and resulting resources by using the separate mutagenesis of heavy and light CDRs as independent sub-libraries and generating combinatorial IgG molecules in CHO cell manufacturing stage, instead of mutagenesis of heavy and light CDRs in one scFv library.

Therefore, in this chapter, several issues raised through the antibody improvement process will be discussed.

Firstly, Herceptin was chosen as a parental antibody in this antibody improvement study for the following reason. Since enhancement of functional activity of antibody can be primarily achieved by improvement of antibody affinity, this study aimed at generating antibody variants improved functional activity through the affinity maturation or/and optimization.

Therefore, to determine anti-tumor activity, anti-proliferative activity against 2 types of HER2 positive cancer cells as a primary criterion was evaluated in combination of well-established antibody engineering methods. Since hu4D5, a commonly used anti-cancer drug, still needs to be improved and information of its CDR residues is available, it was chosen as a parental antibody in this model study. So it was able to monitor enhancement or improvement of functional activity compared to the parental antibody step by step in the process of antibody affinity maturation or optimization.

Secondly, screening of all CDRs is worth considering, although the significant improvement was achieved from only CDR-H3 screening.

To increase probability of isolating the antibody enhanced in functional biological activity, this study used both random

degenerate PCR method targeting specific residues of CDR-H3, L3 and L2 and error-prone PCR method targeting variable regions of the antibody. For the purpose of enhancing functional biological activity of antibody, through setting hu4D5 as a model antibody, the isolated AH06 was screened from the library LN02. However, since AH06 was screened from the "initial" library LN02, "laterally performed or screened" library LN04 and LN05 seems to be ineffective to isolate variants more improved.

However, it was worth attempting in terms of exploring all the possibilities to improve the efficacy of antibody as the most fundamental purpose of antibody engineering. Since the composition of CDR residues varies in different antibodies and is an important factor in determining antigen specificity and binding affinity, various optimization strategies and protocols can be considered.

Therefore, the conclusion of this study changing parent hu4D5 using a variety of methods is that CDR-H3 of parent hu4D5 has more potential to improve functional efficacy and binding affinity to HER2 than the other CDRs, as a result of which this study could identify AH06 as a "better variant sequence".

Thirdly, the orientation of V_L and V_H of the scFv format could make a considerable difference in antibody affinity and activity.

In this study, the scFv antibody format with V_L-linker-V_H was used to isolate variants improved efficacy. There are reports

showing that expression levels in *E. coli* and binding affinity of the scFv having V_L-linker-V_H orientation is slightly more decreased than those of scFv having V_H-linker-V_L orientation (Weatherill et al., 2012), on the contrary, it was also reported that the binding activity of scFv having V_L-linker-V_H orientation is more superior to that of scFv having V_H-linker-V_L orientation (Desplanco et al., 1994).

Therefore, according to the first point that the binding affinity which acts as a selection pressure in panning process can be influenced by the orientation of V_L and V_H of the scFv format, and also different from various antibodies, and the second point that binding capacities (not affinities) of two scFv format generated from hu4D5 were not largely different (when two format were compared as a preliminary data, data not shown), therefore the scFv format having V_L-linker-V_H orientation was used.

Fourthly, the antibody has differential anti-proliferative activity against cancer cell lines, which might affect screening outcomes.

Since Herceptin has been widely and mainly used in breast cancer treatment, the anti-cancer proliferative activity of the antibody variants in breast cancer cell line SK-BR-3 first, and then in gastric cancer cell line NCI-N87 was screened and evaluated. However, it would have been possible to get better clones, if the antibody variants had been screened in NCI-N87 first or co-screened in NCI-N87 and SK-BR-3 cells.

Although AH06 with the strongest binding affinity showed the

most effective anti-proliferative activity, the data (Table 3-4) did not show a direct correlation between antigen binding affinity of antibody and its biological activity. However, it is consistent with the report that the anti-proliferative activity of humAb4D5 variants against HER2 overexpressing SK-BR-3 cells is not simply correlated with their binding affinity for the HER2 (Carter et al., 1992): the variant humAb4D5-3 with a binding affinity similar to that of humAb4D5-2 had a significantly enhanced anti-proliferative activity compared to humAb4D5-2.

6.2 Recommendations

AH06 shows the possibility of a therapeutic antibody.

AH06 showed a 7.2-fold enhanced anti-proliferative activity against NCI-N87 gastric cancer cells compared to hu4D5, although it did not greatly enhance the activity against SK-BR-3 breast cancer cells (Table 3-4). HER2 gene amplification is higher in NCI-N87 compared with SK-BR-3: the HER2 amplification ratios relative to CEP17 (chromosome 17 centromere) were 8.4 and 4.9 in NCI-N87 and SK-BR-3 cells, respectively (Kim et al., 2008), and receptor/ligand avidity generally increases with the density of the receptor on cell surface (Lesley et al., 2000). Therefore, AH06 may

be able to more efficiently bind to and inhibit NCI-N87 cells having a higher density of HER2 than SK-BR-3 cells.

In addition, its anti-cancer activity of AH06 was HER2-sepcific and its effect was confirmed at the level of signal transduction as well, indicating that AH06 is distinctly superior to hu4D5. Therefore, it is able to suggest that AH06 could be clinically developed as a therapeutic anti-cancer antibody over hu4D5 (Herceptin).

Panning strategy using "one pot phage mixture of sublibraries" increased the chance to screen the improved variants compared to that using "each phage library"

Library LN01 and LN02 were randomized at positions of 4 residues and 6 residues, respectively; LN03 was randomized as 2 sub-libraries at different positions of 4 residues and 4 residues, respectively. Since both LN01 and LN02 were derived from CDR-H3 library after generating each phage library of LN01 and LN02 from each constructed DNA library, they were mixed into "one-pot" to perform the panning process. Since both sub-libraries of LN03 were derived from CDR-L3 library, they were mixed in the same manner.

The reason why two phage libraries were mixed into "one-pot mixture" and screened in this manner was that it was more efficient in order to save labor, time and resources than the separate screening with each library. As a result, AH06 was screened and

isolated from LN01 and LN02 phage library mixture, suggesting that it was the economic screening as intended. It might be the same for LN03, although variants isolated from LN03 did not improve functional activity.

The "one-pot mixture" strategy mentioned in Overall Discussion section, if the number of randomizing residues of specific CDR is over 7~8, it is more efficient to make and screen sub-libraries with randomized each 6 residues rather than to randomize the whole residues of those CDRs at a time. Thus, in such a case, after the phage libraries are randomized and expressed in *E. coli* host, the "one-pot mixture" strategy would be preferable.

However, such a "one-pot mixture" strategy would have some limitations and disadvantages as follows. If "undesirable clones" are more amplified due to higher expression level during the phage amplification stage in *E. coli* host although their binding affinities are not superior to "desirable clones", they could be enriched and survived in the course of screening.

Consequently, there is a possibility that "desirable clones" are eventually "naturally-selected" to diminish. In other words, if "one-pot mixture" of phage sub-libraries from the same CDRs is screened, "loss or wash-out of a better candidate" could be one of possible disadvantages or limitations.

As shown here, functional activity of antibodies can be sufficiently improved using the methods such as random mutagenesis using degenerate and error-prone PCR and site-directed mutagenesis at

specific positions of CDRs and variable region. However, since it is practically difficult to randomize and screen all the CDR regions or residues, it is necessary to decide randomizing target CDRs and number of residues.

If there were many residues and CDRs as CDR-H2 to randomize, it is appropriate to make several sub-libraries with a unit of 6 randomized residues for convenient library construction and "full and thorough and without any loss" screening. Since the study could not help considering saving research resources such as cost and labor, and also time which takes about 20~30 days from library construction, several panning protocols, selection of positive clones to novel sequence identification, it would be more proper approach using "one-pot mixture" strategy.

In order to generate randomized libraries in an efficient and productive way, several factors such as labor, time, resources and feasibility should be considered, and particularly the number of CDR residues is a one of most important factors.

To increase the possibility to select variants which has much more anticancer activity, in this study, variants were generated step-by-step through the random degenerate mutagenesis PCR with some positions in CDR-H3, CDR-L3, and CDR-L2, respectively, as well as random error-prone mutagenesis PCR with 2~4 sections of a whole area of variable region. Random degenerate mutagenesis on CDR-H2 that is generally important in antigen-binding and specificity of antibodies was not carried out in this study. As mentioned in

Chapter 3.1 Results, the reason not to randomize CDR-H2 will be described below in detail.

In case of hu4D5 as a model in this study, it has been known that the rest of residues except of 3 exposed residues (50, 56, and 58) of the position 50~65 in CDR-H2 were located inside the variant and did not directly interact with antigen HER2 (Gerstner et al., 2002). Therefore, if the rest residues except for those three residues and CDR-H2 key residue R50 that can significant influence the binding affinity and stability of the antibody were exclude from randomization target positions, in actually, it was only able to randomize positions CDR-H2 Y56, R58 and evaluate the influence for binding affinity without some difficulties.

However, since the results from randomization at positions CDR-H2 Y56 and R58 revealed that the frequencies that appeared as variant residues changed to not original residues but the other different residues were less than 40%, although if those two positions were randomized, it might be practically less effective in residue substitution, we cannot randomize those two positions.

In general, since substitution of antibody variable domain sequences can influence interactions between not only "exposed residues" and its specific antigen, but also antibody internal heavy and light chain, and the resulting structural stability of the antibody can be influenced from such changes, and so, the antibody-antigen binding strength can be changed. Therefore, not only "those exposed residues" involved direct binding to its antigen,

but also "those residues" influencing heavy and light inter-chain interactions (Hawkins et. al, 1993; Chatellier et. al, 1996; Carter et. al, 1992; Schier et. al, 1996; Vajdos et al., 2002) can be randomized as target residues.

In fact, since it is difficult to elucidate what residues act at which position in the situation that there is no modeling analysis data for antibody-antigen binding mode, nor being studied, randomization of all positions in CDR could be the most acceptable strategy for antibody optimization. Therefore, no matter what residues sequences and length of CDRs are, it is necessary to use or adopt productive randomization libraries construction and screening strategies satisfactory in terms of labor, time, resources, easiness and positive outcomes.

However, by the need and possibilities, if this study surely try to randomize 17 residues of CDR-H2, though it was able to omit key residue R50 of CDR-H2 from target residues, the number of remaining target residues for randomization is as many as 16. And if this study construct two sub-libraries sequentially randomizing 8 residues and 8 residues, since two theoretical library sizes are 5.12×10^{10}, respectively, it is necessary to use a huge or enormous costs and times, which means that constructing libraries is practically impossible to do.

Alternatively, if this study construct three sub-libraries sequentially randomizing 6 residues, 6 residues and 4 residues, three theoretical library sizes are 6.4×10^{7}, 6.4×10^{7} and 1.6×10^{5},

respectively. Thus, constructing three sub-libraries is relatively much easier, but in this case, the study must compare or monitor the screening results and try to do in various combinations. And finally, it was unable to construct libraries for CDR-H2 randomization.

For randomization of CDR having more than 10 resides, the most efficient way would be the use of sublibraries: randomization of each 5~6 residues and subsequent mixing of the sublibraries in one-pot.

Nevertheless, if there are many residues consisting of interesting CDRs and randomization is necessary to improve or increase affinity maturation or functional activity, it is able to construct and screen randomized library using sublibraries consisting of 5~6 randomized residues. For example, about 10 “best-binding variants” selected from each library is used at a template for the next step library construction. Thirty~fourty variant DNA extracted from the best-binding variants in the 3~4 libraries is mixed in one-pot and then combinatorial library of best-variants is constructed with ease, and further screening (panning) is performed. By using these methods or strategies, it is supposed that it is able to obtain improved variants more easily.

The purpose of this study is to examine whether the therapeutic efficacy of the antibody can be improved through antibody engineering methods. This study used hu4D5 (Herceptin) as a

model study case, since it has potent anti-cancer activity and high binding affinity (K_D in sub-picomolar range).

Herceptin is well known antibody, and its sequences are already known. Nevertheless, it is still an attractive model to investigate what kinds of random mutagenesis strategies can be used for improvement of binding affinity and functional efficacy, and how much improvement can be achieved from the result.

In addition, this study could suggest basic and simple solutions or applications on how to use of previously available known information for antibody optimization process and how to establish an optimization strategy without any information such as key residues and important positions of antibody-antigen interaction.

If the information is not available, in generally, it is able to get the information for key residues and important positions of CDR regions through analyzing and comparing the results of functional activities and binding affinities (K_D) from alanine scanning mutagenesis.

Therefore, based on the information, it is able to construct and screen libraries randomized at any positions except key and other important residues. This model case study could establish the overall protocol and strategy for the purpose of improving functional activity of the antibody, which can be applicable to any other antibody optimization study.

In this study, although it was unable to randomize all the CDRs of

the parent antibody hu4D5 due to research limitation factors such as resources, labor and time, to isolate the improved variants, this study randomized some of CDR residues generally known to be important for functional activity and binding affinity of the antibody using various methods and strategies. As a result, this study generated the variant AH06 whose binding affinity as well as functional activity is better than those of parent antibody hu4D5, which is very important achievement and meanings.

AH06 showed approximately 7.0-fold enhanced anti-proliferative activity against NCI-N87 gastric cancer cells compared to hu4D5, although it did not greatly enhance the activity against SK-BR-3 breast cancer cells. In addition, its anti-cancer activity was HER2-sepcific and its effect was confirmed at the level of signal transduction as well, indicating that AH06 is distinctly superior to hu4D5. Therefore, this study suggest that AH06 could be clinically developed as a therapeutic anti-cancer antibody over hu4D5 (Herceptin).

In addition, this study was not designed for elucidating novel biological principles, phenomena, and signaling mechanisms or discovering new biomolecules or developing analysis methodology, but it is a planned model study to show how to design strategies or methods to improve functionality and efficacy of antibodies that are currently used for therapeutics and diagnostics in the clinical practice. This study was also performed to test if the strategies and

methods confirmed from this model study could be applied to enhance functionality of other therapeutic antibodies.

By excluding key and other relatively conserved residues from randomization, as this methodology or strategy is general and widely adopted, it was able to reduce the library size and thus save labor, time and related resources for screening.

As this study, it can sufficiently improve functional activities of antibodies with methods for random mutagenesis using degenerate and error-prone PCR and for site-directed mutagenesis at specific positions of CDRs and variable region. However, since it is impossible to randomize and screen all the CDR regions or residues, it is necessary to decide randomizing target CDRs and number of residues.

For this reason, in this study, CDR-H3, L3 and L2 were selected as target CDRs to randomize and screen. In addition, although AH06 isolated from this study is an improved antibody variant, it is unable to conclude that AH06 is ultimately the best antibody derivable from parent hu4D5 and so there is no possibility of getting more improved antibody than AH06. That is, it is possible to be selected or generated as many as better variants than AH06 by the order and combinations of residues far different from those of AH06.

Since it is impossible to construct and screen libraries by randomizing residues in all the possible and theoretical combinations in the antibody optimization process, it is extremely

important to set the quantitative selection criteria which are well describing and properly representing the purpose of antibody optimization such as improvement of functional activity, binding affinity, specificity, effector function, productivity, stability and reduction of immunogenicity.

Therefore, in the study for antibody optimization process, it is economical and important to make Go or No-Go decision step-by-step by monitoring if variants meet quality standards at each screening step. It means that the antibody optimization process is a step to select the variants that meet the requirements among numerous variants.

In summary, the CDR mutagenesis and the combinatorial library expression strategies can be used for optimizing and developing a new antibody as the effective methodology, and thus is more significant than the outcomes in terms of experimental results and technologies described above.

References

Abhinandan, K.R., and Martin, A.C. (2008). Analysis and improvements to Kabat and structurally correct numbering of antibody variable domains. Mol. Immunol. *45*, 3832-3839.

Almagro, J.C., and Fransson, J. (2008). Humanization of antibodies. Front. Biosci. *13*, 1619-1633.

Anneli, D., and Basant, S. (1994). Tryptic map variation of Erythropoietin resulting from carboxypeptidase B-like activity. J. Liq. Chromatogr. *17*, 2777-2789.

Azriel-Rosenfeld, R., Valensi, M., and Benhar, I. (2004). A human synthetic combinatorial library of arrayable single-chain antibodies based on shuffling *in vivo* formed CDRs into general framework regions. J. Mol. Biol. *335*, 177-192.

Azzazy, H.M., and Highsmith, W.E. Jr. (2002). Phage display technology: clinical applications and recent innovations. Clin. Biochem. *35*, 425-445.

Baca, M., Presta, L.G., O'Connor, S.J., and Wells, J.A. (1997). Antibody humanization using monovalent phage display. J. Biol. Chem. *272*, 10678-10684.

Baek, H., Suk, K.H., Kim, Y.H., and Cha, S.H. (2002). An improved helper phage system for efficient isolation of specific antibody molecules in phage display. Nucleic Acids Research. *30*, e18-e26.

Baek, H.J., Hur, B.W., Cho, J.W., Lee, H.K., Kim, N.I., Oh, M.Y., and Cha, S.H. (2004). Isolation of two distinct populations of recombinant antibody molecules specific for rat malonyl-CoA decarboxylase from a semi-synthetic human scFv display library using Ex-phage system. Immunol. Letters. *91*, 163-170.

Barbas, C.F. III, Burton, D.R., and Silverman, G.J. (2004). Phage display: a laboratory manual, 1st Edition (Cold Spring Harbor Laboratory Press)

Barnes, D., and Sato, G. (1991). Methods for growth of cultured cells in serum-free medium. Anal. Biochem. *102*, 255-270.

Barok, M., Isola, J., Pályi-Krekk, Z., Nagy, P., Juhász, I., Vereb, G., Kauraniemi, P., Kapanen, A., Tanner, M., Vereb, G., and Szöllösi, J. (2007). Trastuzumab causes antibody-dependent cellular cytotoxicity-mediated growth inhibition of submacroscopic JIMT-1 breast cancer xenografts despite intrinsic drug resistance. Mol. Cancer Ther. *6*, 2065-2072.

Baselga, J., Albanell, J., Molina, M.A., and Arribas, J. (2001).

Mechanism of action of trastuzumab and scientific update. Semin .Oncol. *28*, 4-11.

Benatuil, L., Perez, J.M., Belk, J., Hsieh, C.M. (2010). An improved yeast transformation method for the generation of very large human antibody libraries. Protein Eng. Des. Sel. *23*, 155-159.

Boder, E.T., and Wittrup, K.D. (1997). Yeast surface display for screening combinatorial polypeptide libraries. Nat. Biotechnol. *15*, 553-557.

Boulianne, G.L., Hozumi, N., Shulman, M.J. (1984). Production of functional chimaeric mouse/human antibody. Nature. *312*, 643-646.

Bryson, C.J., Jones, T.D., and Baker, M.P. (2010). Prediction of immunogenicity of therapeutic proteins: validity of computational tools. BioDrugs. *24*, 1-8.

Baxevanis, C.N., Sotiropoulou, P.A., Sotiriadou, N.N., and Papamichail, M. (2004). Immunobiology of HER-2/neu oncoprotein and its potential application in cancer immunotherapy. Cancer Immunol. Immunother. *53*, 166-175.

Bei, R., Budillon, A., Masuelli, L., Cereda, V., Vitolo, D., Di Gennaro, E., Ripavecchia, V., Palumbo, C., Ionna, F., Losito, S., Modesti, A.,

Kraus, M.H., and Muraro, R. (2004). Frequent overexpression of multiple ErbB receptors by head and neck squamous cell carcinoma contrasts with rare antibody immunity in patients. J. Pathol. *204*, 317-325.

Birch, J.R., and Racher, A.J. (2006). Antibody production. Adv. Drug Deliv. Rev. *58*, 671-685.

Brennan, P.J., Kumagai, T., Berezov, A., Murali, R., and Greene, M. (2000). HER2/neu: mechanisms of dimerization/oligomerization. Oncogene. *19*, 6093-6101.

Bumbaca, D., Boswell, C.A., Fielder, P.J., and Khawli, L.A. (2012). Physiochemical and biochemical factors influencing the pharmacokinetics of antibody therapeutics. AAPS J. *14*, 554-558.

Butler, M. (2005). Animal cell cultures: recent achievements and perspectives in the production of biopharmaceuticals. Appl. Microbiol. Biotechnol. *68*, 283-291.

Calogero, R.A., Cordero, F., Forni, G., and Cavallo, F. (2007). Inflammation and breast cancer. Inflammatory component of mammary carcinogenesis in ErbB2 transgenic mice. Breast Cancer Research. *9*, 211-219.

Carter, P., Presta, L., Gorman, C.M., Ridgway, J.B., Henner, D., Wong, W.L., Rowland, A.M., Kotts, C., Carver, M.E., and Shepard, H.M. (1992). Humanization of an anti-p185 HER2 antibody for human cancer therapy. Proc. Natl. Acad. Sci. *89*, 4285-4289.

Carter-Franklin, J.N., Victa, C., McDonald, P., and Fahrner, R. (2007). Fragments of protein A eluted during protein A affinity chromatography. J. Chromatogr. A. *1163*, 105-111.

Chatellier, J., Van Regenmortel, M.H., Vernet, T., and Altschuh, D. (1996). Functional mapping of conserved residues located at the V_L and V_H domain interface of a Fab. J. Mol. Biol. *264*, 1-6.

Chen, Y., Wiesmann, C., Fuh, G., Li, B., Christinger, H.W., McKay, P., de Vos, A.M., and Lowman, H.B. (1999). Selection and analysis of an optimized anti-VEGF antibody crystal structure of an affinity-matured Fab in complex with antigen. J. Mol. Biol. *293*, 865-881.

Cheng, X., Zhang, Y., Kotani, N., Watanabe, T., Lee, S., Wang, X., Kawashima, I., Tai, T., Taniguchi, N., and Honke, K. (2005). Production of a recombinant single-chain variable-fragment (scFv) antibody against sulfoglycolipid. J. Biochem. *137*, 415–421.

Clackson, T., Hoogenboom, H.R., Griffiths, A.D., and Winter, G. (1991). Making antibody fragments using phage display libraries.

Nature. *352*, 624-628.

Cockett, M.I., Bebbington, C.R., and Yarranton, G.T. (1990). High-level expression of tissue inhibitor of metalloproteinases in Chinese Hamster Ovary cells using glutamine synthetase gene amplification. Biotechnol. *8*, 662-667.

Corisdeo, S., and Wang, B. (2004). Functional expression and display of an antibody Fab fragment in Escherichia coli: study of vector designs and culture conditions. Protein Expr. Purif. *34*, 270-279.

Daëron, M. (1997). Fc receptor biology. Annu. Rev. Immunol. *15*, 203-234.

Davoli, A., Hocevar, B.A., and Brown T.L. (2010). Progression and treatment of HER2-positive breast cancer. Cancer Chemother. Pharmacol. *65*, 611-623.

Derek, A., Rashmi, Korke., Wei-Shou, H. (2007). Application of stoichiometric and kinetic analyses to characterize cell growth and product formation. *In* Methods in Biotechnology, Animal cell biotechnology : methods and protocols. Vol. 24 (Springer), pp. 269-284.

Desplanco, D., King, D.J., Lawson, A.D., and Mountain, A. (1994). Multimerization behavior of single chain Fv variants for the tumour-binding antibody B72.3, Protein Engineering. *7*, 1027-1033.

Ding, L., Azam, M., Lin, Y.H., Sheridan, J., Wei, S., Gupta, G., Singh, R.K., Pauling, M.H., Chu, W., Tran, A., Yu, N.X., Hu, J., Wang, W., Long, H., Xiang, D., Zhu, L., and Hua, S.B. (2010). Generation of high-affinity fully human anti-interleukin-8 antibodies from its cDNA by two-hybrid screening and affinity maturation in yeast. Protein Sci. *19*, 1957-1966.

Dower, W.J., Miller, J.F., and Ragsdale, C.W. (1988). High efficiency transformation of *E. coli* by high voltage electroporation. Nucleic Acids Research. *16*, 6127-6145.

Fahrner, R.L., Knudsen, H.L., Basey, C.D., Galan, W., Feuerhelm, D., Vanderlaan, M., and Blank, G.S. (2001). Industrial purification of pharmaceutical antibodies: development, operation, and validation of chromatography processes. Biotechnol. Genet. Eng. Rev. *18*, 301-327.

Farajnia, S., Ahmadzadeh, V., Tanomand, A., Veisi, K., Khosroshahi, S.A., and Rahbarnia, L. (2014). Development trends for generation of single-chain antibody fragments. Immunopharmacol. Immunotoxicol. *36*, 297-308.

Ferrige, A.G., Seddon, M.J., Jarvis, S.A., Skilling, J., and Aplin, R. (1991). Maximum entropy deconvolution in electrospray mass spectrometry. Rapid Commun. Mass Spectrom. *5*, 374-377.

Franklin, M.C., Carey, K.D., Vajdos, F.F., Leahy, D.J., de Vos, A.M., and Sliwkowski, M.X. (2004). Insights into ErbB signaling from the structure of the ErbB2-pertuzumab complex. Cancer Cell. *5*, 317-328.

Fuchs, P., Dübel, S., Breitling, F., Braunagel, M., Klewinghaus, I., and Little, M. (1992). Recombinant human monoclonal antibodies. Basic principles of the immune system transferred to *E. coli*. Cell Biophys. *21*, 81-91.

Genentech, Inc. (2005). Humanized anti-ErbB2 antibodies and treatment with anti-ErbB2 antibodies. US6949245 (US Patent).

Gerstner, R.B., Carter, P., and Lowman, H.B. (2002). Sequence plasticity in the antigen-binding site of a therapeutic anti-HER2 antibody. J. Mol. Biol. *321*, 851-862.

Giordano, R.J., Cardó-Vila, M., Lahdenranta, J., Pasqualini, R., and Arap, W. (2001). Biopanning and rapid analysis of selective interactive ligands. Nat. Med. *7*, 1249-1253.

Gong, S.J., Jin, C.J., Rha, S.Y., and Chung, H.C. (2004). Growth

inhibitory effects of trastuzumab and chemotherapeutic drugs in gastric cancer cell lines. Cancer Letters. *214*, 215-224.

Grillberger, L., Kreil, T.R., Nasr, S., and Reiter, M. (2009). Emerging trends in plasma-free manufacturing of recombinant protein therapeutics expressed in mammalian cells. Biotechnol. J. *4*, 186-201.

Gu, M.B., Kern, J.A., Todd, P., and Kompala, D.S. (1992). Effect of amplification of dhfr and lac Z genes on growth and beta-galactosidase expression in suspension cultures of recombinant CHO cells. Cytotechnology. *9*, 237-245.

Hamlin, J.L. (1992). Mammalian origins of replication. Bioessays. *14*, 651-659.

Hanes, J., and Plückthun, A. (1997). *In vitro* selection and evolution of functional proteins by using ribosome display. Proc. Natl. Acad. Sci. *94*, 4937-4942.

Harris, R.J., Kabakoff, B., Macchi, F.D., Shen, F.J., Kwong, M., Andya, J.D., Shire, S.J., Bjork, N., Totpal, K., and Chen, A.B. (2001). Identification of multiple sources of charge heterogeneity in a recombinant antibody. J. Chromatogr. B. Biomed. Sci. Appl. *752*, 233-245.

Hawkins, R.E., Russell, S.J., Baier, M., and Winter, G. (1993). The contribution of contact and non-contact residues of antibody in the affinity of binding to antigen. The interaction of mutant D1.3 antibodies with lysozyme. J. Mol. Biol. *234*, 958-964.

Hinton, P.R., Johlfs, M.G., Xiong, J.M., Hanestad, K., Ong, K.C., Bullock, C., Keller, S., Tang, M.T., Tso, J.Y., Vásquez, M., and Tsurushita, N. (2004). Engineered human IgG antibodies with longer serum half-lives in primates. J. Biol. Chem. 279, 6213-6216.

Hoet, R.M., Cohen, E.H., Kent, R.B., Rookey, K., Schoonbroodt, S., Hogan, S., Rem, L., Frans, N., Daukandt, M., Pieters, H., van Hegelsom, R., Neer, N.C., Nastri, H.G., Rondon, I.J., Leeds, J.A., Hufton, S.E., Huang, L., Kashin, I., Devlin, M., Kuang, G., Steukers, M., Viswanathan, M., Nixon, A.E., Sexton, D.J., Hoogenboom, H.R., Ladner, R.C. (2005). Generation of high-affinity human antibodies by combining donor-derived and synthetic complementarity-determining-region diversity. Nat. Biotechnol. *23*, 344-348.

Høgdall, E.V., Christensen, L., Kjaer, S.K., Blaakaer, J., Bock, J.E., Glud, E., Nørgaard-Pedersen, B., and Høgdall, C.K. (2003). Distribution of HER-2 overexpression in ovarian carcinoma tissue and its prognostic value in patients with ovarian carcinoma: from the Danish MALOVA ovarian cancer study. Cancer. *98*, 66-73.

Hoogenboom, H.R., and Chames, P. (2000). Natural and designer binding sites made by phage display technology. Immunol. Today. *21*, 371-378.

Hudis, C.A. (2007). Trastuzumab - Mechanism of action and use in clinical practice. New Engl. J. Medicine. *357*, 39-51.

Hudson, P.J., and Souriau, C. (2003). Engineered antibodies. Nat. Med. *9*, 129-134.

Hudziak, R.M., Lewis, G.D., Winget, M., Fendly, B.M., Shepard, H.M., and Ullrich, A. (1989). p185 HER2 monoclonal antibody has antiproliferative effects *in vitro* and sensitizes human breast tumor cells to tumor necrosis factor. Mol. Cell. Biol. *9*, 1165-1172.

Idusogie, E.E., Wong, P.Y., Presta, L.G., Gazzano-Santoro, H., Totpal, K., Ultsch, M., and Mulkerrin, M.G. (2001). Engineered antibodies with increased activity to recruit complement. J. Immunol. *166*, 2571-2575.

Imai, K., and Takaoka, A. (2006). Comparing antibody and small-molecule therapies for cancer. Nat. Rev. Cancer. *6*, 714-727.

Iscove, N.N., and Melchers, F. (1978). Complete replacement of serum by albumin, transferrin, and soybean lipid in cultures of

lipopolysaccharide-reactive B lymphocytes. J. Exp. Med. *147*, 923-933.

Janice, M.R. (2012). Marketed therapeutic antibodies compendium. mAbs. *3*, 413-415.

Jendeberg, L., Tashiro, M., Tejero, R., Lyons, B.A., Uhlén, M., Montelione, G.T., and Nilsson, B. (1996). The mechanism of binding staphylococcal protein A to immunoglobin G does not involve helix unwinding. Biochemistry. *35*, 22-31.

Johnson, B.E., and Jänne, P.A. (2006). Rationale for a phase II trial of pertuzumab, a HER-2 dimerization inhibitor, in patients with non-small cell lung cancer. Clin. Cancer Res. *12*, 4436s-4440s.

Johnsson, B., Löfås, S., and Lindquist, G. (1991). Immobilization of proteins to a carboxymethyldextran-modified gold surface for biospecific interaction analysis in surface plasmon resonance sensors. Analyt. Biochem. *198*, 268-277.

Jones, P.T., Dear, P.H., Foote, J., Neuberger, M.S., Winter, G. (1986). Replacing the complementarity-determining regions in a human antibody with those from a mouse. Nature. *321*, 522-525.

Joo, H.Y., Hur, B.U., Lee, K.W., Song, S.Y., and Cha, S.H. (2008).

Establishment of a reliable dual-vector system for the phage display of antibody fragments. J. Immunol. Methods. *333*, 24-37.

Kabat, E.A., Wu, T.T., and et al. (1991). Identical V region amino acid sequences and segments of sequences in antibodies of different specificities. Relative contributions of V_H and V_L gene, minigenes, and complementarity-determining regions to binding of antibody-combining sites. J. Immunol. *147*, 1709-1719.

Kaufman, R.J., Wasley, L.C., Spiliotes, A.J., Gossels, S.D., Latt, S.A., Larsen, G.R., and Kay, R.M. (1985). Coamplification and coexpression of human tissue-type plasminogen activator and murine dihydrofolate reductase sequences in Chinese hamster ovary cells. Mol. Cell Biol. *5*, 1750-1759.

Korean Pharmacopoeia (대한약전), General test for "Measurement of pH".

Kay, B.K., Winter, J., and McCafferty, J. (1996). Phage display of peptides and proteins, a laboratory manual, 1st ed. (Academic Press)

Kelley, B. (2009). Industrialization of mAb production technology: the bioprocessing industry at a crossroads. MAbs. *1*, 443-452.

Kelley, R.F., and O'Connell, M.P. (1993). Thermodynamic analysis of an antibody functional epitope. Biochemistry. *32*, 6828-6835.

Kent, U.M. (1999). Purification of antibodies using ion-exchange chromatography. Methods Mol. Biol. *115*, 19-22.

Kettleborough, C.A., Saldanha, J., Heath, V.J., Morrison, C.J., and Bendig, M.M. (1991). Humanization of a mouse monoclonal antibody by CDR-grafting: the importance of framework residues on loop conformation. Protein Eng. *4*, 773-783.

Khazaeli, M.B., Conry, R.M., LoBuglio, A.F. (1994). Human immune response to monoclonal antibodies. J. Immunother. Emphasis. Tumor Immunol. *15*, 42-52.

Kim, E.J., Kim, N.S., and Lee, G.M. (1999). Development of a serum-free medium for dihydrofolate reductase-deficient Chinese hamster ovary cells (DG44) using a statistical design : beneficial effect of weaning of cells. *In Vitro* Cell Dev. Biol. Anim. *35*, 178-182.

Kim, J.W., Kim, H.P., Im, S.A., Kang, S., Hur, H.S., Yoon, Y.K., Oh, D.Y., Kim, J.H., Lee, D.S., Kim, T.Y., and Bang, Y.J. (2008). The growth inhibitory effect of lapatinib, a dual inhibitor of EGFR and HER2 tyrosine kinase, in gastric cancer cell lines. Cancer Letters. *272*, 296-306.

Knappik, A., and Plückthun, A. (1995). Engineered turns of a recombinant antibody improve its *in vivo* folding. Protein Eng. *8*, 81-89.

Knezevic, I., Kang, H.N., and Thorpe, R. (2015). Immunogenicity assessment of monoclonal antibody products: A simulated case study correlating antibody induction with clinical outcomes. Biologicals. *43*, 307-317.

Knight, D.M., Trinh, H., Le, J., Siegel, S., Shealy, D., McDonough, M., Scallon, B., Moore, M.A., Vilcek, J., and Daddona, P. (1993). Construction and initial characterization of a mouse-human chimeric anti-TNF antibody. Mol. Immunol. *30*, 1443-1453.

Kobayashi, N., Oyama, H., Kato, Y., Goto, J., Soderlind, E., and Borrebaeck, C.A. (2010). Two-step *in vitro* antibody affinity maturation enables estradiol-17beta assays with more than 10-fold higher sensitivity. Anal. Chem. *82*, 1027-1038.

Köhler, G., Milstein, C. (1992). Continuous cultures of fused cells secreting antibody of predefined specificity. Biotechnology. *24*, 524-526

Krebber, A., Burmester, J., and Plückthun, A. (1996). Inclusion of an upstream transcriptional terminator in phage display vectors

abolishes background expression of toxic fusions with coat protein g3p. Gene. *178*, 71-74.

Krebs, B., Rauchenberger, R., Reiffert, S., Rothe, C., Tesar, M., Thomassen, E., Cao, M., Dreier, T., Fischer, D., Höss, A., Inge, L., Knappik, A., Marget, M., Pack, P., Meng, X.Q., Schier, R., Söhlemann, P., Winter, J., Wölle, J., and Kretzschmar, T. (2001). High-throughput generation and engineering of recombinant human antibodies. J. Immunol. Methods. *254*, 67-84.

Kubota, T., Niwa, R., Satoh, M., Akinaga, S., Shitara, K., and Hanai, N. (2009). Engineered therapeutic antibodies with improved effector functions. Cancer Sci. *100*, 1566-1572.

Lara, P.N. Jr., Meyers, F.J., Gray, C.R., Edwards, R.G., Gumerlock, P.H., Kauderer, C., Tichauer, G., Twardowski, P., Doroshow, J.H., Gandara, D.R. (2002). HER-2/neu is overexpressed infrequently in patients with prostate carcinoma. Results from the California Cancer Consortium Screening Trial. Cancer. *94*, 2584-2589.

Lazar, G.A., Dang, W., Karki, S., Vafa, O., Peng, J.S., Hyun, L., Chan, C., Chung, H.S., Eivazi, A., Yoder, S.C., Vielmetter, J., Carmichael, D.F., Hayes, R.J., and Dahiyat, B.I. (2006). Engineered antibody Fc variants with enhanced effector function. Proc. Natl. Acad. Sci. *103*, 4005-4010.

Lee, M.S., and Olson, M.A. (2006). Calculation of absolute protein-ligand binding affinity using path and endpoint approaches. Biophys J. *90*, 864-877.

Lei, S., Appert, H.E., Nakata, B., Domenico, D.R., Kim, K., and Howard, J.M. (1995). Overexpression of HER2/neu oncogene in pancreatic cancer correlates with shortened survival. Int. J. Pancreatol. *17*, 15-21.

Lesley, J., Hascall V.C., Tammi, M., and Hyman, R. (2000). Hyaluronan binding by cell surface CD44. J. Biol. Chem. *275*, 26967-26975.

Liang, Y., Benakanakere, I., Besch-Williford, C., Hyder, R.S., Ellersieck, M.R., and Hyder, S.M. (2010). Synthetic progestins induce growth and metastasis of BT-474 human breast cancer xenografts in nude mice. Menopause. *17*, 1040-1047.

Liu, H.F., Ma, J., Winter, C., and Bayer, R. (2010). Recovery and purification process development for monoclonal antibody production. MAbs. *2*, 480-499.

Liu, H., Gaza-Bulseco, G., Faldu, D., Chumsae, C., and Sun, J. (2008). Heterogeneity of monoclonal antibodies. J. Pharm. Sci. *97*, 2426-2447.

Lonberg, N., and Huszar, D. (1995). Human antibodies from transgenic mice. Int. Rev. Immunol. *13*, 65-93.

Lowe, D., Wilkinson T., and Vaughan, T.J., (2012). Affinity maturation approaches for antibody lead optimization. *In* Antibody Drug Discovery, Wood C.R., (London, UK : Imperial College Press). pp.85-120.

Macdonald, R.A., Hosking, C.S., and Jones, C.L. (1988). The measurement of relative antibody affinity by ELISA using thiocyanate elution. J. Immunol. Methods. *106*, 191-194.

Marchalonis, J.J., Adelman, M.K., Schluter, S.F., and Ramsland, P.A. (2006). The antibody repertoire in evolution: chance, selection, and continuity. Dev. Comp. Immunol. *30*, 223-247.

Mariani, E., Mariani, A.R., Monaco, M.C., Lalli, E., Vitale, M. and Facchini, A. (1991). Commercial serum-free media: hybridoma growth and monoclonal antibody production. J. Immunol. Methods. *145*, 175-183.

Marichal-Gallardo, P.A., and Alvarez, M.M. (2012). State-of-the-art in downstream processing of monoclonal antibodies: process trends in design and validation. Biotechnol. Prog. *28*, 899-916.

Matsui, Y., Inomata, M., Tojigamori, M., Sonoda, K., Shiraishi, N., and Kitano, S. (2005). Suppression of tumor growth in human gastric cancer with HER2 overexpression by an anti-HER2 antibody in a murine model. Int. J. Oncol. *27*, 681-685.

Mayumi, O., and Michihiko, K. (2006). Molecular mechanisms of epidermal growth factor receptor (EGFR) activation and response to Gefitinib and other EGFR-targeting drugs. Clin. Cancer Res. *12*, 7242-7251.

Melmer, M., Stangler, T., Schiefermeier, M., Brunner, W., Toll, H., Rupprechter, A., Lindner, W., and Premstaller, A. (2010). HILIC analysis of fluorescence-labeled N-glycans from recombinant biopharmaceuticals. Anal. Bioanal. Chem. *398*, 905-914.

Ménard, S., Casalini, P., Campiglio, M., Pupa, S., Agresti, R, and Tagliabue E. (2001). HER2 overexpression in various tumor types, focussing on its relationship to the development of invasive breast cancer. Ann. Oncol. *12*, S15-S19.

Mineo, J.F., Bordron, A., Quintin-Roué, I., Loisel, S., Ster, K.L., Buhé, V., Lagarde, N., Berthou, C. (2004). Recombinant humanised anti-HER2/neu antibody (Herceptin) induces cellular death of glioblastomas. Br. J. Cancer. *91*, 1195-1199.

MoBiTec. (2000). pSKAN 8 phagemid vector, product information and instructions.

Molina, M.A., Codony-Servat, J., Albanell, J., Rojo, F., Arribas, and J., Baselga, J. (2001). Trastuzumab (herceptin), a humanized anti-Her2 receptor monoclonal antibody, inhibits basal and activated Her2 ectodomain cleavage in breast cancer cells. Cancer Res. *61*, 4744-4749.

Moorhouse, K.G., Nashabeh, W., Deveney, J., Bjork, N.S., Mulkerrin, M.G., and Ryskamp, T. (1997). Validation of an HPLC method for the analysis of the charge heterogeneity of the recombinant monoclonal antibody IDEC-C2B8 after papain digestion. J. Pharm. and Biomed. Anal. *16*, 593-603.

Morrison, S.L., Johnson, M.J., Herzenberg, L.A., Oi, V.T. (1984). Chimeric human antibody molecules: mouse antigen-binding domains with human constant region domains. Proc. Natl. Acad. Sci. *81*, 6851-6855.

Moser, A.C., Hage, D.S. (2011). Immunoaffinity chromatography: an introduction to applications and recent development. Bioanalysis. *2*, 769-790.

Neuberger, M.S., Williams, G.T., Fox, R.O. (1984). Recombinant

antibodies possessing novel effector functions. Nature. *312*, 604-608.

Ng, S.K. (2012). Generation of high-expressing cells by methotrexate amplification of destabilized dihydrofolate reductase selection marker. Methods Mol. Biol. *801*, 161-172.

Nicolas, W., Véronique, D.H., and Martine, J.P. (2008). HER2-positive breast cancer: From Trastuzumab to innovatory anti-HER2 strategies. Clin. Breast Cancer. *8*, 38-49.

Noguchi, A., Mukuria, C.J., Suzuki, E., and Naiki, M. (1995). Immunogenicity of N-glycolylneuraminic acid-containing carbohydrate chains of recombinant human erythropoietin expressed in Chinese hamster ovary cells. J. Biochem. *117*, 59-62.

O'Brien, N.A., Browne, B.C., Chow, L., Wang, Y., Ginther, C., Arboledal, J., Duffy, M.J., Crown, J., O'Donovan, N., and Slamon, J.D. (2010). Activated phosphoinositide 3-kinase/AKT signaling confers resistance to Trastuzumab but not Lapatinib. Mol. Cancer Ther. *9*, 1489-2211.

Oh, M.Y., oung, Joo, H.Y., Hur, B.U., Jeong, Y.H., and Cha, S.H. (2007). Enhancing phage display of antibody fragments using gIII-amber suppression. Gene. *386*, 81-89.

Okines, A., Cunningham, D., Chau, I. (2011). Targeting the human EGFR family in esophagogastric cancer. Nat. Rev. Clin. Oncol. *8*, 492-503.

Ono, M., and Kuwano, M. (2006). Molecular mechanisms of epidermal growth factor receptor (EGFR) activation and response to gefitinib and other EGFR-targeting drugs. Clin. Cancer Res. *12*, 7242-7251.

Parampalli, A., Eskridge, K., Smith, L., Meagher, M.M., Mowry, M.C., and Subramanian, A. (2007). Development of serum-free media in CHO-DG44 cells using a central composite statistical design. Cytotechnology. *54*, 57-68.

Pasqualini, R., and Ruoslahti, E. (1996). Organ targeting *in vivo* using phage display peptide libraries. Nature. *380*, 364-366.

Parsons, H.L., Earnshaw, J.C., Wilton, J., Johnson, K.S., Schueler, P.A., Mahoney, W., and McCafferty, J. (1996). Directing phage selections towards specific epitopes. Protein Eng. *9*, 1043-1049.

Pasqualini, R., and Ruoslahti, E. (1996). Organ targeting *in vivo* using phage display peptide libraries. Nature. *380*, 364-366.

Phumyen, A., Jumnainsong, A., and Leelayuwat, C. (2012).

Improved binding activity of antibodies against major histocompatibility complex Class I chain-related gene A by phage display technology for cancer-targeted therapy. J. Biomed. Biotechnol. *2012*, 1-8.

Prassler, J., Thiel, S., Pracht, C., Polzer, A., Peters, S., Bauer, M., Nörenberg, S., Stark, Y., Kölln, J., Popp, A., Urlinger S., and Enzelberger, M. (2011). HuCAL PLATINUM, a synthetic Fab library optimized for sequence diversity and superior performance in mammalian expression systems. J. Mol. Biol. *413*, 261-278.

Presta, L.G., Gazzano-Santoro, H., Totpal, K., Wong, P.Y., Ultsch, M., Meng, Y.G., and Mulkerrin, M.G. (2000). Mapping of the C1q binding site on rituxan, a chimeric antibody with a human IgG1 Fc. J. Immunol. *164*, 4178-4184.

Rader, C., Cheresh, D.A., and Barbas, C.F.III. (1998). A phage display approach for rapid antibody humanization : designed combinatorial V gene libraries. Proc. Natl. Acad. Sci. *95*, 8910-8915.

Rajpal, A., Beyaz, N., Haber, L., Cappuccilli, G., Yee, H., Bhatt, R.R., Takeuchi, T., Lerner, R.A., and Crea, R. (2005). A general method for greatly improving the affinity of antibodies by using combinatorial libraries. Proc. Natl. Acad. Sci. *102*, 8466-8471.

Reff, M.E., Carner, K., Chambers, K.S., Chinn, P.C., Leonard, J.E., Raab, R., Newman, R.A., Hanna, N., and Anderson, D.R. (1994). Depletion of B cells *in vivo* by a chimeric mouse human monoclonal antibody to CD20. Blood. *83*, 435-445.

Riechmann, L., Clark, M., Waldmann, H., Winter, G. (1988). Reshaping human antibodies for therapy. Nature. *332*, 323-327.

Robert de B., Kees S., Joseph M., Ronald K., and Francesca Q., (1999). Selection of high-affinity phage antibodies from phage display libraries. Nature Biotechnology. *17*, 397-399.

Romond, E.H., Perez, E.A., Bryant, J., Suman, V.J., Geyer, C.E. Jr., Davidson, N.E., Tan-Chiu, E., Martino, S., Paik, S., Kaufman, P.A., Swain, S.M., Pisansky, T.M., Fehrenbacher, L., Kutteh, L.A., Vogel, V.G., Visscher, D.W., Yothers, G., Jenkins, R.B., Brown, A.M., Dakhil, S.R., Mamounas, E.P., Lingle, W.L., Klein, P.M., Ingle, J.N., and Wolmark, N. (2005). Trastuzumab plus adjuvant chemotherapy for operable HER2-positive breast cancer. N. Engl. J. Med. *353*, 1673-1684.

Routier, F.H., Hounsell, E.F., Rudd, P.M., Takahashi, N., Bond, A., Hay, F.C., Alavi, A., Axford, J.S., and Jefferis, R. (1998). Quantitation of the oligosaccharides of human serum IgG from patients with rheumatoid arthritis: a critical evaluation of different

methods. J. Immunol. Methods. *213*, 113-130.

Rowley, M.J., O'Connor, K., and Wijeyewickrema, L. (2004). Phage display for epitope determination: a paradigm for identifying receptor-ligand interactions. Biotechnol. Ann. Rev. *10*, 151-188.

Ryan, M.C., Hering, M., Peckham, D., McDonagh, C.F., Brown, L., Kim, K.M., Meyer, D.L., Zabinski, R.F., Grewal, I.S., and Carter, P.J. (2007). Antibody targeting of B-cell maturation antigen on malignant plasma cells. Mol. Cancer. Ther. *6*, 3009-3018.

Sambrook, J.F., and Russell, D.W. (2001). *In* Molecular cloning : a laboratory manual, 3rd ed. (Cold Spring Harbor Laboratory Press), pp.1.25-1.26.

Scallon, B.J., Moore, M.A., Trinh, H., Knight, D.M., and Ghrayeb, J. (1995). Chimeric anti-TNF-alpha monoclonal antibody cA2 binds recombinant transmembrane TNF-alpha and activates immune effector functions. Cytokine. 7, 251-259.

Schier, R., McCall, A., Adams, G.P., Marshall, K.W., Merritt, H., Yim, M., Crawford, R.S., Weiner, L.M., Marks, C., and Marks, J.D. (1996). Isolation of picomolar affinity anti-c-erbB-2 single-chain Fv by molecular evolution of the complementarity determining regions in the center of the antibody binding site. J. Mol. Biol. *263*,

551-567.

Seliger, B., Rongcun, Y., Atkins, D., Hammers, S., Huber, C., Störkel, S., and Kiessling, R. (2000). HER-2/neu is expressed in human renal cell carcinoma at heterogeneous levels independently of tumor grading and staging and can be recognized by HLA-A2.1-restricted cytotoxic T lymphocytes. Int. J. Cancer. *87*, 349-359.

Shepard, H.M., Lewis, G.D., Sarup, J.C., Fendly, B.M., Maneval, D., Mordenti, J., Figari, I., Kotts, C.E., Palladino, M.A. Jr, Ullrich, A., et al. (1991). Monoclonal antibody therapy of human cancer: taking the HER2 protooncogene to the clinic. J. Clin. Immunol. *11*, 117-127.

Sidhu, S.S, Lowman, H.B., Cunningham, B.C., and Wells, J.A. (2000). Phage display for selection of novel binding peptides. Methods. Enzymol. *328*, 333-363.

Sliwkowski, M.X., Lofgren, J.A., Lewis, G.D., Hotaling, T.E., Fendly, B.M., and Fox, J.A. (1999). Nonclinical studies addressing the mechanism of action of trastuzumab (Herceptin). Semin. Oncol. *26*, 60-70.

Soltes, G., Barker, H., Marmai, K., Pun, E., Yuen, A., and Wiersma, E.J. (2003). A new helper phage and phagemid vector system improves viral display of antibody Fab fragments and avoids

propagation of insert-less virions. J. Immunol. Methods. *274*, 233–244.

Song, S.Y., Hur, B.U., Lee, K.W., Choi, H.J., Kim, S.S., Kang, K., and Cha, S.H. (2009). Successful application of the dual-vector system II in creating a reliable phage-displayed combinatorial Fab library. Mol. Cells. *27*, 313-319.

Steiner, D., Forrer, P., Stumpp, M.T., and Plückthun, A. (2006). Signal sequences directing cotranslational translocation expand the range of proteins amenable to phage display. Nature Biotechnol. *24*, 823-831.

Strohl, W.R. (2009). Optimization of Fc-mediated effector functions of monoclonal antibodies. Curr. Opin. Biotechnol. *20*, 685-691.

Swanton, C., Futreal, A., and Eisen, T. (2006). Her2-targeted therapies in non-small cell lung cancer. Clin. Cancer Res. *12*, 4377s-4383s.

Tjio, J. H., and Puck, T.T. (1958). Genetics of somatic mammalian cells. II. Chromosomal constitution of cells in tissue culture. J. Exp. Med. *108*, 259–268.

Trill, J.J., Shatzman, A.R., and Ganguly, S. (1995). Production of

monoclonal antibodies in COS and CHO cells. Curr. Opin .Biotechnol. *6*, 553-560.

Urlaub. G., Käs, E., Carothers, A.M., and Chasin, L.A. (1983). Deletion of the diploid dihydrofolate reductase locus from cultured mammalian cells. Cell. *33*, 405-412.

USPC (2005). General chapters, 85. Bacterial endotoxin test.

Shukla, A.A., Hubbard, B., Tressel, T., Guhan, S., and Low, D. (2007). Downstream processing of monoclonal antibodies--application of platform approaches. J. Chromatogr. B Analyt. Technol. Biomed. Life Sci. *848*, 28-39.

Vaccaro, C., Zhou, J., Ober, R.J., and Ward, E.S. (2005). Engineering the Fc region of immunoglobulin G to modulate *in vivo* antibody levels. Nat. Biotechnol. *23*, 1283-1288.

Vajdos, F.F., Adams, C.W., Breece, T.N., Presta, L.G., de Vos, A.M., Sidhu, S.S. (2002). Comprehensive functional maps of the antigen-binding site of an anti-ErbB2 antibody obtained with shotgun scanning mutagenesis. J. Mol. Biol. *320*, 415-428.

Valabrega, G., Montemurro, F., and Aglietta, M. (2007). Trastuzumab: mechanism of action, resistance and future

perspectives in HER2-overexpressing breast cancer. Ann. Oncol. *18*, 977-984.

Verhoeyen, M., Milstein, C., Winter, G. (1988). Reshaping human antibodies: grafting an antilysozyme activity. Science. *239*, 1534-1536.

Vieira, J., and Messing, J. (1987). Production of single-stranded plasmid DNA. Methods Enzymol. *153*, 3-11.

Wang, Z., Wang, Y., Li, Z., Li, J., and Dong, Z. (2000). Humanization of a mouse monoclonal antibody neutralizing TNF-alpha by guided selection. J. Immunol. Methods. *241*, 171-184.

Watzka, H., Pfizenmaier, K., and Moosmayer, D. (1998). Guided selection of antibody fragments specific for human interferon gamma receptor 1 from a human V_H- and V_L-gene repertoire. Immunotechnol. *3*, 279-291.

Weatherill, E.E., Cain, K.L., Heywood, S.P., Compson, J. E., Heads, J.T., Adams, R. and Humphreys, D.P. (2012). Towards a universal disulphide stabilised single chain Fv format: importance of interchain disulphide bond location and V_L-V_H orientation. Protein Engineering, Design & Selection. *25*, 321-329.

Werner, R.G., Noé, W., Kopp, K., Schlüter, M. (1998). Appropriate mammalian expression systems for biopharmaceuticals. Arzneimittelforschung. *48*, 870-880.

Whenham, N., D'Hondt, V., and Piccart, M.J. (2008). HER2-positive breast cancer: from trastuzumab to innovatory anti-HER2 strategies. Clin. Breast Cancer *8*, 38-49.

Winter, G., Griffiths, A.D., Hawkins, R.E., and Hoogenboom, H.R. (1994). Making antibodies by phage display technology. Ann. Rev. Immunol. *12*, 433-455.

Witzeneder, K., Lindenmair, A., Gabriel, C., Höller, K., Theiß, D., Redl, H., and Hennerbichler, S. (2013). Transfus. Med. Hemother. *40*, 417-423.

Wurm, F.M. (2004). Production of recombinant protein therapeutics in cultivated mammalian cells. Nat. Biotechnol. *22*, 1393-1398.

Xu, Z., Davis, H.M., and Zhou, H. (2015). Clinical impact of concomitant immunomodulators on biologic therapy: Pharmacokinetics, immunogenicity, efficacy and safety. J. Clin. Pharmacol. *55*, S60-S74.

Yakes, F.M., Chinratanalab, W., Ritter, C.A., King, W., Seelig, S.,

and Arteaga, C.L. (2002). Herceptin-induced inhibition of phosphatidylinositol-3 kinase and Akt is required for antibody-mediated effects on p27, cyclin D1, and antitumor action. Cancer Res. *62*, 4132-4141.

Yamamoto, A., Ochiai, M., Fujiwara, H., Asakawa, S., Ichinohe, K., Kataoka, M., Toyoizumi, H., and Horiuchi, Y. (2000). Evaluation of the applicability of the bacterial endotoxin test to antibiotic products. Biologicals. *28*, 155-167.

Yan, X., and Xu, Z. (2006). Ribosome-display technology: applications for directed evolution of functional proteins. Drug Discov. Today. *11*, 911-916.

Yang, G.H., Yoon, S.O., Jang, M.H., and Hong, H.J. (2007). Affinity maturation of an anti-hepatitis B virus PreS1 humanized antibody by phage display. J. Microbiol. *45*, 528-533.

Yang, G., Truong, L.D., Wheeler, T.M., and Thompson, T.C. (1999). Caveolin-1 expression in clinically confined human prostate cancer: a novel prognostic marker. Cancer Res. *59*, 5719-23.

Yang, X.D., Jia, X.C., Corvalan, J.R., Wang, P., and Davis, C.G. (2001). Development of ABX-EGF, a fully human anti-EGF receptor monoclonal antibody, for cancer therapy. Crit. Rev. Oncol. Hematol.

38, 17-23.

Yoon, S.O., Lee, T.S., Kim, S.J., Jang, M.H., Kang. Y.J., Park, J.H., Kim, K.S., Lee, H.S., Ryu, C.J., Gonzales, N.R., Kashmiri, S.V.S., Lim, S.M., Choi, C.W., and Hong, H.J. (2006). Construction, affinity maturation, and biological characterization of an anti-tumor-associated glycoprotein-72 humanized antibody. J. Biol. Chem. *281*, 6985-6992.

Zou, W., Ueda, M., Murai, T., and Tanaka, A. (2000). Establishment of a simple system to analyse the molecular interaction in the agglutination of *Saccharomyces cerevisiae*. Yeast. *16*, 995-1000.

초 록

항 HER2 항체 hu4D5 (Trastuzumab, Herceptin) 보다 치료활성이 향상된 biobetter 를 도출하고, 항체 최적화 기술을 응용하기 위한 하나의 모델로서 hu4D5 를 이용하였다. hu4D5 의 CDR-H3, L3 및 L2의 몇몇 위치에 대하여 무작위 돌연변이를 유도한 scFv 라이브러리를 구축하고, 파아지 디스플레이를 이용한 가혹 조건에서 선별하는 방법을 통하여 유방암 세포 에 대한 세포증식저해활성을 일차적 선정 기준으로 스크리닝하였다.

139종의 변이체중에서, AH06 이 hu4D5 에 비하여 위암 세포에 대한 세포증식저해활성 (IC_{50}: 0.81 nM)과 HER2에 대한 친화도 (K_D: 60 pM)가 각각 7.2-fold 및 7.4-fold로 향상되는 등, 가장 우수한 효능을 나타내었다.

AH06 항체는 HER2 도메인 IV에 특이적으로 결합하며, HER2 이외의 다른 수용체에는 교차 반응성을 가지고 있지 않았으며 위암 세포 NCI-N87에서 인산화-HER2와 인산화-AKT 수준을 hu4D5 와 유사한 수준으로 억제하지만, 하위 신호전달에서 p27 수준은 좀더 많이 증가시켰다.

결합 에너지 계산 결과, AH06 의 CDR-H3의 W98, F100c, A101, L102로의 아미노산 잔기 변화가 HER2에 대한 결합을 안정화시키는 것으로 나타났다. 분자 모델링으로 시뮬레이션한 결과, AH06 내의 W98 의 aromatic ring 과 항원 HER2 도메인 IV 내의 I613 의 aliphatic group 사이에 직접적인 소수성 상호작용 및 CDR-H3 F100c 의 phenyl ring 과 V_L 의 Y36, P44 및 F98 로 구성된 소수성 치환기 사이의 사슬간 소수성 상호작용들의 상승효과에 의하여 HER2에 대한 친화도가 향상된 것으로 추론되었다.

AH16 항체 발현 벡터를 제조하였고, 15 계대까지 발현량과 세포성장속도가 일정하게 유지되는 AH16F1-3-14-80-26 clone을 최종 생산세포주 (stable cell line)으로 선별하였다. 1종의 기본 배지와 3종의 첨가물을 선정하였고, 이의 최적 조합 배지를 이용한 최종 생산성은 플라스크 상에서 약 1.3g/L 이었다.

1차 Protein A 레진 과 2단계의 이온교환 크로마토그래피 등 3단계의 순차적 정제를 통하여 수율 93.8%, 순도 99.9% 의 공정을 하였고, non-Protein A 공정으로서 양이온 교환 크로마토그래피를 이용하여 HCP (host cell protein), HCD (host cell DNA) 같은 불순물을 효과적으로 분리 할 수 있었으며, 수율은 99%, 순도는 97.5% 였다.

AH16 원료의약품 (API: active pharmaceutical ingredients)의 구조, 물리 화학적 특성, 면역학적, 생물학적 특성을 분석한 결과, AH16 API는 자체적으로 설정한 “기준 및 시험법” 항목에 부합되었다.

본 연구를 통하여 다양한 치료용 선도 항체의 효능 개량에 필요한 upstream 항체공학 기술과 항체 생산에 필요한 downstream 바이오공정 기술을 확립, 응용하였다.

주제어: 항체공학, 항체 최적화, HER2, 파아지 디스플레이, 무작위 돌연변이, 세포증식 저해활성, 결합 친화도, Herceptin, 바이오공정 개발, 생산세포주, 배양 공정, 정제 공정

학번: 2004-30222